AGU PUBLICATIONS

Reviews of Geophysics

REVIEW ARTICLE
10.1002/2017RG000579

Key Points:
- PTHA quantifies the probability that different hazard intensity levels will be exceeded in a given time window at a specific place
- PTHA is the first step toward tsunami risk assessment and risk reduction planning
- A comprehensive review of PTHA is discussed for seismic and nonseismic tsunami sources with uncertainty quantification methods

Supporting Information:
- Supporting Information S1
- Data Set S1

Correspondence to:
A. Grezio,
anita.grezio@ingv.it

Citation:
Grezio, A., Babeyko, A., Baptista, M. A., Behrens, J., Costa, A., Davies, G., … Thio, H. K. (2017). Probabilistic Tsunami Hazard Analysis: Multiple sources and global applications. *Reviews of Geophysics*, *55*, 1158–1198. https://doi.org/10.1002/2017RG000579

Received 7 JUL 2017
Accepted 2 NOV 2017
Accepted article online 14 NOV 2017
Published online 27 DEC 2017

Probabilistic Tsunami Hazard Analysis: Multiple Sources and Global Applications

Anita Grezio[1], Andrey Babeyko[2], Maria Ana Baptista[3], Jörn Behrens[4], Antonio Costa[1], Gareth Davies[5], Eric L. Geist[6], Sylfest Glimsdal[7], Frank I. González[8], Jonathan Griffin[5], Carl B. Harbitz[6], Randall J. LeVeque[8], Stefano Lorito[9], Finn Løvholt[7], Rachid Omira[3], Christof Mueller[10], Raphaël Paris[11], Tom Parsons[6], Jascha Polet[12], William Power[10], Jacopo Selva[1], Mathilde B. Sørensen[13], and Hong Kie Thio[14]

[1]Istituto Nazionale di Geofisica e Vulcanologia, Bologna, Italy, [2]Deutsches GeoForschungsZentrum (GFZ), Germany, [3]Instituto Português do Mar e da Atmosfera, Universidade de Lisboa, Portugal, [4]Department of Mathematics, Universität Hamburg, Hamburg, Germany, [5]Geoscience Australia, Canberra, ACT, Australia, [6]U.S. Geological Survey, Reston, VA, USA, [7]Norwegian Geotechnical Institute, Oslo, Norway, [8]Department of Earth and Space Sciences, University of Washington, Seattle, WA, USA, [9]Istituto Nazionale di Geofisica e Vulcanologia, Roma, Italy, [10]Institute of Geological and Nuclear Sciences (GNS), Lower Hutt, New Zealand, [11]Laboratoire Magmas et Volcans, Université Clermont Auvergne, Clermont-Ferrand, France, [12]Department of Geological Sciences, California State Polytechnic University, Pomona, CA, USA, [13]Department of Earth Science, University of Bergen, Bergen, Norway, [14]AECOM, Los Angeles, CA, USA

Abstract Applying probabilistic methods to infrequent but devastating natural events is intrinsically challenging. For tsunami analyses, a suite of geophysical assessments should be in principle evaluated because of the different causes generating tsunamis (earthquakes, landslides, volcanic activity, meteorological events, and asteroid impacts) with varying mean recurrence rates. Probabilistic Tsunami Hazard Analyses (PTHAs) are conducted in different areas of the world at global, regional, and local scales with the aim of understanding tsunami hazard to inform tsunami risk reduction activities. PTHAs enhance knowledge of the potential tsunamigenic threat by estimating the probability of exceeding specific levels of tsunami intensity metrics (e.g., run-up or maximum inundation heights) within a certain period of time (exposure time) at given locations (target sites); these estimates can be summarized in hazard maps or hazard curves. This discussion presents a broad overview of PTHA, including (i) sources and mechanisms of tsunami generation, emphasizing the variety and complexity of the tsunami sources and their generation mechanisms, (ii) developments in modeling the propagation and impact of tsunami waves, and (iii) statistical procedures for tsunami hazard estimates that include the associated epistemic and aleatoric uncertainties. Key elements in understanding the potential tsunami hazard are discussed, in light of the rapid development of PTHA methods during the last decade and the globally distributed applications, including the importance of considering multiple sources, their relative intensities, probabilities of occurrence, and uncertainties in an integrated and consistent probabilistic framework.

1. Introduction

Tsunamis occur infrequently compared to many other natural hazards. Yet they can have devastating consequences. The infrequency of tsunami events in coastal areas, particularly where preceding events occurred well before living memory, makes tsunami hazard assessment a challenging task. Recently, Probabilistic Tsunami Hazard Analysis (PTHA) has been developed to quantify tsunami hazard at return periods extending from hundreds to thousands of years, beyond the limited historical observational records. PTHA therefore provides crucial information that underpins society's tsunami risk management measures.

A brief look at the history of tsunamis shows that many times society has been caught unprepared, and tsunami risk management strategies have been developed in response to major tsunami disasters (see https://www.nasa.gov/vision/earth/lookingatearth/indonesia_quake.html and http://www.esa.int/About_Us/ESRIN/Mapping_Japan_s_changed_landscape_from_space). The first tsunami warning system was established in Japan following the 1933 Sanriku Tsunami. Similarly, the U.S. tsunami warning center in Hawaii was established following the 1946 Unimak tsunami. Pacific Rim countries worked together to

establish the Pacific Tsunami Warning Centre (International Tsunami Information Center, 2015) following the 1964 M_w 9.2 Great Alaska earthquake and Tsunami, and the 1960 Valdivia M_w 9.3–9.6 earthquake and tsunami in Chile (Abe, 1979; Cisternas et al., 2005; Fujii & Satake, 2013; Lomnitz, 2004; Liu et al., 1995; Watanabe, 1972).

Although tsunami research had demonstrated that large megathrust earthquakes capable of generating transoceanic tsunami had occurred on the Sunda Arc in the past (Cummins, 2004; Latief et al., 2000; Newcomb & McCann, 1987; Natawidjaja et al., 2004; Zachariasen et al., 1999), tsunami early warning systems had not been established in the Indian Ocean at the time of the 2004 Indian Ocean Tsunami, in which more than 225,000 people died (Emergency Events Database (EM-DAT), 2017). Again, it was only following this major disaster that Intergovernmental Oceanographic Commission of UNESCO received the mandate from the international community to coordinate the establishment of regional tsunami early warning systems in the Indian Ocean (Indian Ocean Tsunami Warning and Mitigation System, IOTWS), the North-eastern Atlantic and the Mediterranean Sea (North-eastern Atlantic, the Mediterranean and Connected Seas Tsunami Warning and Mitigation System, NEAMTWS), and the Caribbean region (Caribbean and Adjacent Regions Early Warning System, CARIBE-EWS). Additionally, national tsunami early warning systems were established in the Indian Ocean (e.g., Indonesian Tsunami Early Warning Systems, Ina-TEWS) (Lauterjung et al., 2010; Taubenböck et al., 2009; Setiyono et al., 2017).

Prior to the Indian Ocean Tsunami, only a handful of PTHA's (e.g., Lin & Tung, 1982; Rikitake & Aida, 1988) had been conducted. However, the PTHA method gained momentum from 2004 and onward due to the many tsunami hazard assessments (including deterministic hazard studies) needed to inform risk reduction activities. Progress in developing modern PTHA techniques were achieved by Geist and Parsons (2006), and a series of studies building on their methodology followed later (e.g., Burbidge et al., 2008; Griffin et al., 2016; Heidarzaed & Kijko, 2011; Hoechner et al., 2016; Horspool et al., 2014; Shin et al., 2015; Suppasri et al., 2012; Taubenböck et al., 2008; Yadav, Tripathi, et al., 2013; Yadav, Tsapanos, et al., 2013).

The scale of the disaster caused by the 11 March 2011 M_w 9.0 Tohoku earthquake and Tsunami, Japan (Baba et al., 2017; Fujii et al., 2011; Gusman et al., 2012; Ito et al., 2011; Koketsu et al., 2011; Romano et al., 2012, 2014; Satake et al., 2013; Simons et al., 2011; Yoshida et al., 2011), with more than 19,800 fatalities and USD210 billion in damages (EM-DAT, 2017) in a country that has invested much effort on tsunami preparation, again demonstrated that there exist limitations in our understanding of tsunami hazard and risk. In particular, this event highlighted the need for incorporating more complex phenomena such as variable slip (e.g., Davies et al., 2015; Goda et al., 2014) and quantification of source uncertainties (e.g., Selva et al., 2016) in PTHA analysis.

While this led some to debate the fundamental value of probabilistic hazard assessment (see Stein et al., 2012 and reply by Frankel, 2013), a more measured approach undertaken in this paper is to review the current state of PTHA practice and identify the issues that remain unresolved and should be subjects of active research.

Complying with the most used PSHA (Probabilistic Seismic Hazard Analysis) convention and hazard/risk terminology PTHA analysis indicates a general study on probabilistic tsunami hazard and an explicative quantification in which the method is more important than the actual values obtained. PTHA assessment indicates official computations for which the tsunami hazard values matter for the subsequent use of risk level acceptance by end users.

PTHA methodologies provide a framework for assessing the likelihood of a given measure of tsunami intensity (e.g., maximum run-up height) being exceeded at a particular location within a given time period. As historical tsunami catalogs are almost inherently incomplete, numerical models of tsunami generation, propagation, and inundation (e.g., Geist & Lynett, 2014) are combined with source probabilities to provide quantitative estimates of the probability of exceedance of different levels of a given tsunami metric.

Onshore, tsunami metrics used for PTHA typically include tsunami height, inundation depth, and current velocity, as well as important derived quantities that relate to hydrodynamic forces, such as momentum flux. Offshore, the seaward distance to low hazard regions where current speeds are minimal is important, and indices that relate damage in harbors to current speed have also been developed (Lynett et al., 2014). Nearshore drawdown metrics serve to identify regions that may become so shallow that vessels may capsize or cooling water intakes of nuclear power plants might be exposed. In practical applications, these metrics are frequently displayed on maps that help guide decision makers. Finally, these metrics are a key component of tsunami risk assessment (Wood et al., 2015), being used as input to loss models that estimate damage to the built environment, economic impact, and fatalities; in turn, they help setting priorities for the expenditure of

financial and human resources on risk mitigation efforts (Chock, 2015; Løvholt, Griffin, et al., 2015, Suppasri et al., 2016; Thio et al., 2017; Wei et al., 2017; Yeh, 2010).

The most common cause of tsunami are submarine earthquakes, which include the majority of events with a high number of casualties (Lay, 2015; Lorito et al., 2016; Okal, 2015; Satake & Atwater, 2007; Synolakis & Bernard, 2006). To this end, PTHA methodologies have been applied in many different regions of the world, and PTHAs have been undertaken at different scales, local, regional, and global, to inform different policy decisions. Coarse grained global-scale PTHAs (Davies et al., 2017; Løvholt et al., 2014; Løvholt, Griffin, et al., 2015) have been developed for consistent multihazard risk assessment used by the United Nations Office for Disaster Risk Reduction to prioritize resources for Disaster Risk Management. A number of regional and national-scale PTHAs have been undertaken in the Pacific Ocean (Annaka et al., 2007; Burroughs & Tebbens, 2005; Dall'Osso et al., 2014; De Risi & Goda, 2016; Downes & Stirling, 2001; Geist & Parsons, 2006; González et al., 2009; Gubler et al., 2013; Jaimes et al., 2016; Jingming et al., 2016; Lane et al., 2013; Liu et al., 2007; Knighton & Bastidas, 2015; Orfanogiannaki & Papadopoulos, 2007; Power et al., 2013; Rikitake & Aida, 1988; Sakai et al., 2006; Smit et al., 2017; Tatsumi et al., 2014; Thio et al., 2007), in the Indian Ocean (Burbidge et al., 2008; Heidarzaed & Kijko, 2011; Hoechner et al., 2016; Horspool et al., 2014; Shin et al., 2015; Suppasri et al., 2012; Thio et al., 2007; Yadav et al., 2013; Yadav et al., 2013), in the Atlantic Ocean (e.g., Geist & Parsons, 2009; Leonard et al., 2014; Omira et al., 2015; Parsons & Geist, 2009) and in the Mediterranean Sea (e.g., Lorito et al., 2015; Selva et al., 2016; Sørensen et al., 2012). These studies are used to prioritize high hazard locations for more detailed studies and identify the tsunami sources that contribute most to the hazard at a particular location. However, many tsunami risk management measures (e.g., planning evacuation routes) require high-resolution local-scale information. Local-scale onshore PTHAs face computational challenges due to the need to model nonlinear inundation processes and generally rely on a reduced set of scenarios (González et al., 2009; Lorito et al., 2015; Wei et al., 2017; Thio et al., 2010). In many cases national or regional PTHA are used to define a set of scenarios representative of a given probability that are then used to model inundation, rather than undertaking an exhaustive local-scale PTHA.

PTHA methods for nonearthquake sources are less well established. Determining rates of occurrence tends to be more problematic for nonearthquake sources compared with earthquake sources because they often lack any clear time dependence, and source mechanisms can be strongly nonlinear. Probabilistic hazard assessments of tsunamis from submarine mass failures, some including the potential for earthquake triggering, have been undertaken for the U.S. Atlantic (Geist & Parsons, 2010; Grilli et al., 2009; Lynett & Martinez, 2012; Maretzki et al., 2007; ten Brink et al., 2009, 2014) and Pacific margins (Watts, 2004), the Canadian coast (Leonard et al., 2014), New Zealand coasts (Lane, Mountjoy, Power, & Mueller, 2016), and the Tyrrhenian Sea (e.g., Grezio et al., 2012, 2015). Probabilistic analysis of meteotsunamis were introduced by Geist et al. (2014) and Šepić, Medugorac, et al. (2016) for the northeast U.S. coastlines and the Balearic Islands, Spain, respectively. A probabilistic hazard assessment of tsunamis due to meteor impacts was undertaken by Ward and Asphaug (2000) in consideration of the fact that small bodies (diameter <1 km) could statistically represent the most likely scenario for a future meteorite collision and generation/propagation of large waves, sometimes traveling a large distance from the point of impact (Gisler et al., 2011; Glimsdal et al., 2007; Korycansky & Lynett, 2007; Rumpf et al., 2017; Wünnemann et al., 2010). An attempt to undertake PTHA for volcanic sources was considered in recent studies related to underwater explosions in the Campi Flegrei, Italy (*EU ASTARTE Project*-Assessment, Strategy and Risk Reduction for Tsunami in Europe) and pyroclastic flows from Vesuvio, Naples (*Italian ByMuR Project*-Bayesian Multi-Risk Assessment: A case study for natural risks in the city of Naples).

This paper reviews the current state of PTHA methods and the related unresolved issues that challenge the tsunami science community. The paper is organized into four preceding sections. Section 2 provides a detailed background of the nature of tsunami sources and their hydrodynamic modeling, including earthquakes, tsunami earthquakes, landslides, volcanoes, meteotsunamis, and asteroid impacts. It is mainly present to provide introductory information of the effect of the individual sources on PTHA. Section 3 reviews the basic principles of the PTHA method and derivations of tsunami probabilities. Section 4 provides a review of methods that may be used to quantify tsunami uncertainties. Finally, future challenges for future hazard assessments are discussed in section 5.

2. Tsunami Generation and Propagation: Causes, Mechanisms, and Modeling

Most destructive tsunamis in recent history have been caused by earthquakes, and thus, much of the effort devoted to PTHA has been directed at characterizing seismic sources. However, in some parts of the globe the major causes of catastrophic tsunamis are nonseismic, including landslides, volcanic activity, atmospheric disturbances, and meteorite impacts. Ideally, PTHAs should combine all tsunamigenic sources in a joint probabilistic analysis (e.g., Grezio et al., 2015). In practice, tsunami studies commonly treat the different classes of tsunami sources individually in PTHAs, as different tsunami sources face different challenges and exhibit different sets of background data. This necessitates the source specific overviews given below (Figure 1). In addition, a review of tsunami propagation and inundation modeling techniques applied in PTHA is presented in section 2.6.

2.1. Earthquakes Generating Tsunamis

Earthquakes under the ocean (or lake) bottom can cause sudden deformation of the seafloor, which, in turn, displaces the water column above the source giving rise to a tsunami. We review a range of features associated with an earthquake rupture that control its tsunamigenic potential. While large magnitude ruptures tend to produce larger tsunamis, there are still additional contributing factors that include, for example, the earthquake's focal depth and mechanism, and the amount and distribution of slip. We introduce some of the effects of this variability on modeling, describe a variety of earthquake scaling laws, and discuss issues of earthquake forecasting that influence tsunami forecasting in the PTHA context. We will also describe a special class of earthquakes, "tsunami earthquakes" that produce anomalously large tsunamis in respect to their seismic magnitudes (section 2.1.1).

Earthquakes, within or in the vicinity of subduction zones where oceanic plates converge beneath another tectonic plate, are the most common, but not the exclusive, cause of significant tsunamis (e.g., National Geophysical Data Center/World Data Service (NGDC/WDS): Global Historical Tsunami Database. National Geophysical Data Center, NOAA. doi:10.7289/V5PN93H7). Subduction zones are capable of generating different types of ruptures: (1) classical interplate thrusts which are the primary tsunami triggers (Satake & Tanioka, 1999), (2) outer-rise normal faults (Abe, 1978; Gusman et al., 2009), (3) intraslab events (Heidarzadeh & Satake, 2014), and (4) crustal earthquakes within the overriding continental plate (Power et al., 2017). The subduction zone process itself has been reviewed elsewhere (Stern, 2002).

The dominant earthquake mechanism, which is the relative offset direction of tectonic blocks subjected to shear faulting, depends on the tectonic environment. Plate motions create regional stresses that can cause parts of the lithosphere to compress, extend, or be offset laterally; as a result, earthquakes will feature reverse (thrust), normal, and strike-slip focal mechanisms, respectively. Combinations of strike slip with reverse or normal mechanisms are classified as oblique earthquakes. When an earthquake occurs offshore or in the vicinity of the coast, it may result in a rapid coseismic displacement of the sea bottom perturbing the entire water column above it. The vertical displacement of the water column gives rise to a tsunami. This vertical displacement results primarily due to the corresponding vertical displacement of the sea bottom. But also horizontal coseismic displacements of the sea bottom topography characterized by significant slopes (e.g., subduction zone trench) are suggested to contribute to the tsunami generation (Tanioka & Satake, 1996; Song et al., 2017). Analysis of past tsunamis suggests that the ratio of the horizontal components of bottom deformation to the total displaced water volume ranges between 0.07% and 55%, with an average being about 14% (Nosov et al., 2014).

Larger earthquake magnitudes generally produce greater fault slip and hence cause larger coseismic crustal deformation, which in turn generate larger tsunamis. The energy radiated by an earthquake can be approximately related to the seismic moment M_0 (in units of N m), derived from an equivalent set of double-couple forces acting on the points of a finite (extended) fault plane. The earthquake moment magnitude used in standard seismological observatory practice M_w is related to M_0 by

$$M_w = (\log_{10} M_0 - 9.1)/1.5 \quad (1)$$

(Kanamori, 1977). However, particularly in the near field of the earthquake source, the complexity of initial field shape (e.g., the aspect ratio or characteristic wavelengths of the displacement) influences the size and the characteristics of the tsunami. Also, other earthquake properties impact on the initial field, such as earthquake focal depth, faulting mechanism and aspect ratio, slip amount and distribution, and heterogeneity of slip over the fault plane.

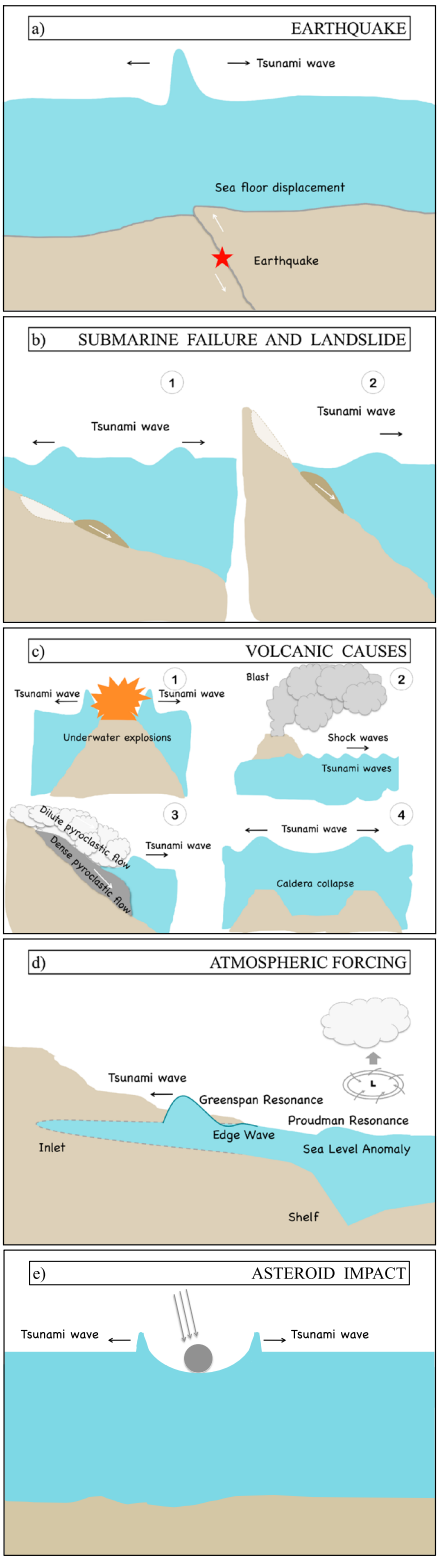

Figure 1. Sources of tsunami waves: (a) earthquakes causing seafloor deformations and subsequent displacements of the water column above; (b) submarine (1) and subaerial (2) mass failures; (c) volcanic activity including (1) underwater explosion, (2) blast exciting free waves in the atmosphere which transfers energy to water, (3) pyroclastic flows, and (4) rapid ground deformations or caldera collapses; (d) *Proudman* resonance or *Greespan* resonance occurring after atmospheric disturbances with further amplification of the long ocean waves because of the shelf resonance; and (e) oceanic impacts of asteroids and comets.

Another factor controlling the efficiency of tsunami generation by large earthquakes may be temporal evolution of the seafloor displacement (Le Gal et al., 2017). A rupture velocity of 1 km/s and a rise time of 180 s yielded the best fit between tide gauge data and model simulations in the 2004 Sumatra-Andaman earthquake (Fujii & Satake, 2007).

For practical reasons, and to limit the computational cost, several approximations are commonly made in earthquake source modeling for PTHA (see the review by Geist & Oglesb, 2014). It is often assumed that a uniform displacement takes place on a rectangular planar fault buried in a homogeneous elastic half-space, and that the coseismic seafloor displacement happens instantaneously with the fault displacement (slip). Sometimes, only the vertical component of the deformation is taken into account, while the horizontal displacement is neglected. The translation of the fault movement into the seafloor movement is often accomplished based on a *Green*'s function solution to the elastic half-space problem (Okada, 1985). This model yields a steady state solution that describes the seafloor deformation due to uniform slip over a rectangular dislocation patch. The seafloor deformation is then transferred exactly into a sea level vertical perturbation. Examples of complexities that are not usually taken into account in this modeling technique are (1) the topography of the seafloor, which can be influential if there is a large horizontal movement; (2) the fact that the Earth is not a homogeneous isotropic elastic material; (3) the geometry of the fault surface in reality may be curved along strike or downdip; and (4) that earthquake slip and coseismic displacement are not uniformly distributed and not instantaneous.

Methods that employ a layered model for the elastic properties of the Earth are also available (Wald & Graves, 2001; Wang et al., 2003) and have been used in some PTHA studies (e.g., Horspool et al., 2014). More complex three-dimensional models of the Earth and fault plane are possible using finite element models (e.g., Romano et al., 2014). Nonuniform distribution of slip plays an important part in assessing the impact of local tsunamis (e.g., Geist & Dmowska, 1999). Modeling this effect can be performed with stochastic slip distributions which also include correlation length scales that may be anisotropic (Davies et al., 2015; Geist, 2002; LeVeque et al., 2016). This is commonly done by dividing the rupture plane into several subfaults located on a regular grid and assigning varying slip to each of these subfaults. Once the amount of slip has been assigned to each subfault, surface displacements are subsequently computed for each of these, and the linearity of each solution allows superposition over all the slip patches. Stochastic slip methods have been used to provide earthquake source models for inundation studies at a limited number of locations (e.g., Geist & Oglesby, 2014; Goda et al., 2014; Griffin et al., 2016; Mueller et al., 2015). Hence, stochastic slip models can generate a set of possible heterogeneous rupture scenarios for tsunami generation. However, while they can represent the total moment of an earthquake, they may or may not recreate a justifiable stress drop pattern or friction law on the fault. Thus, stochastic slip realizations could include unrealistic and/or unlikely slip patterns. Because of this, studies with stochastically generated scenarios may be not fully probabilistic because they do not assign probabilities to different slip distributions. Today, only a few studies integrate rupture complexity into the PTHA process (e.g., Li et al., 2016).

The assumption that complex rupture happens instantaneously across the whole rupture interface is still very common. In reality, earthquake rupture nucleates at the hypocenter and then travels from there across the rupture interface with varying speed and amount of slip. The kinematics of this effect can be incorporated in the modeling process by defining an empirical velocity function for the rupture propagation. It is common to assume that this effect can be translated to the seafloor by sequentially "activating" the individual surface displacements for each subfault. However, this is still a kinematic approach. Earthquake rupture is a dynamic process that can be modeled as such (e.g., Kozdon & Dunham, 2014; Murphy et al., 2016; Ryan et al., 2015). In such models the nonuniform distribution of slip would be part of the dynamic simulation as would be the time history of the rupture process.

A PTHA that includes seismic sources must inherently contain an earthquake forecast. It requires estimated rates of tsunamigenic earthquake from all potential sources that can affect the site of interest. We introduce some basic concepts here and give further details for typical PTHA applications in section 3.2. The magnitude-frequency distribution of earthquakes is well described up to a certain upper magnitude threshold by the *Gutenberg-Richter* relation (Gutenberg & Richter, 1941, 1944), which shows that the log of earthquake frequency follows an inverse linear trend versus magnitude. Thus, the long-term rate of the less frequent, largest events can be extrapolated from the trend of lower magnitude events. However, rates of the highest magnitudes are subject to uncertainty because the linear shape of the distribution breaks down at the

high end, and there typically are not enough observations to constrain it (e.g., Kagan, 2002; Geist & Parsons, 2014). Alternatively, a rough estimate of the long-term earthquake rate can be drawn by considering the ratio of the observed strain rate and strain drop during earthquakes. Since relative rates of motion at plate boundaries are generally faster than those in plate interiors, the same holds for large earthquake recurrence times, which are roughly on the order of $10^2 - 10^3$ years at the boundaries and $10^3 - 10^4$ in plate interiors.

Some earthquake forecasts are built around the concept of time dependence (e.g., Field et al., 2015), where the probability of an earthquake is lowest just after an earthquake releases stress and increases as tectonic motions rebuild stress on the locked fault; this concept is known as elastic rebound (Reid, 1910). Earthquakes generally do not occur regularly in time, though some faults demonstrate quasi-periodicity (Parsons, 2008). There are several factors that complicate recurrence. For example, Shimazaki and Nakata (1980) raised the possibility that earthquakes are either time or slip predictable, with either the time or slip of the next earthquake depends on the slip of the past one. The uncertainty results from time predictability having a stress threshold above which the fault always fails, whereas in slip predictability there is a base stress state to which the fault always returns. Additional uncertainties result from nonuniform tectonic loading, the complexity of the dynamic rupture process that controls the scaling of the parameters describing the earthquake, static and dynamic stress transfer caused by earthquakes on adjacent faults, frictional and material heterogeneities, and viscoelastic mantle response (e.g., Kanamori & Brodsky, 2004; Wang et al., 2012). Earthquake interactions via static stress transfer can lead to tsunamis caused not by a mainshock but instead excited by a triggered aftershock (e.g., Geist & Parsons, 2005).

2.1.1. Tsunami Earthquakes

Tsunami earthquakes comprise a specific subset of tsunamigenic earthquakes, the latter of which are all earthquakes that excite a tsunami. Kanamori (1972) defined a "tsunami earthquake" as "an earthquake that produces a large size tsunami relative to the value of its surface wave magnitude (M_s)." Polet and Kanamori (2016) modified this definition to include only earthquakes that directly cause a regional and/or teleseismic tsunami that is greater in amplitude than would be typically expected from their seismic moment magnitude. This definition excludes seismic events that were followed by tsunamis directly caused by slides or slumps resulting from the original earthquake, as was the case for example for the 1992 Flores earthquake (Hidayat et al., 1995) and the 1998 Papua New Guinea earthquake (Synolakis et al., 2002), as well as events that only very locally caused large tsunamis as a result of, for example, focusing effects due bathymetry (e.g., Satake and Kanamori, 1991) or directivity effects combined with the shape of the coastline (e.g., Dengler et al., 2009). Examples of tsunami earthquakes include the 1896 Sanriku event near the coast of Japan (Hatori, 1967), two events near the Kurile Islands: one in 1963 and the other in 1975 (Fukao, 1979), the 1992 Nicaragua earthquake (Kanamori & Kikuchi, 1993), the Peru earthquake 4 years later (Heinrich et al., 1998), the 2006 Java earthquake (Mori et al., 2007), and the 2010 Mentawai earthquake (Newman et al., 2011). Seno and Hirata (2007) suggest that the great 2004 Sumatra-Andaman earthquake also may have included a tsunami earthquake component, because tsunamis larger than expected from seismic slip occurred, possibly due to slow rupture on the shallow subduction boundary. These characteristics can all likely be related to the location of these events in the shallow-most part of the subduction zone near the trench; furthermore, shoaling amplification of tsunamis sourced in deep water is considerably greater than typical subduction earthquakes that rupture largely beneath the shelf and slope. Similarly, the 2011 Tohoku earthquake could be considered a combination of a tsunami earthquake with an earthquake that produced deeper slip, such as the 869 Jogan earthquake in the same region (Satake et al., 2013).

Tsunami earthquakes appear to have the following characteristics in common: a "slow" source process, as indicated by comparison of various types of seismic magnitude (Pelayo & Wiens, 1992), as well as analysis of source spectra (Polet & Kanamori, 2000), centroid time (Polet & Kanamori, 2000), rupture velocities (e.g., Newman et al., 2011), and energy to moment ratios (Newman & Okal, 1998), a centroid location that is very close to the trench (Polet & Kanamori, 2000) and a preponderance of intraplate aftershocks as compared to interface earthquakes (e.g., Polet & Thio, 2003). These characteristics can all likely be related to the location of these events in the shallow subduction zone near the trench; shoaling amplification of tsunamis sourced in deep water is considerably greater than typical subduction earthquakes that rupture largely beneath the shelf and slope.

Due to the slow character of their source processes, the seismic moment of tsunami earthquakes may be underestimated. However, with the recent inclusion of very long period seismic waveform data in the

calculation of moment magnitude, this effect has likely become insignificant (Duputel et al., 2012; Kanamori & Rivera, 2008). The presence of low velocity sediments (i.e., having a low shear modulus μ) in the very shallow rupture area of tsunami earthquakes may produce greater slip than would be expected for earthquakes of the same magnitude in areas without these sediments (Okal, 1988). Hence, as an example, a high probability for a low shear modulus would imply a larger conditional probability of occurrence of tsunami earthquakes in PTHA modeling.

Splay faulting, thrusts within the accretionary wedge of subduction zones, may also play a significant role in increasing surface deformation (e.g., Fukao, 1979; Park et al., 2002). Additionally, the shallow depth of this slip may produce relatively greater displacement of the ocean floor and therefore excite larger tsunamis, although this may not be significant for the longer period waves that dominate at greater distances (Ward, 2002). Furthermore, at very shallow depths, the dip of the subducting plate is expected to be very small. Since only the product of dip and moment is resolved when inverting Rayleigh waves for source mechanisms of shallow thrust events (Kanamori & Given, 1981), overestimating dip by only a few degrees could lead to underestimating moment and thus slip, by a factor of 2. It has also been suggested that the horizontal deformation of the ocean floor may act to displace great volumes of water (Tanioka & Satake, 1996) but is mainly neglected in tsunami modeling. Finally, the shallow slip and unusual aftershock sequences of tsunami earthquakes may be related to the subduction of bathymetric features that enhance local normal stress (e.g., Scholz & Small, 1997; Tanioka et al., 1997) and/or modify the fluid pressure, introducing variations in the effective basal friction (Seno, 2002).

Many of these factors have been combined in a model for tsunami earthquakes that represents these events as slip at unusually shallow depths that would typically be dominated by creep processes (Scholz, 1990). The existence of localized asperities or patches of unstable friction in a typically stable or conditionally stable region enables their nucleation (Bilek & Lay, 2002). Localized areas of elevated fluid pressure surrounding the asperities may aid in the propagation of the seismic slip by creating zones of nearly zero friction (Seno, 2002). These asperities may be created by the subduction of bathymetric features like seamounts or ridges or by horst-and-graben structures formed at the top of the subducting plate, which would act as buckets for sediment subduction (e.g., Polet & Kanamori, 2000; Tanioka et al., 1997). The stress release on these asperities would be near complete, and any additional unloading of stress on the plate interface due to the rupture may occur mostly through creep, with the relatively large static stress change in the outer rise generating normal faulting aftershocks (Dmowska et al., 1996).

2.2. Landslide Tsunamis

Landslide tsunamis vary greatly in terms of characteristics and coastal impact depending on their sizes and origins. Enormous submarine landslides with volumes of several thousand cubic kilometers may cause extreme tsunamis with regional impact (Masson et al., 2006), with the 8150 year B.P. Storegga Slide (Bondevik et al., 2005; Harbitz, 1992) and the 1929 Grand Banks landslides as the standout examples (Fine et al., 2005). Volcano flank collapses and preceding debris avalanches also represent large-volume sources of tsunamis with potential distant destruction (e.g., Abadie et al., 2012; Løvholt et al., 2008), although supporting field evidence is presently limited (see also section 2.3). However, most landslides involve smaller volumes and produce only local tsunamis (Harbitz et al., 2014).

The initial landslide acceleration, speed, volume, and configuration (length, width, and thickness) govern tsunami generation for subaqueous landslides (Løvholt, Pedersen, et al., 2015). Short tsunami generation time scales (Hammack, 1973; Løvholt, Pedersen, et al., 2015; Watts, 2000) render rapidly accelerating landslides more tsunamigenic, as this restricts destructive interference between wave crests and troughs generated by the frontal and rear parts of the slide, respectively. Conversely, slow landslide evolution, retrogression, and acceleration may render event giant landslides weak tsunami generators (Løvholt et al., 2017). Short time scales are characteristic for submarine slumps such the 1998 Papua New Guinea tsunami (Synolakis et al., 2002; Tappin et al., 2008) and partly explains why this tsunami was so destructive. Submarine landslides are most often subcritical, which means that the landslide moves slower than the leading tsunami wave celerity. The ratio of the landslide speed to the linear hydrostatic wave celerity, defined as the *Froude* number (*Fr*), is a key factor in determining the landslide's tsunamigenic potential. Because the wave celerity increases with water depth, landslides located in shallower waters have larger *Froude* numbers and are more efficient tsunami generators (Harbitz et al., 2014).

Subaerial landslides often hit the water body at high speeds, thus giving rise to a different generation mechanism than what is observed for submerged landslides. For large *Froude* numbers, an impact crater is formed (Fritz et al., 2003), and dispersive waves are generated. The initial height of such tsunamis also primarily depends on the *Froude* number (measured at a characteristic reference water depth) as well as the frontal area of the landslide (e.g., Fritz et al., 2004; Mohammed & Fritz, 2012). Later investigations have attempted to unify the expression for the tsunamigenic power in terms of the impulse product parameter that contains information on various slide parameters including the density of the landslide (e.g., Heller & Spinneken, 2013).

The characteristics in tsunami generation discussed above raises challenges related to landslide-induced PTHA, as the tsunami generation is much more sensitive to the landslide dynamics compared to earthquakes. The landslide dynamics have large epistemic uncertainties, as the material properties that determine the speed and acceleration are often unknown (see also section 4). Further, the *Froude* number effect discussed implies that a small shallow landslide may impose a larger tsunami hazard than a relatively larger slide volume situated in deeper water (Tinti et al., 2001; Okal & Synolakis, 2003; Ward, 2001). Finally, it is often difficult determine if the full landslide volume will be effective, or if the landslide will evolve in a cascading manner with many individual failures (see Haugen et al., 2005).

Deep-water waves from giant submarine landslides are believed to be long and more comparable large earthquake tsunamis (Løvholt et al., 2017; Løvholt, Pedersen, et al., 2015). Yet landslides often give rise to shorter wave components that are not tackled by long-wave models. For instance, impulsive events such as slumps generate shorter waves. Consequently, landslide tsunamis are often dispersive (e.g., Glimsdal et al., 2013; Grilli & Watts, 2005; Løvholt, Pedersen, et al., 2015; Lynett & Liu, 2002).

Landslide tsunami source models (i.e., describing the volumetric landslide emplacement processes) are mostly depth averaged. These vary considerably in complexity. The simplest models assume a translational block or rotational slump (Bondevik et al., 2005; Grilli & Watts, 2005). Landslide flow models include viscous shallow-water type models (e.g., Fine et al., 2005), *Coulomb*-type friction or granular landslide models (e.g., Giachetti et al., 2011; Grilli et al., 2017; Kelfoun, 2011), or layered viscoplastic models including yield strength remolding. The latter may be used also to model retrogressive failure, which may be important for large clay-rich submarine landslides (Haugen et al., 2005; Løvholt et al., 2016, Løvholt, Pedersen, et al., 2015). However, for other and more impulsive types of landslides, only the initial landslide motion influences tsunami generation in a significant way, and the postfailure deformation may be neglected (Grilli and Watts, 2005; Løvholt, Pedersen, et al., 2015). In a probabilistic assessment, this type of behavior may be favorable as it simplifies the source description. There is however, still a long way to go in order to understand when the postfailure can be neglected in (probabilistic) modeling of tsunami generation. For subaerial landslide tsunamis, numerical models based on primitive equation sets (*Euler* or *Navier-Stokes*) are generally needed to model tsunami generation and early propagation in detail (e.g., Abadie et al., 2012; Crosta et al., 2016), although the far-field propagation may be treated by dispersive wave models (e.g., Gylfadottir et al., 2017). For a rigorous review of landslide tsunami models, see Yavari-Ramshe and Ataie-Ashtiani (2016).

Landslides and volcanoes constitute about 15% of all known tsunami sources (Harbitz et al., 2014). Giant submarine landslides involving volumes hundreds to thousands of cubic kilometers are rare, and their occurrence is likely geologically controlled (time intervals may exceed hundred ka), indicating very low return periods for giant submarine landslide tsunamis (e.g., Solheim et al., 2005). However, large-scale debris flows surrounding active volcanoes or submarine landslides initiated by sediment supply in river deltas may have shorter return periods.

While our historical record is too short to be used to determine landslide probability of occurrence, we may estimate probabilities from geomarine field investigations. Statistical landslide data from the Mediterranean Sea indicate that landslide frequency is larger in tectonically active regions, whereas they may reach more extreme volumes in passive margins (Urgeles & Camerlenghi, 2013). Further, a review of submarine landslide occurrence in active margins is found in Kawamura et al. (2014). However, records from submarine geomorphology are biased toward Holocene events (Camerlenghi et al., 2010). Seismic profiles and stratigraphic investigations of the seabed combined with dating techniques can provide information about the recurrence rate in a specific location (Geist & Parsons, 2010). Paleotsunami deposits are also used to determine return periods, even though it is normally challenging to relate the deposits to specific sources.

2.3. Volcanic Causes of Tsunamis

A volcanic tsunami can be generated by mechanisms that include eruptive processes, rapid ground deformation, or flank instability and failure (Paris, 2015). Specific source mechanisms of volcanic tsunamis include underwater explosions, pyroclastic flows, lava, and lahars entering the water, slope failures, volcanic earthquakes, shock waves from large explosions, and caldera subsidence (Begét, 2000; Day, 2015; Latter, 1981; Kienle et al., 1987; Paris, 2015). Volcanic tsunamis are generally characterized by short-period waves, greater dispersion, and limited far-field effects compared to earthquake-generated tsunamis, but the diversity of source mechanisms imply different types of waves (e.g., Choi et al., 2003; Le Méhauté & Wang, 1996; Nomanbhoy & Satake, 1995; Maeno & Imamura, 2011; Ulvrova, Paris, et al., 2016; Watts & Waythomas, 2003; Yokoyama, 1987). Owing to the diversity of complexity of these sources, inclusion of volcanic tsunamis into PTHA developed slowly.

In the historical record, volcanic tsunamis represent a low-frequency hazard (about 5% of all recorded tsunamis) but the largest events are particularly deadly, four of them being ranked in the twenty deadliest volcanic disasters (Auker et al., 2013; Paris, 2015; Paris et al., 2014).

The generation of tsunamis by slope failures on the flanks of volcanoes is not systematically associated to volcanic activity, and the source mechanisms involved are similar to other landslide-induced tsunamis (cf. section 2.2 of this review). For these reasons, volcanic PTHA studies may inherit many of the same challenges as landslide PTHA, but spanning a greater variability of tsunami generation mechanisms than landslides. At the same time, their location is more spatially confined than any possible submarine landslide occurring on a continental slope. There is no specificity, except that volcanic edifices are by their nature unstable due to structural and lithological discontinuities, hydrothermal alteration, magmatic intrusions, and high lava accumulation rates (e.g., Keating & McGuire, 2000). Three kinds of tsunamis generated by volcano flank collapse can be distinguished: (1) Landslides such as the Iliwerung 1979 (Lassa, 2009) or Stromboli 2002 events (Bonaccorso et al., 2003; Tinti et al., 2006) produce local tsunamis only, because their duration (minutes), and moderate size ($<100 \times 10^6$ m) reduce their far-field impact. The 2002 tsunamis at Stromboli volcano had wave run-ups up to 8 m on the coasts of Stromboli Island, but limited effect on the coasts at a distance of more than 200 km from the volcano (Maramai et al., 2005). (2) Large debris avalanches of stratovolcanoes imply volumes >1 km^3 (e.g., the 1741 Oshima-Oshima eruption, Satake & Kato, 2001), and their impact is regional. With a volume of 5 km^3 the collapse of Ritter Island (Papua New Guinea) in 1888 was the largest historical volcano flank failure and the tsunami devastated all the coasts of the Bismarck Sea at distances up to 500 km from the volcano (Ward & Day, 2003). (3) Tsunami conglomerates found at unusually high elevations in Hawaii, the Cape Verde, and Canary Islands represent geological evidence of megatsunamis generated by massive (tens to hundreds of cubic kilometers) flank failures of oceanic shield volcanoes (Moore & Moore, 1984; McMurtry et al., 2004; Pérez Torrado et al., 2006; Paris et al., 2011; Ramalho et al., 2015). Recent studies suggest that these failures are often retrogressive (Hunt et al., 2013; Giachetti et al., 2011) and sometimes coupled with major explosive eruptions (Paris et al., 2017).

As illustrated by controversies regarding the 1883 Krakatau tsunami, determining the cause of tsunamis generated during large caldera-forming eruptions is difficult because different tsunamigenic processes were likely involved: pyroclastic flows and underwater pyroclastic ponds, underwater explosions, earthquakes, slope failures, shock waves, and the caldera collapse itself (Paris, 2015). Experimental and numerical simulations coupled with field data (observations, geology) progressively increased our knowledge of the physical processes and main parameters implied in volcanic tsunamis. Ulvrova, Paris, et al. (2016) demonstrated that the short duration (<10 minutes) required for a caldera subsidence to generate a tsunami is often unrealistic as caldera collapses typically last from few to several hours (e.g., Folch & Marti, 2009; Stix & Kobayashi, 2008). In the case of underwater eruptions, the expansion, rise, and gravitational collapse of the water crater produced by the explosion itself can produce tsunamis, depending on the water depth and energy of explosion (e.g., Le Méhauté & Wang, 1996). The best documented example is the 1996 tsunami in Karymsky Lake (Belousov et al., 2000; Torsvik et al., 2010; Ulvrova et al., 2014).

Small tsunamis were generated by pyroclastic flows during the 1997 and 2003 collapses of lava dome at Montserrat volcano (Pelinovsky et al., 2004). The collapse of large volcanic plumes (*Plinian* eruptions) also produces pyroclastic flows that are potentially tsunamigenic, as happened during the 1883 Krakatau eruption (e.g., Carey et al., 2000). The main parameters controlling the generation of tsunami by a pyroclastic flow are the thickness and bulk density of the dense part of the flow, its preservation or disaggregation underwater,

the angle of incidence, and the discharge rate at the shoreline (Maeno & Imamura, 2011; Watts & Waythomas, 2003). However, mechanisms of interaction between pyroclastic flow and water as well as the conditions required to generate a tsunami remain partly elusive because of the lack of observational and experimental data (Allen et al., 2011; Freundt, 2003; Legros & Druitt, 2000). The 15–30 m high waves observed in the Sunda Strait during the 1883 Krakatau eruption were triggered by pyroclastic flows, but the worldwide tsunami recorded by the tide gauges was most probably the result of phase coupling between shock waves (explosions) and long-period sea waves (Choi et al., 2003; Yokoyama, 1987).

Earthquakes preceding or accompanying volcanic eruptions can also generate tsunamis. However, only volcanotectonic earthquakes (i.e., the so-called high-frequency (HF) volcanic earthquakes resulting from the accumulation of stress during magma emplacement) can involve ground deformation large enough to generate tsunamis of small magnitude (Paris, 2015). They are often characterized by seismic swarms at shallow depth (<10 km), with magnitudes typically lower than $M_s = 6$ (Begét, 2000; Latter, 1981). However, larger-magnitude tectonic earthquakes along volcanic flanks, such as the 1975 Kalapana Hawaii earthquake, can generate regional tsunamis (Ma et al., 1999).

A preliminary framework for the PTHA of tsunamis generated by submarine volcanic eruptions has been developed by Ulvrova, Selva, et al. (2016) using probability for eruptions of different size, a parameterization of the initial surface displacement as a function of explosion energy for a given depth, and a numerical wave propagation model for each source. Tsunamis generated from submarine part of the Campi Flegrei caldera, Italy, are presented as an example. Maretzki et al. (2007) and Grilli et al. (2009) included a possible collapse of the Cumbre Vieja volcano in the Canary Islands as a tsunami source in their PTHA for the U.S. northeast coast. Further research in developing PTHA for volcanic tsunamis is needed: similar approaches could be extended to the other volcanic phenomena able to generate tsunamis.

2.4. Meteotsunamis

High-energy atmospheric disturbances (thunderstorms, tropical and extra-tropical storms, atmospheric pressure jumps, frontal passages, gales, squalls, tornados, atmospheric convection cells, jet streams, and atmospheric gravity waves) are recognized to produce significant sea level response over a broad frequency band (Rabinovich & Monserrat, 1998). Atmospheric pressure changes can force the ocean to respond through the generation of small sea level oscillations. However, if resonance occurs between the atmospheric forcing and the ocean then the small oscillations become amplified leading to significant waves with periods in the range of 2 minutes to 2 hours (Pattiaratchi & Wijeratne, 2015). Because of their generation origin and characteristics, the term "meteorological tsunamis" or "meteotsunamis" was introduced to define this kind of waves (Defant, 1961; Monserrat et al., 2006). Common types of resonance leading to meteotsunami's generation are the *Proudman* resonance (Proudman, 1929) and the *Greenspan* resonance (Greenspan, 1956) (the former occurring if the translational speed U of the atmospheric disturbance is equal or nearly equal to the phase speed c of the long wave and the latter if the alongshore component of the atmospheric disturbance velocity is equal to the phase speed of an edge wave generated along the coastlines). During the resonance process, the atmospheric disturbances moving above the ocean surface can give rise to significant long ocean waves by continuously pumping additional energy into these waves. The energetic ocean waves arriving at the coast (bay, inlet, or harbor) can become destructive due to the combination of other amplification mechanisms, including shoaling and local resonance effects (also applicable to tsunamis of other origins). Tanaka et al. (2014) showed that the incident meteotsunami waves became more amplified due to the harbor resonance in Sakutsu Bay, Japan. Anderson et al. (2015) highlighted the dangerous effects of meteotsunami wave reflection and energy focusing in the enclosed basin of the Lake Erie, U.S.

Even moderate meteotsunamis can have damaging impacts on boats and ships in harbors and small embayments (Thomson et al., 2009). Meteotsunami hazard is increased by additional sources of energy: (1) the wind stress (Bechle & Wu, 2014; De Jong & Battjes, 2004; Dragani et al., 2014; Pellikka et al., 2014; Whitmore & Knight, 2014), (2) the local high tide level (Horvath & Vilibic, 2014), and (3) a higher water level from a storm surge or high mean seasonal sea level (Pattiaratchi & Wijeratne, 2014).

There are regions where the temporal and spatial occurrences of the meteotsunamis are higher compared to the seismically induced tsunamis because the combination of the resonant factors is more common (Bechle et al., 2016; Wang et al., 1987). For this reason recent studies in the Great Lakes and the Mediterranean Sea aimed to forecast destructive events and support early warning systems (Anderson et al., 2015; Vilibić et al., 2016). Renault et al. (2011) used a coupled atmosphere-ocean modeling system to reproduce the whole

process, from atmospheric source to meteotsunami ocean dynamics: with further improvements, this system may eventually be used in operational forecasting of a meteotsunami events. Šepić, Vilibić, et al. (2016) constructed an atmospheric index to evaluate the meteotsunamis probability of occurrence with critical meteorological synoptic conditions above the Balearic Islands for a possible warning system. A framework for the PTHA of meteotsunamis has been introduced by Geist et al. (2014) in the northeast U.S. In its general form, the analysis aggregates the hazard from different possible sources (squall lines, atmospheric gravity waves, etc.) and uses a numerical wave propagation model for each source and parameter combination. This is similar to both probabilistic tsunami hazard analysis (PTHA) and probabilistic storm surge forecasting that develops hazard assessments from parameterization and sampling of source processes. The annual rate of exceedance as a function of the maximum event amplitude and the calculated number of meteotsunamis above a certain threshold is compared to the number of historically observed meteotsunamis and their occurrence in time.

In other coastal zones estimating the recurrence interval of meteotsunamis using continuous records or historical catalogs remains difficult and further developments can be introduced to quantify the likelihood of meteotsunami occurrence in a PTHA framework.

2.5. Asteroid Impacts

One framework for the PTHA for asteroid impacts is given by Ward and Asphaug (2000). The asteroid density, ratios, and impact velocity are linked to energy considerations and scaling of the generated craters. The initial cavity generates the tsunami waves and attenuation relations, based on a large set of simulations, determine the tsunami amplitude as a function of the distance. By coupling the tsunami amplitude/distance information with the statistics of asteroid impacts, the probabilistic hazard is found by integrating contribution over all impactor sizes and locations. The probabilistic hazard is finally given as the likelihood of impact of tsunamis for a given tsunami height in 1,000 years.

According to Earth Impact Database (Earth Impact Database (EID), 2017), there are today 190 known impacts on Earth. Only a few are found in the sea, even though the sea covers about two thirds of the surface of the Earth. The underreported number of impacts in sea may be due to the following: (1) it is easier to discover impacts on land than in the sea, (2) impacts of smaller bodies into deep sea may not create craters, and (3) due to plate tectonics, the sea bed is younger than the land continents and older impact craters have disappeared.

Oceanic impacts of asteroids and comets may produce huge waves that remain strongly nonlinear during propagation over hundreds or thousands of kilometers (Wünnemann & Weiss, 2015). Also, dispersive effects remain important for a long period of time after the generation (Glimsdal et al., 2007). Tsunamis from asteroid impacts may behave similarly to subaerial landslide tsunamis during generation and initial propagation (see section 2.2), but nonlinearity will typically be important farther away from the source for asteroid impact tsunamis. To this end, one feature that needs to be captured is undular bores. Glimsdal et al. (2007) demonstrated that such bores were formed for example for the Mjølnir asteroid impact.

We may categorize impact tsunamis into three classes. The first class comprises asteroids having diameter much less than the water depth (diameter-to-depth ratio less than 0.1, say). These impactors will produce a surface cavity in the sea with rim elevations (Artemieva & Shuvalov, 2002; Gault & Sonett, 1982; Gisler et al., 2011; Wünnemann et al., 2010). In this case the waves will be shorter than the water depth and therefore highly dispersive. An example is the Pliocene Eltanin impact where no clearly pronounced seabed crater was formed during the impact and the shock wave was not strong enough to melt the seabed (Gersonde et al., 1997; Shuvalov & Trubetskaya, 2007). During impact, the seabed was dry and the tsunami surface elevation was modeled to be about 1 km at a distance of 20 km from the impact center (Shuvalov, 2003).

The second class includes large objects that lead to crater formation and a temporarily dry seabed. Examples are found in simulations of the 10 km diameter bolide that formed the Chicxulub crater in the Gulf of Mexico 65 Ma ago (Matsui et al., 2002) and the Mjølnir impact in the Barents Sea about 142 Ma ago (Glimsdal et al., 2007). Here the tsunami generation is characterized by intense wave breaking and resurgence into the seabed crater. Given that the crater radius is large compared to the water depth, long waves with large amplitudes can be formed. Subsequently, these waves will behave very differently from both earthquake and deep-water impact tsunamis. These violent tsunamis may lead to strong mixing and sediment transport that may change the environment with drastic consequences for marine life even when propagating across the ocean.

Airburst asteroids represent the third class, recently investigated by Gisler et al. (2017) and Patchett et al. (2017). They pointed out that (1) airbursts happen when the asteroids interaction with the atmosphere causes

it to explode before impacting the surface provoking the transition of kinetic energy from the asteroid into the water to be more coherent and changing the likelihood of tsunami generation and (2) a more oblique angle increases the amount of time the asteroid spends in the atmosphere and therefore increases the amount of ablation opportunity before the impact (possibly making a smaller impactor) which could possibly push the water in a more coherent direction increasing the likelihood of tsunami generation.

For the study of impact and tsunami generation, models that are based on the primitive equations (e.g., of *Navier-Stokes* type models) are applicable. Such multiphysics hydrocodes must handle several different phases (air, water, and Earth crust), free surface, thermodynamics, and turbulence.

PTHA considering asteroid impacts are not produced on global or regional scales. Recently Rumpf et al. (2017) evaluated asteroid impact effects in a probabilistic hazard analysis considering both impact scenarios over land and water masses. The analysis covered a wide range of possible impact conditions in terms of impact speed, angle, and size concluding there is a significant difference in expected loss for airburst and surface impacts. Moreover, the average impact dangerous effects over land are an order of magnitude more dangerous than one over water. Tsunamis, which were the most significant effect for water impacts, were less important globally because the initial wave height restriction due to the sea depth and wave height attenuation over distance.

2.6. Tsunami Modeling

In PTHA studies, tsunami hazard is expressed by "hazard metrics" that provide a quantitative estimate of tsunami intensity, such as maximum values of tsunami run-up, inundation depth, or current speed and these metrics might be summarized on a map of the region. Due to the infrequent nature of tsunamis, historical data on these metrics are very sparse and irregular. The few available events are just a small sample of thousands or millions of possible tsunami scenarios. Lack of empirical observations makes numerical modeling of tsunami generation and propagation the main tool to establish links between source parameters and hazard metrics (compared to Ground Motion Prediction Equations, GMPEs, in PSHA), and software used to model the generation and propagation of a tsunami from its source to the target area of interest becomes a critical component of PTHA assessment. This software must produce an accurate representation of realistic tsunami behavior, by solving a system of partial differential equations. Except for very idealized situations, these equations must be solved approximately, typically by discretizing the equations on a finite grid and using standard numerical techniques such as finite difference, finite element, or finite volume methods to advance the solution in time. Computational efficiency is particularly important in PTHA applications, where a large number of tsunami simulations may be required. Numerous tsunami models have been developed, and we will not attempt to cite them all in this summary. Benchmarking and validation of models against exact solutions for simplified problems, laboratory experiments, and/or past tsunami events is an important aspect of developing or selecting a model (e.g., Horrillo et al., 2014; Pedersen, 2008; Synolakis et al., 2008).

The first question to address is what mathematical model of the fluid dynamics should be used, that is, what system of partial differential equations should be discretized. The answer will depend on the particular application. The three-dimensional *Navier-Stokes* equations with a free surface could provide a very accurate model. However, in most cases this is computationally much too costly, and for most tsunami applications the vertical structure of the flow does not need to be modeled directly. Instead, two-dimensional depth-averaged systems of equations can generally be used to obtain sufficiently accurate results with far less computing time than would be needed to solve the three-dimensional equations (e.g., Kowalik & Murty, 1993). The simplest such approximation is the long-wave or shallow-water equations (also called the *Saint Venant* equations), derived by assuming that the waves of interest have a long wavelength relative to the depth of the fluid. These equations are a good approximation for tsunamis generated by subduction zone earthquakes, since the seafloor deformation over a large region generally leads to tsunamis with a wavelength of several tens of kilometers or more, compared to the average ocean depth of 4 km. For propagation in the open ocean linearized shallow-water equations can be used, since the tsunami amplitude is small relative to the depth. In very shallow coastal parts as well as by simulation of wave inundation, full nonlinear shallow-water equations must be solved.

However, there are situations in which the shallow-water equations are inadequate (Kirby et al., 2013), in particular for short wavelength tsunamis that arise from phenomena that are more localized than subduction zone earthquakes, such as landslides or asteroid impacts (e.g., Glimsdal et al., 2013). More complicated two-dimensional depth-averaged equations can be derived from the three-dimensional *Navier-Stokes*

equations by making different assumptions on the vertical structure and keeping additional terms in asymptotic expansions. This leads to the appearance of higher-order derivative terms in the resulting partial differential equations and so must generally be solved using implicit time-stepping algorithms. As a result they are more computationally demanding than the shallow-water equations, although still much cheaper than full three-dimensional simulations. Many different sets of depth-averaged dispersive equations and layered nonhydrostatic models have been proposed and studied as better approximations for short wavelength tsunamis, (e.g., Bonneton et al., 2011; Fuhrman & Madsen, 2009; Kennedy et al., 2000; Kim et al., 2009; Lynett et al., 2002; Løvholt et al., 2008; Ma et al., 2012; Nwogu, 1993; Shi et al., 2012).

While the long-wave assumptions discussed in the preceding paragraphs are most often appropriate for modeling tsunami propagation, short scales and rapid source motion may lead to nonhydrostatic effect in the generation phase. For sources with very long depth perturbations, such as large earthquakes with uniform slip, it may be sufficient to copy the modeled seabed displacement to the sea surface. However, for shorter sources the water column effectively works as a low-pass filter: short wavelength perturbations will be suppressed. The filtering effect of the water column increases with depth and wave number (Kajiura, 1963; Satake, 2007; Nosov & Kolesov, 2011). Thus, horizontal wavelengths of displacement less than 3 times the water depth are effectively attenuated during tsunami generation. For subaqueous landslides, short wavelengths may also be introduced due to rapid accelerations, and in this case low-pass filters are also needed to convey landslide-induced seabed changes into local tsunami generation (Løvholt, Pedersen, et al., 2015). While one filtering operation may be sufficient for earthquakes (when assumed instantaneous), the filtering must be conducted for different steps of landslide advance.

Early approaches to tsunami hazard assessment were often based on approximating the solution at offshore locations, using reflecting boundary conditions at a fixed isobaths (typically, between 10 and 100 m), rather than attempting to directly model the inundation on shore. From the offshore wave height, various empirical models can be used to estimate the onshore run-up. One simple approach is to assume amplification due to solitary shaped wave (e.g., Synolakis, 1987, 1991). Another method is to use *Green*'s law to account for shoaling up to a reference water depth and use this as a proxy for the run-up height. Recently, Løvholt et al. (2012) proposed a method that combines computationally effective long-wave propagation models with nearshore 1-D wave simulations at a much finer numerical grid using linear theory. This method can incorporate different wave periods and polarities but is still a very rough method that inherit large uncertainties. Nevertheless, these approaches are still widely used for PTHA in cases when it is impractical or impossible to perform a large number of fine-scale 2-D simulations at all coastal locations of interest (see, e.g., Geist & Parsons, 2006; Sorensen et al., 2012; Thio et al., 2007).

The detailed PTHA analysis of a specific coastal community is usually performed using high-resolution inundation modeling (González et al., 2009; Lorito et al., 2015; Omira et al., 2015), at least close to the target area (e.g., 10 m resolution or finer depending on the type of application). With depth-averaged equations, one of the variables is the depth of the fluid at each point, and inundation is often modeled by allowing the depth to be zero in some grid cells (dry land) and nonzero elsewhere, with sophisticated techniques often used to advance the solution near the wet-dry interface, allowing cells to transition between wet and dry (e.g., LeVeque et al., 2011; Titov & Synolakis, 1995).

In order to apply high-resolution inundation modeling for detailed PTHA, the following conditions should be met: (1) The availability of high-resolution and precise bathymetry and topography data for the target area, or else inundation results, could be inaccurate and potentially misleading (Behrens et al., 2009; Griffin et al., 2015). Even with highly accurate elevation data, models based on digital terrain models (DTM), where surface features such as trees and buildings are removed from the elevation model, may give significantly larger inundation extents compared with digital surface models (DSM) that include these features in the elevation model. Ignoring surface features may result in overestimates of inundation extent (Kaiser et al., 2011) while including all features in the elevation model may underestimate inundation (Griffin et al., 2015). Griffin et al. (2015) found the use of DTM combined with appropriate choices of *Manning*'s roughness coefficients best reproduced observed inundation extent. Wang et al. (2017) found that maximum flow depths and speeds in models where buildings were explicitly included in the elevation model could be 50% higher compared with models that used *Manning*'s roughness coefficients to account for buildings; however, the inundation extent was similar. Therefore, there is still a need for further research on how best to quantify surface roughness features (Griffin et al., 2015; Kaiser et al., 2011). To this end, note also that there are theoretical limitations of the

Manning's friction approach for modeling tsunami inundation (see, e.g., Antuono et al., 2012). It is recommended that sensitivity analysis to elevation data, and the method used to include surface features should be undertaken to understand potential uncertainties before employed inundation modeling (Behrens et al., 2009). (2) The parameterization of the selected scenarios should be appropriate and their discretization fine enough to capture uncertainty in the source, including the range of magnitudes, source zone, and rupture complexity (slip distributions). For local-scale studies the number of possible tsunami sources, and hence inundation scenarios, can usually be restricted to be computationally affordable for simulation on fine grids while still properly representing all significant sources for the required range of probability of exceedances (González et al., 2009). Deaggregation analysis of regional or global-scale PTHA can be used to inform the selection of scenarios. Consideration of rupture complexity, which has a first-order effect on flow depth and inundation extent for local tsunami sources, can be undertaken through brute force simulation of many scenarios (e.g., Griffin et al., 2016; Muhammad et al., 2016). Alternatively computational effort can be saved through application of magnitude corrections to uniform slip models to account for uncertainty in the slip distribution and avoid underestimating the potential inundation extent (Mueller et al., 2015). Nevertheless, methods for assessing the probability of alternative slip distributions for incorporation into PTHA remains an area of research (Murphy et al., 2016).

It is not possible to model the entire ocean at the fine scale needed for an inundation study, nor is it necessary. In the ocean, where the wavelength is long, it may be possible to use a grid resolution of several kilometers. Tsunami software must provide the ability to use much finer computational grids in some region than in others, either by continuously varying cell sizes (e.g., Harig et al., 2008) or with nested levels of grids at different resolutions. Adaptive mesh refinement is sometimes used to dynamically adjust the grids in order to efficiently follow a propagating tsunami (e.g., LeVeque et al., 2011; Popinet, 2011).

3. PTHA Methodology

The purpose of a PTHA is to find the probability that a certain tsunami hazard metric, such as maximum wave amplitude, is exceeded. The most basic outcome of such an analysis is typically expressed as a hazard curve, which shows exceedance level of the hazard metric as a function of probability, with the probability often expressed as a rate of exceedance per year. The actual hazard metric can be chosen depending on the problem to be addressed. The most common metric is maximum wave amplitude, but for inundation in subduction zone environments, where ground uplift and subsidence are integral parts of the inundation process, flow depth is a more appropriate parameter. In ports and harbors, maximum currents may be more useful.

In the simplest case, consider a PTHA where almost all aleatory and epistemic uncertainties (defined in section 4) are ignored. Suppose the PTHA includes a finite set of hypothetical tsunamigenic events $e \in E$, with each individual event e recurring randomly in time and independently of all other events (i.e., as a *Poisson* process), with a known mean annual rate $\lambda(e)$ (events/year). For example, E could be a set of tsunamigenic earthquake scenarios representing all possible earthquakes affecting the site of interest, and for each earthquake event e, the mean annual rate $\lambda(e)$ might be derived based on a regional earthquake magnitude-frequency relation (see section 3.2). Suppose further that for all $e \in E$, the (spatially variable) tsunami intensity parameter $I(x|e)$ is known at a set of locations $x \in X$. For example, $I(x|e)$ might be taken as the peak wave height at location x due to the tsunami generated by event e. In practice, tsunami intensity measures are often derived by numerical modeling tsunami propagation for all events $e \in E$ and storing the results at a set of points $x \in X$ (see section 2.6), although statistical approaches can also be used (see section 3.3; Geist & Parsons, 2016). Under these conditions, the tsunami hazard curve at any location x describes the mean annual rate λ (events/year) at which *any* tsunami event occurs at location x with intensity $I(x)$ greater than some threshold I_0:

$$\lambda\left(I(x) > I_0\right) = \sum_{e \in E} \left(\mathbb{I}_{I(x|e) > I_0}\, \lambda(e)\right) \tag{2}$$

Here $\mathbb{I}_{I(x|e) > I_0}$ is an indicator function which takes the value 1 if $I(x|e) > I_0$, and zero otherwise. Equation (2) should be considered as a hazard curve specific to location x, which maps values of the tsunami intensity I_0 to their rate of exceedance λ (Figure 2).

The rate of exceedance is often transformed into other equivalent measures to aid its interpretation. For example, it may be converted into the probability of exceedance once or more in a given time period

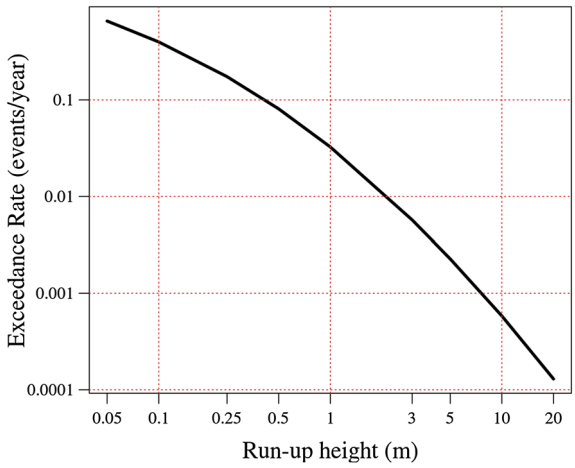

Figure 2. A hazard curve offshore of Sydney (Davies et al., 2017).

(with duration ΔT in years), denoted $P\left(I(x) > I_0, \Delta T\right)$). This is computed as

$$P\left(I(x) > I_0, \Delta T\right) = 1 - \exp\left(-\lambda\left(I(x) > I_0\right)\Delta T\right) \quad (3)$$

Alternatively, the rate of exceedance may be converted into the mean time between events (i.e., the return period R_p in years):

$$R_p\left(I(x) > I_0\right) = \frac{1}{\lambda\left(I(x) > I_0\right)} \quad (4)$$

Equations (2)–(4) may also be inverted to find the intensity value I_0 associated with a given rate/probability/return period. Often hazard maps rely on this to depict spatial variations in the tsunami intensity parameter for a fixed rate of exceedance (Figure 3). Probability maps are also sometimes used, which represent the rate of exceedance or the average return period for a fixed value of the tsunami intensity parameter (e.g., the coastal distribution of the return periods for 1 m tsunami height, Figure 4). In contrast, hazard curves depict the relationship between the tsunami intensity value I_0 and its return period, for a specific location x.

3.1. Source Parameters

Traditionally, all of the different tsunamigenic sources described in sections 2.1 through 2.5—earthquakes, landslides, volcanoes, atmospheric disturbances, and asteroid impacts—are treated separately when doing PTHA assessments. Among these five source types, earthquakes are the more frequent tsunami triggers and are the type whose source parameters we discuss here. Fortunately, for a seismic-based PTHA (SPTHA) earthquake sources are also the most studied and constrained by instrumental observations regarding their annual rates (historical seismicity, *Gutenberg-Richter* distribution for magnitudes) as well as source parameters (rupture locations, focal mechanisms, etc.). However, this also brings a computational challenge: despite this knowledge, we still have to deal with huge variability in earthquake source parameters that need to be explored in a comprehensive PTHA study.

In particular, this variability includes spatiotemporal distribution of tsunamigenic seismicity as well as variability in local earthquake source parameters. The latter implies fault orientation (strike and dip angles), dimensions, faulting style (rake or slip angle), and slip distribution of potential ruptures. Not all of these parameters are fully independent. Thus, rupture dimensions and mean slip are generally correlated with the

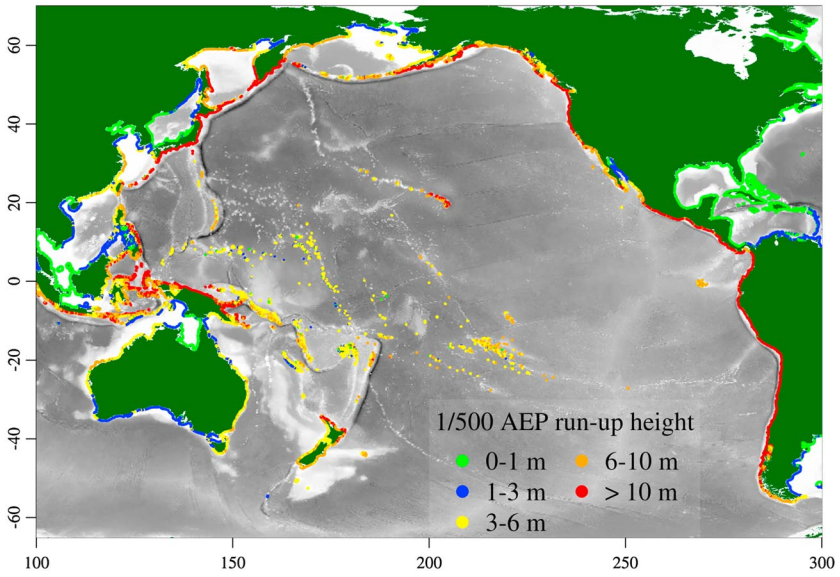

Figure 3. A hazard map showing the run-up height with 1/500 annual exceedence probability (AEP). The wave height points are located in ~100 m depth, but the values at the points refer to onshore run-up height. For individual scenarios, the onshore run-up height is derived from the offshore wave time series using "crude theory combined with statistical adjustments" (details in Davies et al. (2017)).

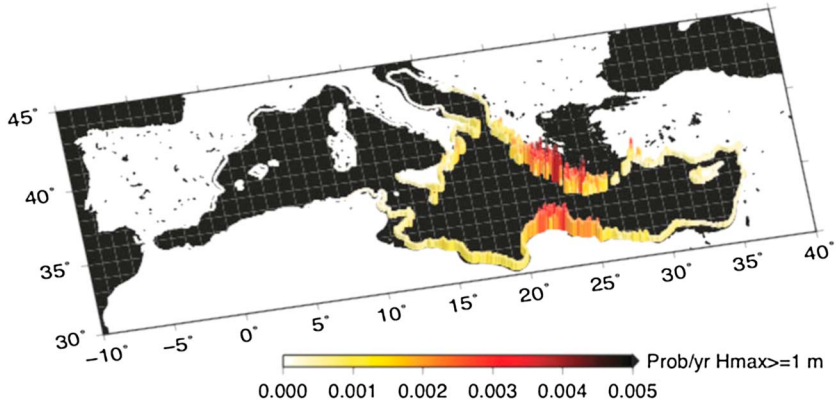

Figure 4. A probability map showing the annual exceedance probability (AEP) for offshore maximum wave height of 1 m, due to earthquakes on the western portion of the Hellenic Arc; tsunamis are simulated at the 50 m isobath and extrapolated to 1 m depth with the *Green*'s law (modified after Lorito et al., 2015 see details therein).

earthquake magnitude (e.g., Blaser et al., 2010; Murotani et al., 2013; Strasser et al., 2010; Wells & Coppersmith, 1994). Consequently, the magnitude is often adopted as a primary parameter which can be, for example, sampled directly from the *Gutenberg-Richter* distribution, whereas rupture size and overall slip are later estimated using scaling laws and the relation between seismic moment and slip:

$$M_0 = \mu \cdot D \cdot L \cdot W \tag{5}$$

here M_0 is seismic moment, D is mean slip, L and W are fault dimensions, and μ stands for rigidity (or shear modulus) of the ruptured media.

However, caution is needed to avoid systematic bias of PTHA results in using this approach. The rigidity parameter μ depends on the rock type and depth and varies in a wide range up to ∼30–75 GPa for intact rocks. Bilek and Lay (2002) reported rigidity values as low as ∼1 GPa at a very shallow depths for the Alaska-Aleutian seismogenic subduction zone. Because for a given seismic moment there is a trade-off between rigidity and slip, not accounting for spatial rigidity variations in rigidity in depth and space, which are typically poorly constrained, may lead to a systematic bias in PTHA results.

Nowadays, SPTHA studies are mostly carried out within a computational framework, that is, source parameters and hazard metric at a target site are linked via numerical simulation of tsunami generation and propagation described in the previous sections. One could say that in SPTHA, numerical simulations substitute empirical GMPEs used in PSHA. Not all of the above listed seismic source parameters are equally important for every SPTHA assessment. Each particular study tries to find an optimal balance between the necessity to incorporate all relevant sources, on one hand, and computational costs, on another hand. The latter may rapidly become computationally unaffordable, especially when using extended PTHA metrics such as probabilistic inundation maps at target sites.

Identifying the range of relevant seismic sources and the way of their discretization is mandatory for every SPTHA study. In regions where long-term tsunami hazard is dominated by subduction sources, variability of focal mechanisms as well as rupture location and orientation can be significantly reduced according to the seismotectonic model of the corresponding subduction zone (Burbidge et al., 2008; González et al., 2009; Rikitake & Aida, 1988). Geodynamic plate convergent rates may also be used to constrain temporal parametrization of earthquake occurrence rates (e.g., Bird & Kagan, 2004).

Subduction zones account for the vast majority of tsunamigenic earthquakes worldwide. At the same time, they are relatively easy to geometrically parameterize on a large scale. This one reason is why global-scale PTHA studies are, basically, restricted to the subduction sources with coarse-scale discretization (Davies et al., 2017; Løvholt et al., 2012, 2014).

Alternatively, in a smaller region dominated by a large number of crustal faults with different orientations and focal mechanisms like the Mediterranean Sea, source parameters exhibit large natural variability. Tsunamigenic seismicity cannot be reduced to a limited number of representative scenarios in this case. Sampling within the broad range of source parameters is unavoidable resulting in hundreds of thousands of tsunami propagation scenarios (Selva et al., 2016; Sørensen et al., 2012).

Following the challenge to compute PTHA inundation maps while exploring many thousands of potential sources, several authors have used a two-step approach (Lorito et al., 2015; Thio et al., 2010, 2017). In the first step, offshore exceedance amplitudes are computed using a very efficient *Green*'s function summation method, which takes advantage of the linear behavior of waves in deeper water and allows the integration over thousands of events. Aleatory variability terms that are not included in the source characterization (e.g., the error in the propagation models, tides) can be included at this stage as well (Thio et al., 2010). In the second stage, fully nonlinear local inundation computations are carried out for a select number of scenarios that conform to the offshore exceedance amplitudes. The scenarios are selected on the basis of the source disaggregation for the target area by clustering all sources that would produce similar wave height profiles along a sufficiently extended set of control points in front of the target coast. This is based on the assumption that similar effects for a specific target site will correspond to a roughly similar inundation pattern. Lorito et al. (2015) perform a hierarchical cluster analysis on the set of sources which passed the first stage so that one single simulation for each cluster may be chosen as representative of any source belonging to it. The one representative event source for each cluster is defined as the one which has the closest profile to the cluster centroid, that is, the one that has the minimum distance from the average profile in the cluster. In practice, only one source for each cluster will be used for inundation modeling. The probability of occurrence for the entire set of scenarios belonging to a cluster is then attributed to the relative representative source event scenario.

3.2. Source Probability

Specification of source probabilities in PTHA involves estimating the rate of occurrence for each source type in each region as well as determining the optimal size distribution. Again, using earthquakes sources as an example, the *Gutenberg-Richter* magnitude-frequency relation for a given region supplies both the occurrence rate and size distribution

$$\log N(m) = a - bm \tag{6}$$

where $N(m)$ is the number of earthquakes greater than or equal to m and the two parameters include the activity or occurrence rate (a value) and power law magnitude exponent (b value). The underlying seismic moment distribution for the *Gutenberg-Richter* relation is the *Pareto* distribution (Kagan, 2002) specified by $1 - P(M) = (M_t/M)^{\beta}$ where P is the cumulative distribution function, M_t is the minimum seismic moment threshold, and shape parameter $\beta = 2/3b$.

Several probability models have been used to specify how an earthquake size distribution is limited at large seismic moment. For example, a *Pareto* distribution can be either truncated or tapered in either the density or cumulative form (Kagan, 2002). The truncated *Pareto* distributions are specified by a "hard" maximum seismic moment, whereas the tapered *Pareto* distributions are specified by a "soft" corner seismic moment. Procedures to estimate these parameters are given in Kagan (2002). Other seismic moment distribution models are based on extreme value theory (e.g., Pisarenko et al., 2014).

Although the *Gutenberg-Richter* relationship provides a good description for many areas in the world, for some individual fault sources the number of large earthquakes is strongly underpredicted when trying to extrapolate from the smaller magnitude earthquake distribution. Alternative distributions that emphasize the larger-magnitude earthquakes are the Characteristic earthquake distribution (Schwartz & Coppersmith, 1984), which is a combination of *Gutenberg-Richter* for the smaller magnitudes and an elevated rate at the larger-magnitude end, and the Maximum magnitude model (e.g., Wesnousky, 1986) where the earthquake magnitude (*Gaussian*) distribution is concentrated around a Maximum magnitude that is based on magnitude-area scaling relations (e.g., Strasser et al., 2010).

The rate parameter for seismic sources can be determined empirically from catalog data, although records are typically short or lack detail. Alternatively, rates can be estimated from a seismic moment balance across a plate boundary or fault system. This exercise is similar to requirements of PSHA (Cornell, 1968) and requires an estimation of fault slip rates, their seismogenic areas, a seismic coupling coefficient, and a magnitude frequency distribution shape. Ideally, the slip rate and seismic coupling coefficient are known for faults used in PTHA. However, direct slip rate measures for offshore faults are difficult to acquire. Geodetic strain rates or known plate convergence rates can serve as proxies for megathrust slip rates at major subduction zones (e.g., Bird & Kagan, 2004), though the proportion of outer rise and splay fault earthquakes add complications. Modeling tectonic deformation forced by relative plate motions can yield more detailed estimates of slip rates along an irregularly shaped subduction zone and related faults (e.g., Parsons & Geist, 2009). The relationship between occurrence rate $\lambda(e)$, seismic moment rate, and parameters of the modified *Pareto* distributions

is given by Kagan (2002). (Davies et al., 2017) explain how uncertainties in the rate parameter are incorporated, and how source zones with nonuniform dimensions are considered in PTHA.

For nonseismic tsunami sources, a size distribution other than a modified form of the *Pareto* distribution may be optimal. For example, whereas in some cases submarine landslide sizes (volumes and areas) follow a *Pareto* distribution (Lane, Mountjoy, Power, & Popinet, 2016; ten Brink et al., 2006), in other cases a lognormal distribution is a better fit (Chaytor et al., 2009). For landslide sources, ten Brink et al. (2016) have developed empirical relationships linking occurrence rates to earthquake frequency and sedimentation rates. Care must be taken in estimating the occurrence rate parameter $\lambda(e)$ directly where there are few data and/or where the observations are subject to significant uncertainty, such as dating geologic event horizons. Several studies have indicated that age uncertainty and open time intervals (i.e., before the first event and after the last) affect rate estimates (e.g., Parsons, 2008a). *Bayesian* and *Monte Carlo* methods are most often used to estimate occurrence rate and its uncertainty (Geist et al., 2013; Nomura et al., 2011; Parsons, 2008a, 2012; Savage, 1994).

3.3. Empirical Methods

Empirical tsunami data such as tide gauge, paleotsunami deposits, or eye witness observations can be used to test PTHA calculations (e.g., Horspool et al., 2014), or to develop a tsunami hazard estimate directly, in the absence of a comprehensive PTHA study. Such empirical estimates might provide an initial prior for PTHA that encompasses very large areas, and that can be updated with numerical modeling or other information as it becomes available. Most empirical observations are drawn from specific locations (particularly in the case of tide gauges) and may thus be strongly influenced by local topography/bathymetry. Thus, extrapolation to other sites across even small ($\leq$1 km) distances might overestimate or underestimate wave height or run-up. However, empirical data have been shown to provide information in PTHA that numerical modeling calculations do not, particularly in regional settings where it can difficult to account for every possible tsunami source (e.g., Geist & Parsons, 2006, Parsons & Geist, 2009). Additionally in PSHA, empirical data are often given strong weighting compared with model-derived results (see, e.g., Field et al., 2015).

Notwithstanding the sparsity of tsunami data mentioned in section 2.6, at some tide gauge stations, there is an instrumental catalog of tsunami events with sufficient length to develop empirical estimation of tsunami probability. From the station catalog data, a size distribution can be fit and, assuming the data follow a *Poisson process*, a hazard curve can be estimated. Empirical analysis can also be expanded to use additional data to assess tsunami hazards in broad regions (Fernandez et al., 2000; Leonard et al., 2014; Kulikov et al., 2005). However, with empirical tsunami analysis there is the need to account for effects of catalog completeness and undersampling.

For a given station or local event catalog, an empirical distribution function (EDF) can be obtained. A probability model can be fit to the data, using parameter estimation techniques such as maximum likelihood or method of moments (e.g., Kagan, 2002; Kagan & Schoenberg, 2001). If the distribution were correct, the EDF would converge to the model distribution as the number of events approaches infinity. The optimal model for most tide gauge station catalogs, specifically those in the Pacific, appears to be a modified form of a *Pareto* distribution (see section 3.2). Both truncated (Burroughs & Tebbens, 2005; Kim & Choi, 2012) and tapered (Geist & Parsons, 2014) modifications of the *Pareto* distribution have been used in past studies. An exponential size distribution is also indicated for tsunamis by Kaistrenko (2011). Alternate probability models can be evaluated by the Akaike Information Criterion (AIC), which measures goodness of fit (e.g., Utsu, 1999). The model with the smaller AIC is considered the better fit.

As indicated in Geist and Parsons (2006), it is critical to account for the statistical effects of catalog completeness and undersampling of large events when performing an empirical analysis. Geist and Parsons (2011) indicate that the starting year that the global tsunami catalog can be considered completely depends on the minimum size threshold. The minimum threshold for tide gauge observations is nominally 0.1 m, starting circa 1960 when tsunami observations from tide gauge stations started to become routine and systematic. Prior to that, a 1 m threshold for catalog completeness could be considered starting circa 1890 for the global catalog, relying more on eyewitness observations. Different station catalogs will likely have different thresholds and starting years for completeness.

One way in which the effects of undersampling can be analyzed is to determine confidence intervals of distribution parameters that dictate the tail shape, and the effect of record-breaking events. For the tapered *Pareto* size distribution, for example, Geist and Parsons (2014) indicate that in many cases the upper confidence

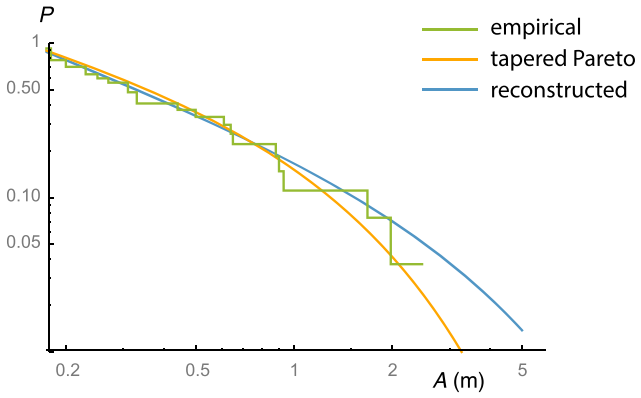

Figure 5. Comparison of complementary cumulative distribution functions of tsunami amplitude at the Crescent City, CA tide gauge station derived from empirical methods. (green line) Raw, empirical distribution function of station catalog data. (orange line) Maximum likelihood fit of data to tapered *Pareto* distribution. (blue line) Reconstructed distribution using earthquake magnitude distribution from Pacific subduction zones, scaling, and aggregation (see Geist and Parsons (2016), for details).

bound for the corner amplitude parameter tends to infinity. Thus, in these cases the pure *Pareto* distribution cannot be rejected given the data. Moreover, estimates of the corner amplitude are unstable over time, even with samples containing thousands of observations, owing to the occurrence of one or more record-breaking events which dominate the fit (Geist & Parsons, 2014; Kagan & Schoenberg, 2001; Zöller, 2013). Undersampled empirical distributions can take the appearance of being depleted in large amplitudes, relative to a pure *Pareto* distribution, or dominated by one or more large events. Both of these appearances in the empirical distribution can be artifacts of undersampling.

Geist and Parsons (2016) indicate that the station-specific model distribution can be made more robust, particularly in the Pacific, by using the extensive catalog of subduction zone earthquakes. Building on previous research establishing an empirical relationship between earthquake and tsunami magnitude (Abe, 1995; Comer, 1980), the procedure consists of four steps: (1) define the distribution of seismic moment at subduction zones, (2) establish a source-station scaling relation from regression analysis, (3) transform the seismic moment distribution to a tsunami amplitude distribution for each subduction zone, and (4) mix the transformed distribution for all subduction zones to an aggregate tsunami amplitude distribution specific to the tide gauge station. Geist and Parsons (2016) demonstrate that this procedure lessens the effects of undersampling at the tail of the distribution function. An example of an empirical hazard curve calculated using this procedure is shown in Figure 5. Kaistrenko (2011) has developed a similar procedure transforming smoothly varying amplitudes from the open ocean to broad regions of the coastline.

As with defining source probability, the assumed interevent distribution is one following a stationary *Poisson* process. However, temporal clustering of global tsunami events is indicated by examining the distribution of interevent times (Geist & Parsons, 2011). This clustering affects the short-term probability of a tsunami occurring soon after previous event has occurred (Corral, 2005). Additionally, eyewitness or paleotsunami records at a given site are usually too short to fully determine the interevent distribution empirically. Because long intervals are those most likely to be missing from the catalog, a simple mean of intervals will tend to skew from the true parent distribution mean. This effect can be corrected for, and uncertainties assessed through *Monte Carlo, Bayesian*, or other fitting methods (e.g., Nomura et al., 2011; Parsons, 2008a, 2012).

3.4. Hazard Maps and Hazard Curves

Hazard curves, hazard maps and probability maps are the main means by which PTHA results are communicated. Hazard curves describe the rate (events/year) of exceedance as a function of the tsunami intensity measure (e.g., peak wave height) at one or more locations of interest. As illustrated by Geist and Lynett (2014), hazard maps and probability maps are obtained by horizontal and vertical cuts, respectively, of the hazard curves. As a result, a geographical representations either of the tsunami intensity distribution associated to a selected rate or return period (hazard map) or of the rate associated to a selected tsunami intensity (probability map), is obtained. These computations involve integrating over all hypothetical tsunami events in the PTHA (as in equations (3)–(5)), but they are often generalized to include quantified aleatory and epistemic uncertainties. We outline the main aspects of hazard curve and map computations below but defer full discussion of the inclusion of aleatory and epistemic uncertainties to section 4.

Typically hazard curves are generalized using integration to include quantified aleatory uncertainties (i.e., random uncertainties, such as the unknown tidal stage at the time the tsunami arrives), whereas a range of methods are used to treat epistemic uncertainties (i.e., associated with lack of knowledge). Aleatory uncertainties are often used to account for simplifications in our representations of tsunami events. For example, it is common for the earthquake-tsunami events included in PTHA to be reduced to a few scenarios from a limited range of magnitude categories, thus ignoring stochastic variations in the earthquake slip geometry, and random oceanographic influences such as tidal variations during the tsunami (Davies et al., 2017; Horspool et al., 2014). Real earthquake tsunamis are thus expected to deviate from the modeled PTHA scenarios. One way to account for such deviations is to assume they lead to random variations in the tsunami

intensity parameter $I(x|e)$. To include this in equation (2), the indicator function is replaced with a statistical model giving the probability that the tsunami intensity threshold is exceeded (denoted $P(I(x|e) > I_0)$), that is,

$$\lambda\left(I(x) > I_0\right) = \sum_{e \in E} \left(P(I(x|e) > I_0)\right) \lambda(e) \tag{7}$$

Various methods for computing $P(I(x|e) > I_0)$ to account for particular aleatory uncertainties are described in section 4 and the broader literature (Adams et al., 2014; Davies et al., 2017; Horspool et al., 2014). See also the tutorial provided in the supporting information in the form of interactive Jupyter notebooks, available at the Github repository https://github.com/rjleveque/ptha_rog and archived at https://doi.org/10.5281/zenodo.816290 Zenodo data repository.

The treatment of epistemic uncertainties in hazard curve computation is less straightforward. Whereas aleatory uncertainties represent random variations and so can be "integrated out" of the hazard curves (e.g., equation (7)), it may not always be desirable to treat epistemic uncertainties in this way, since unlike the intrinsically random aleatory uncertainties, their effect will not integrate out over sufficiently long observational time periods. We defer full discussion of these issues to section 4.

3.5. Verification With Observations

There are different aspects of PTHA that can be verified with observations, such as assumptions, numerical modeling, and the resulting hazard curves. In terms of tsunami propagation and run-up modeling, for example, performance of different numerical codes are importantly verified with respect to analytic, laboratory, and field survey benchmarks (Synolakis et al., 2008). Uncertainty of the tsunami model with respect to observations can be parameterized and incorporated in PTHA (see section 4). The results from PTHA itself, namely, the hazard curve, can also be tested. These tests can range from a simple visual inspection relative to an empirical hazard curve to more statistically rigorous tests relative to observations.

In its simplest form, PTHA results that include forecasts near 0% or 100% probability can be verified or refuted with a single observation. For example, in an early tsunami probability study, Rikitake and Aida (1988) used a time-dependent, characteristic source model offshore Japan to calculate the probability of different wave height exceedance levels between the years 2000 and 2010. For much of the Tohoku coastline, 0% probability was indicated for some of the higher exceedance wave heights (i.e., 5, 7, 10 m) because incomplete historical run-up values were relied on in the absence of a fault model. As a result, these levels were exceeded by the 2011 Tohoku-Oki earthquake (Mori et al., 2011). Even though this event occurred outside of the authors' forecast window, it is not hard to imagine that their methodology would produce similar probabilities for the year 2011 with the data available at the forecast time.

Often, modern PTHA results are not specific to a time window and inclusion of uncertainty results in forecasts that are rarely near 0 or 100% probability. A hazard curve computed from PTHA, however, can be compared with an empirical hazard curve. Because PTHA conceptually includes all sources and does not suffer from the effects of undersampling, the rate from an empirical hazard curve should not exceed that from a PTHA-derived hazard curve for any given exceedance run-up level. If the computed rate is exceeded by the empirical rate, missing sources or incomplete uncertainty parameterization may be indicated. In cases where computational PTHA includes only one source, for example, earthquakes, then the catalog data can be alternatively included into PTHA using a *Bayesian* scheme, rather than being used for verification (see section 4.3.3).

Both parametric and nonparametric statistical tests can also be used to verify the results. Parametric tests can be used if both the computed and empirical data are fit with the same distribution model. For the tapered *Pareto* distribution, for example, Kagan (1997) describes two tests to determine the homogeneity of the power law exponent β, whereas the likelihood ratio test can be used to compare estimates of the corner amplitude. Nonparametric tests can be used to compare the empirical and computed cumulative distributions: for example, the two-sample *Kolmogorov-Smirnov* test. The comparison might have to be performed on a restricted range of sizes to account for the effects of completeness and undersampling, thus injecting some subjectivity to the test. Several other types of statistical tests developed for earthquake forecasts, such as those described by Schorlemmer et al. (2007) and Kagan (2014), can be adapted for PTHA.

4. Aleatory Variability and Epistemic Uncertainty

Because large tsunamis tend to be relatively rare, uncertainty quantification for PTHA generally involves a mixture of empirical analyses and subjective judgment. Whereas some uncertainties are quantified based

on the observed frequency of occurrence (such as small and intermediate earthquake recurrence), in general the rarity of large tsunami means that judgment is required to quantify other uncertainties, which is a subjective approach (Vick, 2002).

For instance, we may characterize the recurrence of intermediate earthquakes in terms of a *Gutenberg-Richter* relation, constrained by a catalog of historical earthquakes. The assumption is that the mean rate of earthquakes above any magnitude is stationary, so the catalog represents a homogenous sample of the long-term seismic behavior of a source. For large earthquakes however, the recurrence times are often so long relative to our historic record, even when paleoseismic/tsunami data are included, that the recurrence properties of these events cannot be reliably constrained by extrapolation of observed earthquake occurrence. We therefore need to introduce the concept of judgment, where we use our current understanding of earthquake processes, including analyses of similar tectonic structures elsewhere and other information, such as local geological conditions and strain rates, to make assumptions on the nature and recurrence of large earthquakes.

This introduces subjectivity into the assessment, which depends on the observer rather than the observations, and will inevitably cause results to differ from one practitioner to the other. A rigorous PTHA model therefore includes the use of strategies enabling expression of alternative understandings of the same process, for example, large earthquake recurrence, weighted by the subjective credibility within the reference community, in order to quantify a technical community distribution determining "*the center, the body, and the range of technical interpretations that the larger technical community would have if they were to conduct the study*" (Bommer, 2012; Marzocchi et al., 2015; Senior Seismic Hazard Analysis Committee (SSHAC), 1997; U.S. Nuclear Regulatory Commission (USNRC) 2012).

4.1. Aleatory Variability

Aleatory variability refers to the unpredictability (or randomness) of a physical process. This randomness is expressed through the objective probability of the PTHA. This unpredictability does not reduce with additional data, as what may be reduced is only our knowledge in modeling the process (i.e., epistemic uncertainties). Typically, the aleatory variability is expressed as a distribution function (e.g., *Gauss and Poisson*) that describes the outcome of a process. The first, most fundamental aleatory variability is encountered in the occurrence time of source events (earthquakes, landslides, eruptions), which is often assumed to follow a *Poisson* (i.e., time-independent) distribution, for example, the probability of an event occurring does not depend on the elapsed time since the last event on the system.

Aleatory variability is often considered in the following fields:

- Source mechanism — The spatial distribution of earthquakes is not homogeneous over the Earth's surface. The majority of the observed seismicity worldwide is concentrated on faults around the boundaries between adjoining tectonic plates. These interplate earthquakes occur at well-defined plate boundaries, such as the San Andreas Fault in California or the northeast Japan subduction zone offshore Tohoku region. The high earthquake rates and known relative motion vectors make plate boundary earthquake rates relatively quantifiable. More difficult to constrain are intraplate (crustal) earthquakes that occur away from plate boundaries and to provide quantitative methods to examine off-fault mechanism variability (Bird & Kagan, 2004; Kagan, 1992). Low activity rates mean that many intraplate faults may be unidentified; generally historic and current strain and seismicity patterns are used to anticipate areas where future earthquakes may occur (e.g., Selva et al., 2016; Stein & Mazzotti, 2007). Interplate and intraplate earthquakes are only end members of a likely continuum of cases, which includes intermediate tectonic environments such as diffuse margins and/or diffuse seismicity surrounding plate boundaries. Even if the impact of this off-fault seismicity is usually neglected in most of PTHA, recently, Selva et al. (2016) proposed a method to include the "background" seismicity and its variability in hazard quantification. The contribution of this background seismicity may indeed be fundamental in specific tectonic contexts (e.g., Caribbean and Mediterranean).
- Source magnitude — For earthquakes, individual scaling relations mentioned in the epistemic section provide not only mean relations but also the standard deviation which can be used in sampling the magnitude distribution of events. In general, the volume of mass that is displaced, whether by earthquake, landslide, or meteorite, has a random element which is an aleatory term.
- Slip distribution — It is still a quite common practice to represent earthquake sources with uniform slip on a rectangular fault, even though seismic source studies have shown that the slip of large earthquakes is typically strongly nonuniform with ruptures consisting of patches of high slip (asperities) over lower slip

background. Murotani et al. (2008) inverted the slip distributions of several subduction zone earthquakes and found the ratio of maximum to average slip ranged from 2 to 4. To account for the slip variability, Thio et al. (2017) represented every scenario by three instances in which one third of the rupture belongs to an asperity with twice the average slip and the other two thirds of the rupture possess half the average slip. This way, there is a smaller possibility that in some areas the hazard is overestimated or underestimated due to incomplete or overlapping asperity coverage offshore. Aleatoric variability related to the slip distribution can also be accommodated by a *Monte Carlo* approach that uses stochastic slip models to integrate over a large number of semirandomized slip models (e.g., LeVeque et al., 2016). Also, the rake is heterogeneous, but typically, the effects on the tsunami are not as great as slip magnitude.

- Tides — In reality, coastal tsunami impact depends also on the actual tide level (Mofjeld et al., 2007). Since it is not possible to foresee, at which time of the day tsunami will hit the coast, numerical scenarios in PTHA studies refer to the average sea level. Tidal effect becomes, thus, another source of aleatoric uncertainty. In most tsunami models the sea level can be adjusted to model the effect of a tsunami at different tide stages, and multiple simulations can be combined with statistical information about the tide at the location of interest (Adams et al., 2014) resulting in a local probability density function to quantify the tidal uncertainty. For the linear case, tidal variability can most easily be included through a convolution of a sufficiently long tidal record and the actual tsunami time series. The convolution is necessary over a simple multiplication of the distribution functions since the tsunami waves tend to consist of multiple arrivals in time with similar amplitudes so that the probability of coincident tsunami and tidal highs increases with increasing "ringing" of the tsunami waves.
- Modeling — Because realistic earthquakes are usually more variable than the scenarios included in PTHA, the computed tsunami intensity (e.g., run-up) is not expected to give a highly accurate representation of the tsunami intensity of real events. Nevertheless, model results do show correlation with observations, and we may treat the difference as a random process. For example, we can parameterize the aleatoric uncertainty due to modeling for the tsunami run-up as a lognormal distribution, for which the bias and standard deviation may be estimated by comparing modeled tsunamis against observations for well-constrained historical events (Choi et al., 2002).

4.2. Epistemic Uncertainty

As mentioned before, a probabilistic analysis is more than an expression of objective probabilities (defined in terms of long-run frequencies) of a hazard level being exceeded. It also contains a component that expresses limitations in our understanding of natural processes and different opinions regarding these processes, resulting in uncertainty on quantifying these objective probabilities. This is referred to as epistemic uncertainty and is usually accounted for by introducing alternative and scientifically acceptable quantifications, and by weighting them according for their subjective credibility. Different techniques exist to manage such alternatives, as will be discussed in section 4.3. Epistemic uncertainties may be reduced over time as our knowledge of the relevant physical processes improves, so that our subjectivity in defining the alternatives decreased. For example, new evidence may be used to falsify one model (or to weight it less).

The following examples illustrate typical epistemic uncertainties.

For seismic sources:

- Seismic zonation. Similar to PSHA, PTHA studies imply seismic zonation models to separate dominant seismicity into relatively homogeneous zones. All earthquakes in a zone are assumed to follow the common distribution of focal mechanisms as well as magnitude-frequency distribution. Zonation is being done by an expert who considers different available tectonic and seismic data sets and, hence, depends on data availability and expert's opinion.
- Characterization of offshore faults. Compared to onshore faults, offshore faults are generally less well-known, and different models for the fault maps may exist, or the degree of knowledge of offshore structures may be highly variable (e.g., Basili et al., 2013).
- Scaling relations. They are equations that relate different measures associated to earthquake and fault size to each other. Various authors have established empirical relationships between rupture length, width, slip, and magnitude (e.g., Murotani et al., 2008; Strasser et al., 2010).
- Rupture segmentation. Segmentation models describe whether ruptures on fault systems follow repeated segment or can break over multiple segments, therefore affecting the maximum magnitude and rupture extent.

- Updip and downdip rupture limits. Whether ruptures break to the surface or not can have profound implications for the tsunami generation. The downdip rupture extent has implications for the maximum slip as well as uplift or subsidence patterns along the coastline.
- Seismic slip rates. Although convergence rates for subduction zones are generally well known, the fraction of the convergence that is accommodated by seismic (or more accurately tsunamigenic) slip varies between different subduction zones and even within the same subduction zone.

For landslide sources:

- Probability of and location of failure. Quantifying local probability of landslide release is normally associated with large epistemic uncertainty, both because detailed geotechnical and geophysical properties are normally not known over large portions of the possible failure area. Second, it is because of the complex interaction between possible earthquake triggers and landslide failure mechanisms. Geological structures that may prevent a landslide to fail are usually not known, unless detailed site investigation data exist. Moreover, the complex interaction between possible earthquake triggers and landslide failure mechanisms introduces uncertainties.
- Landslide dynamics. Different models exists for the landslide rheology, for example, viscous, granular, and viscoplastic, see section 2.2. Different models, as well as different model parameters could usually span a rather wide parameter space. A fundamental problem here is that we do not have time-dependent data of the landslide dynamics and their parameter values in order to constrain their tsunamigenesis.

For volcanic sources:

- Volcanic vent positions for underwater explosions. This information for most submarine or submerged part of volcanoes is difficult to constrain because main indicators of structural weakness, such as faults and past vents are usually unknown.
- Models for tsunami generation from pyroclastic flows. Different models of pyroclastic flows entering into the water exist (e.g., simplified and multiphase) that may be coupled in different ways to generate tsunamis (including pressure changes), but there are still large uncertainties in modeling the proper dynamics;
- Flank instability. Large uncertainties are related to probability assessment of size and timing of flank failure due to heterogeneities of the volcano edifices and their complex interaction with fluid circulation, magma intrusions, and material weakening;
- Other potential sources. Other sources of tsunami have been proposed, such as caldera collapse, shock waves, and lava entering in the sea (Paris et al., 2014), but the tsunamigenic potential of these sources is still not well constrained.

For meteotsunamis:

- Observation and modeling of the atmospheric phenomena. The atmospheric mesoscale structures and associated tsunamigenic surface pressure disturbances are inadequately observed and are still not properly reproduced by atmospheric models.
- Initial and boundary conditions. Atmospheric simulations exhibit a strong sensitivity to the initial and boundary conditions of the source mechanisms and generation of the atmospheric gravity waves.
- Low temporal and spatial resolution. They determine some differences between model and observations. Such differences would lead to different oceanic response in terms of oscillation amplitude (Renault et al., 2011; Vilibić et al., 2016). Also, they can produce some biases both in location and timing of the convective system or the gravity waves, because the reproduction of mesoscale processes is not preserved. This implies the development of new parameterization schemes within models as well as more accuracy of the bathymetry and increasing resolution of the coastline configuration (not just due to a pure increase of the model resolution) to reproduce feasible physics at these spatial and temporal scales (Renault et al., 2011; Vilibić et al., 2016).
- Tsunamigenic atmospheric disturbances and specific weather conditions. Their correlations require further investigations.

For asteroid impacts:

- Input parameters. Impactor size, density, impact speed, and angle are insufficiently observed.
- Impacts. Their modeling present limitations,especially the formation of the crater (water and crust) before tsunami waves are formed.

- Impact frequency. The reconstruction of the discovered crater structures in the ocean crust may not reflect the real impact frequency at Earth's surface for the quantification of the hazard (Wünnemann et al., 2010).
- Sea depth and bathymetry. They must be assumed for reconstruction of past events with uncertain evaluation of the tsunami height from paleodeposits.

For tsunami generation and propagation modeling:

- Topobathymetric model. High resolution and data accuracy are required.
- Crustal model. Homogeneous half-space, 1-D layered, 3-D finite element model consider different levels of approximations and present different degrees of computational complexities..
- Translation of the sea bottom deformation to the sea surface. The uncertainty reductions concern both no filtering and way to implement filtering).
- Wave propagation. Modeling the linear/nonlinear long waves presents higher approximations.
- Coastal impact. Coastal features representations affect both the treatment of the projection from offshore positions and the direct inundation simulations.

4.3. Quantification of Epistemic Uncertainty

4.3.1. Logic Tree

The use of the logic tree framework has almost become standard practice in PSHA, and it has also found its applications in PTHA, and less frequently in the PVHA (Probabilistic Volcanic Hazard Analysis). Part of the popularity of logic trees is related to the fact that they are technically easy to implement. It is a powerful tool to organize one's thinking in situations where alternative models, in which the analysts have different degrees of confidence, might apply.

The logic tree is then one of the several flavors of graphical probability trees (issue tree, event tree, fault tree, etc.) that aim to dissect a specific problem into its basic components. The structure and the kind of the tree are defined according to its practical use. The different branches of the logic trees used in hazard assessments are meant to describe the epistemic uncertainties related to the different components (nodes) of the hazard model. Each branch is an alternative model and is assigned an associated weight.

The branches emerging from each node must represent a Mutually Exclusive and Collectively Exhaustive (MECE) set of events, in order to meet the *Kolmogorov* axioms for probabilities (Bommer & Scherbaum, 2008; Kulkarni et al., 1984). Referencing from Bommer and Scherbaum (2008): «*the mutually exclusivity requires that the model on one of the branches is applicable but not a combination of models, while the collective exhaustiveness requires that one of the models in the model set considered fully applies*». In the probability tree, probabilities are combined through the law of total probability:

$$P(E) = \sum_{i=1}^{N} P(E \cap H_i) = \sum_{i=1}^{N} P(E|H_i)P(H_i) \tag{8}$$

where E is the event of interest and H_i represents the ith alternative model. In equation (8), it is assumed that H_i represents a countable partition of the sample space, which is the MECE set of events. In their current application, the weights $P(H_i)$ express the "degree of belief" of the hazard analyst(s) in the corresponding model H_i, and they are subsequently treated as (subjective) probabilities to calculate a distribution of hazard curves (Bommer & Scherbaum, 2008). From these curves, the mean model is assessed. In some cases, it has been argued that the hazard should be represented by a percentile (e.g., 84%) instead of the average (Abrahamson & Bommer, 2005). The use of percentiles is questioned by other practitioners who assert that a logic tree can provide only one number; for example, Musson (2005) affirmed «*Each fractile, as a statement of probabilistic hazard, is false. True probabilism has to take into account all uncertainties, and none of the fractile curves do this. Only the mean curve does this*».

The most important consequence of the probabilistic interpretation of the logic tree is that one path of the tree must represent the truth. Since no practitioner believes that one of the paths of the logic tree represents the true hazard, the MECE assumption is pragmatically resumed replacing the term "true" with "the one that should be used" (Scherbaum & Kuehn, 2011). Also, trying to meet the requirements of the MECE is in general a difficult task. As discussed in Bommer and Scherbaum (2008), the MECE criterion easily may lead practitioners to include many branches (following the reasoning that more branches, i.e., alternative models, increase the chance that the true model is among the options), as well as many sections. On the other hand, more branches also increase the chances of model redundancy, automatically violating the condition of mutual

exclusivity (Burnham & Anderson, 2002). In addition, the practical achievement of mutual exclusivity is even more complicated because of the subtle nature of the interdependence of models.

Given the complexity and the criticality of the selection of the alternatives and the quantification of their weights, when the assessment may have regulatory concern (e.g., for national hazard quantifications, or for critical infrastructures), this task is usually associated to multiple-expert process (e.g., SSHAC, 1997), as discussed in section 4.4.

4.3.2. Ensemble Modeling

Epistemic uncertainty arising from the adoption of alternative modeling procedures can be quantified by modeling the different objective probability values. This variability can be interpreted in the framework of ensemble modeling (Araújo & New, 2007; Cloke & Pappenberger, 2009; Marzocchi et al., 2015; Selva et al., 2016; Toth & Kalnay, 1993), as introduced by Marzocchi et al. (2015) and Selva et al. (2016) for PSHA and PTHA, respectively. In this framework, aleatory uncertainty is quantified by an objective probability θ that represents the expected long-run frequencies of random events within the model of the system. Epistemic uncertainties measure the lack of knowledge in the estimation of θ. This uncertainty is quantified through a probability distribution, described by subjective probabilities, that describes epistemic uncertainty. This probability distribution represents the technical community distribution (e.g., Bommer, 2012; SSHAC, 1997; USNRC, 2012).

To quantify such community distribution, a finite set of alternative models is defined $\{\theta_i, \omega_i\}$ $(i = 1, \ldots, N)$, where θ_i and ω_i are the outcome and the weight of the ith model. As for the *Bayesian* case below, in hazard assessments, the θ parameters being quantified are usually the exceedance probabilities of a given tsunami intensity at one site as $\theta = P(Z > z_t; x, \Delta T)$. Different from a logic tree, in which one model is consider the "true" model (or the one that should be used (Scherbaum & Kuehn, 2011)), in ensemble modeling, the models are just considered as samples of the unknown parent distribution $f(\theta)$, the community distribution (Marzocchi et al., 2015):

$$\theta_i \sim f(\theta) \tag{9}$$

This has several important consequences: (i) weights have no probabilistic interpretations; (ii) alternative models should not represent a mutually exclusive and collectively exhaustive set; (iii) gaps between models and tails are still part of the community distributions; and (iv) in case of many alternative models, one can sample from these models to set the ensemble (see Marzocchi et al., 2015; Selva et al., 2016). The community distribution $f(\theta)$ may be either parametric or nonparametric, single, or multimodal, depending on the specific application. Also, it represents a "unified model" describing the state of knowledge about the frequency θ; thus, it is compatible with all the *Bayesian* methods in which frequencies are the object of the inference (e.g., Gelman et al., 2013; Grezio et al., 2010, 2012; Marzocchi et al., 2010; Selva & Sandri, 2013), as the ones discussed in section 4.3.3. In this case, $f(\theta)$ may play the role of the *prior* distribution before evidence about probability of tsunami intensity is updated through the *Bayes'* theorem (equation (10)).

In order to produce a consistent ensemble model, the set of samples and weights $\{\theta_i, \omega_i\}$ should represent an unbiased sample of the epistemic uncertainty (see discussion in Marzocchi et al., 2015). This set should consistently represent the variability of models and opinions within the reference community. Therefore, as in the case of logic trees, the development of alternatives and the quantification of weights should emerge from a multiple-expert process (e.g., SSHAC, 1997), as discussed in section 4.4.

4.3.3. Bayesian Methods

Bayesian methods provide a means to merge all relevant available information to assess both aleatory and epistemic uncertainties in PTHA. By following a *Bayesian* structure to calculate the probability of tsunami intensity at a given point, we can systematically quantify each source of lack of knowledge (epistemic uncertainty) and inherent natural variability (aleatory uncertainty) that usually must be modeled with uncertain parameters. Therefore, in a *Bayesian* approach, the epistemic uncertainties are related to unknown parameters representing the tsunami intensity of the hazard analysis, whereas the aleatory uncertainties are represented by the probability density functions (PDFs) modeling the selected parameters.

The θ parameters being quantified are usually the exceedance probabilities of a given tsunami intensity at one site as $\theta = p(Z > z_t; x, \Delta T)$, where Z is the physical variable expressed in terms of defined specific thresholds z_t per unit time interval ΔT that denotes the tsunami intensity required to evaluate the hazard. Before considering independent observations, the θ parameters are modeled on the basis of the current state of knowledge (i.e., the estimated possible range of the parameter values) with the relative uncertainty

and expressed through the prior PDF $P(\theta)$. This *prior* distribution can be built by fitting series of alternative and scientifically acceptable models, potentially weighting them depending on their credibility, as, for example, the output of a logic tree or an ensemble model (Grezio et al., 2010; Selva et al., 2010; Selva & Sandri, 2013).

If the observed data events are given as $Y = \{y_1, , y_i, , y_n\}$, then *Bayes'* theorem yields an updated (*posterior*) probability distribution $P(\theta|Y)$ in light of the event data as

$$P(\theta|Y) = P(\theta)L(Y|\theta)/P(Y) \tag{10}$$

where the notation $P(\cdot)$ is the probability PDF, $P(\cdot|\cdot)$ is the conditional PDF, $L(Y|\theta)$ is the likelihood function that represents the information about θ contained in the data Y, and $P(Y)$ is a normalization constant ensuring that the *posterior* probability distribution integrates to 1 (e.g., Gelman et al., 2013). The results of a *Bayesian* analysis are conditional on the knowledge or assumptions used to construct the statistical models that represent the prior PDFs of the θ parameters, and the likelihood functions that link the observations Y to the parameters.

Bayesian procedures have been applied in a variety of ways in PTHA uncertainty evaluations. Shin et al. (2015) employed a *Bayesian* approach to account for the uncertainty of earthquake occurrence corresponding to specific return periods within the Kamchatka-Kuril-Japan Trench. By assuming a *Poisson* process, Butler et al. (2016) used standard *Bayesian* procedures to estimate the probability of mega seismic events in the Aleutian Islands on the basis of paleodata. Uncertainties in both seismic input parameters and earthquake slip distribution were quantified in the Sumatra area using a *Bayesian* Network by Blaser et al. (2011), where the relationships between discrete variables were evaluated by conditional probability distributions at each node. In their automated process, variable probabilities could be updated by new observations to proceed in any direction across the network of variables in an early warning process.

Dettmer et al. (2016) considered the initial sea surface displacement during the 2011 Japan tsunami to avoid assumptions associated with the earthquake rupture, which varied across the source region with more parameters introduced where the source was well resolved, and/or had significant complexity. Similarly, Tatsumi et al. (2014) developed a *Bayesian* near-field tsunami forecasting method for the initial sea surface displacement by estimating uncertainty through the use of tsunami waveforms observed at offshore locations in the western and central region of Japan in an inverse problem procedure. The *posterior* distribution was conditioned to the observations, and the *posterior* mean was regarded as a point forecast. Sampling from the *posterior* distribution could quantify the uncertainty in the forecasts of the initial sea surface displacements. Further, Yadav et al. (2013) considered the tsunami intensity, comprehensive of the slope frequency relationship and tsunami activity rate, and the relative uncertainties in a *Bayesian* statistical frame where the occurrences of the tsunami events followed a *Poisson* distribution. Data from an Indian Ocean tsunami catalog (complete for tsunami intensity values greater than 2.0) were included covering a 210 year period (1797–2006).

Knighton and Bastidas (2015) proposed weighting the *prior* distribution by the epistemic uncertainties of the tsunami generation and propagation model in the Aleutian Islands region. The aleatory uncertainty was defined by implementing a binomial probability model defined by the number of tsunamigenic events that overcame a critical threshold within a specific period. The available tsunami catalog of run-up data refined the *posterior* distribution of the tsunami hazard for a specific facility or structure. Selva et al. (2016) adopted an ensemble modeling approach to explore the aleatory uncertainty using alternative probability distributions of semi-informative prior combinations of angles to establish the focal mechanism of submarine earthquakes, which were updated by considering historical catalogs in the Mediterranean Sea.

Grezio et al. (2010, 2012, 2017) estimated run-up exceedance rates and run-up forecast with weighting factors based on subjective estimation of the variance and past tsunami data in the Messina Strait Area. Parsons and Geist (2009) developed a tsunami forecast for the Caribbean region using both empirical catalog and numerical models of wave height with the likelihood function weighting the multiple independent run-up rate distributions. The *Bayesian* method underlined that the empirical catalog was not a complete record of all possible interplate tsunami sources, and the numerical model did not account for accommodating intraplate fault and/or landslide sources.

4.4. Multiple-Expert Processes

The management of scientific and technical controversies within a multiple-expert environment is critical for any hazard/risk assessment project, with the goal of producing a robust quantification of the community distribution. As discussed in section 4.3, the development of alternatives and the quantification of their weights

are the basis for this quantification and the results are often critically dependent on these subjective choices (e.g., Bernreuter et al., 1989; Paté-Cornell, 1996). The need for involving multiple experts necessarily increases as the relevance and the regulatory concern increase (e.g., Intergovernmental Panel on Climate Change (IPCC), 1998; Woessner et al., 2015). Indeed, the multiple-expert involvement may favor a better constraint of the community distribution (e.g., SSHAC, 1997), to help deal with potential subjective choices (e.g., Morgan, 2014), as well as to minimize possible a posteriori critiques if a forecast model fails (e.g., Marzocchi & Zechar, 2011). Therefore, there are numerous documented examples of assessments produced in a multiexpert context (e.g., in Araújo & New 2007; Babuscia & Cheung, 2014; Bommer, 2012; Bommer & Scherbaum, 2008; Boring et al., 2005; Budnitz et al., 1998; Cloke & Pappenberger, 2009; Cooke, 1991; Cooke & Goossens, 1999; Hora, 2007; IPCC, 1998; Linstone & Turoff, 1975; Knoll et al., 2009; Kulkarni et al., 1984; Marzocchi & Zechar, 2014; SSHAC, 1997; Toth & Kalnay, 1993; U.S. Environmental Protection Agency, 2011).

The most applied and referenced protocol is the one developed by the (SSHAC) in 1997 (SSHAC, 1997), and its subsequent specifications and integrations (e.g., Hanks et al., 2009; Coppersmith et al., 2010; USNRC, 2012), hereinafter referred to as SSHAC guidelines. The main motivation for establishing SSHAC and the SSHAC process was the existence of incompatible hazard estimates provided by different yet highly respected groups, which had stalled the U.S. Nuclear Regulatory Commission with regard to their PSHA regulatory concerns. One of the most relevant conclusion in SSHAC guidelines/recommendations about uncertainty management and use of experts is that differences in PSHA assessments are often due to procedural rather than technical differences, and so a great effort has been put in establishing appropriate procedures.

The SSHAC guidelines are primarily based on four levels (1 – 4) of complexity spanning the range from the simplest and least resource intensive (Level 1) to the most complex and resource intensive studies (Level 4). The completeness and the level of assurance of each SSHAC level are based on how extensively the uncertainties are treated in the assessment. All levels are a composition of different participants engaging different roles and responsibilities, such as Project Sponsor, Project Manager, Participatory Peer Review Panel, Technical Integrator, hazard analyst, resource experts, and evaluator experts and proponent experts. A generic summary of important attributes in different levels is presented in USNRC (2012).

When the regulatory concern is not the highest possible (e.g., for Nuclear Commission Issuances), and/or in small/medium size projects, applicability of the full SHAAC procedure may not be feasible. Furthermore, the group interaction and face-to-face meetings between the experts can be challenging for the undesirable effects of personalities and reputations that unavoidably may bias the group quantification (e.g., Aspinall & Cooke, 2013; Bedford & Cooke, 2001). Lastly, some "technical neutrality" is desired, since what really matters is the standardization of the process, not the specific tool (e.g., a logic tree or an ensemble) to be used.

A more flexible management of subjectivity in probabilistic single/multihazard/risk assessments has been addressed within a structured Multiple-Expert Management Protocol (*EU STREST project*-Harmonized approach to stress tests for critical infrastructures against natural hazards, deliverable D3.1 and in Selva et al., 2015) with a development of this approach applied specifically to SPTHA (*EU TSUMAPS-NEAM project*-Probabilistic TSUnami Hazard MAPS for the NEAM, North East Atlantic and Mediterranean Region). The procedure for the management of subjective choices and uncertainty quantification is rooted in a clear definition of roles and interactions among the different experts, structured elicitations based on mathematical aggregation of a pool of experts, and in participatory independent reviews. This is achieved by the coordination with a technical integrator and a project manager, within a formalized process. The purpose of the protocol is (i) to establish roles and responsibility, in order to guarantee transparency, independency of roles, accountability and achievement of procedural consensus; (ii) to homogenize the management of decision making for subjective choices, guaranteeing documented, and trackable decision making; and (iii) to establish homogeneous principles for the management of alternative and scientifically acceptable implementations for quantifying community distribution. This flexible process foresees three main project phases (preassessment, assessment, and outreach), with two internal reviews at the end of the preassessment and assessment phases, finalized through a formal agreement between management and reviewers. Critical decisions are taken during the first two phases. In both cases, the starting point for decisions is constituted by two formal solicitations of feedback from a pool of experts. Decisions are then taken and documented by the management of the project, and subsequently reviewed by independent experts. The details of this process are presented in the deliverable D8.39 of the *EU ASTARTE project*).

5. Discussion, Concluding Remarks, and Future Perspectives

Probabilistic Tsunami Hazard Analysis (PTHA) is quickly becoming standard practice for tsunami hazard assessment around the world. Applications have included the development of probabilistic inundation maps at different scales (Davies et al., 2017; González et al., 2009). PTHA is most applicable for long-term coastal planning hazard zonation, mitigation, and multihazard assessment. In contrast to deterministic assessments, however, where the probability associated with specific scenarios can vary greatly and is often poorly defined, PTHA defines hazards at specific and sometimes multiple mean return times. Where scenario based deterministic methods lack a structured approach for taking into account how data and subjective choices determine the construction of the scenario chosen, PTHA offers structured and rigorous procedures that allows for tracing and weighting how these input influences the output. PTHA calculates tsunami hazard curves in aggregate form, resulting from the combined influence of multiple source regions and, conceivably, multiple types of sources. PTHA also explicitly includes multiple types (epistemic and aleatory) and sources of uncertainty.

There remain, however, several important aspects of PTHA that need to be addressed in future research. While there has been significant progress in the development of progressively more advanced PTHA methods, we lack standards on how to conduct PTHA assessments, and more widely, probabilistic risk assessments. This is particularly important as the diversity of PTHA methods develops into different directions, for instance related to different geographical scales (e.g., regional or local studies), the level of sophistication, or application (e.g. regional screening study versus a critical facility). An initiative referred to as the Global Tsunami Model (GTM, http://www.globaltsunamimodel.org/) has the development of this type of standards as one of its main aims. In order to accomplish standards and good practices for PTHA and related studies, the specific challenges discussed below are all relevant.

We have little systematic data to build probability models for some seismic source zones, such as shallow megathrust areas near the trench that host tsunami earthquake and outer-rise faults. Incorporation of landslide tsunamis into PTHA is also particularly difficult, owing to the lack of an instrumental record of occurrence and measurements of source processes, such as the time history of landslide movement and deformation. Other nonseismic sources such as volcanic tsunamis have similar data challenges with regard to PTHA. However, some sources such as atmospheric tsunamis have significant amounts of data that can be immediately accessed to build probabilistic models.

One of the other significant challenges that PTHA faces is the comprehensive and systematic treatment of uncertainty. Because the tsunami risk is often expected to be dominated by sources with large return periods with associated large uncertainties in the return periods, these uncertainties have a larger impact on our quantification of the risk compared to many other natural hazards. One of the main tasks for the community will be to develop a set of standards that allows for incorporating uncertainties in a sound and feasible way.

Unlike probabilistic seismic hazard analysis, source-to-site path effects are computed numerically. Thus, performing numerical simulations for multiple values of source parameters quickly becomes an insurmountable computational problem. Source selection strategies, event tree, and ensemble modeling methods are currently being developed to address the problem (Lorito et al., 2015; Selva et al., 2016; Thio et al., 2010, 2017). Empirical scaling relations (e.g., for quantifying run-up heights) and derived uncertainty distributions can also help address this computational challenge (Løvholt et al., 2012). However, using these simplified methodologies implies increased (epistemic) uncertainties.

By definition, the epistemic uncertainties affecting a PTHA have the potential to be reduced through further increases in scientific knowledge. For instance, the maximum magnitude earthquake, which can possibly occur on any given source zone (denoted $M_{w_{max}}$), is often highly uncertain, particularly where no large historic earthquakes have occurred. Berryman et al. (2015) suggest plausible ranges for $M_{w_{max}}$ on most large global subduction zones which often cover more than one moment magnitude unit (and sometimes more than two, e.g., the Marianas trench). This translates into substantial epistemic uncertainties in PTHA run-up exceedance rates, as tsunami hazard is often dominated by large, infrequent events (Davies et al., 2017). However, at some time in the future we expect an earthquake exceeding the lower $M_{w_{max}}$ estimate will occur on one of these source zones, and this will reduce epistemic uncertainties in $M_{w_{max}}$ and lead to higher confidence that the source zone can generate large tsunami. Paleotsunami research (e.g., Atwater et al., 1995) can lead to a similar reduction in epistemic uncertainties, by better constraining $M_{w_{max}}$ and the rate of large tsunami events.

Growth in knowledge may also lead to the realization that previous quantifications of epistemic uncertainties are unrealistic. This may cause quantified epistemic uncertainties to increase, as prior errors are corrected, and previously "black swans" become "white swans" (Paté-Cornell, 2012). For example, prior to the M_w 9.1–9.3 2004 Indian Ocean earthquake-tsunami, it was widely considered that large ($>M_w$ 8.5) earthquakes only occur when young lithosphere is undergoing rapid subduction (Ruff & Kanamori, 1980). Re-examination of this hypothesis with greatly improved data more than 20 years later suggested it was incorrect, with the 2004 event being a clear counterexample (Stein & Okal, 2007). This in turn led to the higher $M_{w_{max}}$ values being considered in PTHA for other areas with no such large historical events (e.g., Burbidge et al., 2008). Similarly, prior to the 2011 Tohoku tsunami, most estimates of $M_{w_{max}}$ in that area ranged from ~7.5 to 8.6 (Kagan & Jackson, 2013), and although higher values were derived from seismic moment conservation type analyses (McCaffrey, 2008; Kagan & Jackson, 2013), they were not generally included in applied tsunami hazard studies. The lower $M_{w_{max}}$ values were contradicted by the 2011 M_w 9.1 earthquake-tsunami, which clearly demonstrated the potential for epistemic uncertainties to be poorly quantified (Okal, 2015; Synolakis & Kânoglu, 2015).

Finally, the next step and important application of PTHA is applying the results to calculate tsunami exposure and risk. Tsunami population exposure combines inundation estimates with coastal population data sets, typically on an annual basis (Løvholt et al., 2012; Løvholt, Griffin, et al., 2015). Further, tsunami risk combines the calculations of PTHA, exposure, and fragility. Tsunami risk calculations can refer to both human populations as well as infrastructure. Thus, development of future probabilistic risk assessments will rely critically on developing tsunami fragility curves as well as systematic standards for PTHA calculations. The end product can greatly enhance tsunami risk reduction efforts.

Acknowledgments
The contributions from Finn Løvholt, Carl Harbitz, and Sylfest Glimsdal are been funded by the Research Council of Norway project Tsunamis induced by large landslides (NFR 231252/F20). Gareth Davies and Jonathan Griffin publish with the permission of the CEO, Geoscience Australia. Part of this work was supported by the EU ASTARTE project within the FP7-ENV2013 6.4-3 grant 603839. The data used in the paper and the supporting information are listed in the references and repository at https://github.com/rjleveque/ptharog and https://doi.org/10.5281/zenodo.816290. We thank the Editor Mark Moldwin, the reviewer Linlin Li, and the anonymous reviewer for their valuable comments which improved the quality of the paper.

References

Abadie, S., Harris, J. C., Grilli, S. T., & Fabre, R. (2012). Numerical modeling of tsunami waves generated by the flank collapse of the Cumbre Vieja volcano (La Palma, Canary Islands): Tsunami source and near field effects. *Journal of Geophysical Research*, *117*, C05030. https://doi.org/10.1029/2011JC007646

Abe, K. (1978). A dislocation model of the 1933 Sanriku earthquake consistent with the tsunami waves. *Journal of Physics of the Earth*, *26*(4), 381–396.

Abe, K. (1979). Size of great earthquakes of 1837–1974 inferred from tsunami data. *Journal of Geophysical Research*, *84*(B4), 1561–1568.

Abe, K. (1995). Estimate of tsunami runup heights from earthquake magnitudes. In Y. Tsuchiya & N. Shuto (Eds.), *Tsunami: Progress in prediction, disaster prevention and warning* (pp. 21–35). Dordrecht: Kluwer Academic Publishers.

Abrahamson, N. A., & Bommer, J. J. (2005). Probability and uncertainty in seismic hazard analysis. *Earthquake Spectra*, *21*(2), 603–607.

Adams, L. M., LeVeque, R. J., & González, F. I. (2014). The Pattern Method for incorporating tidal uncertainty into Probabilistic Tsunami Hazard Assessment (PTHA). *Natural Hazards*, *76*(1), 19–39. https://doi.org/10.1007/s11069-014-1482-z

Allen, S. R., Freundt, A., & Kurokawa, K. (2011). Characteristics of submarine pumice-rich density current deposits sources from turbulent mixing of subaerial pyroclastic flow at the shoreline: Field and experimental assessment. *Bulletin of Volcanology*, *74*, 657–675.

Anderson, E. J., Bechle, A. J., Wu, C. H., Schwab, D. J., Mann, G. E., & Lombardy, K. A. (2015). Reconstruction of a meteotsunami in Lake Erie on 27 May 2012: Roles of atmospheric conditions on hydrodynamic response in enclosed basins. *Journal of Geophysical Research: Oceans*, *120*, 8020–8030. https://doi.org/10.1002/2015JC010883

Annaka, T., Satake, K., Sakakiyama, T., Kanagisawa, Y., & Shuto, N. (2007). Logic-tree approach for probabilistic tsunami hazard analysis and its applications to the Japanese coasts. *Pure and Applied Geophysics*, *164*, 577–592.

Antuono, M., Soldini, L., & Brocchini, M. (2012). On the role of the Chezy frictional term near the shoreline. *Theoretical and Computational Fluid Dynamics*, *26*(1), 105–116.

Artemieva, N. A., & Shuvalov, V. V. (2002). Shock metamorphism on the ocean floor (numerical simulations). *Deep Sea Research Part II*, *49*(6), 959–968.

Araújo, M. B., & New, M. (2007). Ensemble forecasting of species distributions. *Trends in Ecology and Evolution*, *22*, 42–47. https://doi.org/10.1016/j.tree.2006.09.010

Aspinall, W. P., & Cooke, R. M. (2013). Quantifying scientific uncertainty from expert judgement elicitation. In J. C. Rougier, R. S. J. Sparks & L. Hill (Eds.), *Risk and uncertainty assessment for natural hazards* (Chapter 4, pp. 64–99). Cambridge: Cambridge University Press.

Atwater, B. F., Nelson, A. R., Clague, J. J., Carver, G. A., Yamaguchi, D. K., Bobrowsky, P. T., … Reinhard, M. A. (1995). Summary of coastal geologic evidence for past great earthquakes at the Cascadia subduction zone. *Earthquake Spectra*, *11*(1), 1–18.

Auker, M. R., Sparks, R. S. J., Siebert, L., Crosweller, H. S., & Ewert, J. (2013). A statistical analysis of the global historical volcanic fatalities record. *Journal of Applied Volcanology*, *2*, 2.

Baba, T., Allgeyer, S., Hossen, J., Cummins, P. R., Tsushima, H., Imai, K., … Kato, T. (2017). Accurate numerical simulation of the far-field tsunami caused by the 2011 Tohoku earthquake, including the effects of Boussinesq dispersion, seawater density stratification, elastic loading, and gravitational potential change. *Ocean Modelling*, *111*, 46–54.

Babuscia, A., & Cheung, K. (2014). An approach to perform expert elicitation for engineering design risk analysis: Methodology and experimental results. *Journal of the Royal Statistical Society: Series A*, *177*, Part 2, 475–497.

Basili, R., Tiberti, M. M., Kastelic, V., Romano, F., Piatanesi, A., Selva, J., & Lorito, S. (2013). Integrating geologic fault data into tsunami hazard studies. *Natural Hazards and Earth System Science*, *13*, 1025–1050.

Bechle, A. J., & Wu, C. H. (2014). The Lake Michigan meteotsunamis of 1954 revisited. *Natural Hazards*, *74*(1), 155–177.

Bechle, A. J., Wu, C. H., Kristovich, D. A. R., Anderson, E. J., Schwab, D. J., & Rabinovich, A. B. (2016). Meteotsunamis in the Laurentian Great Lakes. *Science Reports*, *6*, 37832. https://doi.org/10.1038/srep37832

Bedford, T., & Cooke, R. (2001). *Probabilistic risk analysis: Foundations and methods*. Cambridge, UK: Cambridge University Press.

Begét, J. E. (2000). Volcanic Tsunamis. In H. Sigurdsson, et al. (Eds.), *Encyplopedia of volcanoes* (pp. 1005–1013). London, UK: Academic Press.

Behrens, J., Pranowo, W. S., & Wekerle, C. (2009). Credible worst case tsunami scenario simulation for Padang. hdl:10013/epic.51625.d001.

Belousov, A., Voight, B., Belousova, M., & Muravyev, Y. (2000). Tsunamis generated by underwater volcanic explosions: Unique data from 1996 eruption in Karymskoye Lake, Kamchatka, Russia. *Pure and Applied Geophysics*, *157*, 1135–1143.
Bernreuter, D. L., Savy, J. B., Mensing, R. W., & Chen, J. C. (1989). Seismic hazard characterization of 69 nuclear plant sites east of the rocky mountains, *Vols. 1-8, prepared for Division of Engineering and System Technology, Office of Nuclear Reactor Regulation*. Washington: U.S. Nuclear Regulatory Commission. NUREG/CR-5250 UCID-21517.
Berryman, K., Wallace, L., Hayes, G., Bird, P., Wang, K., Basili, R., … Costa, C. (2015). The GEM faulted earth subduction interface characterisation project. *Version 2.0, April 2015, GEM Faulted Earth Project*.
Bilek, S. L., & Lay, T. (2002). Tsunami earthquakes possibly widespread manifestations of frictional conditional stability. *Geophysical Research Letters*, *29*(14), 18-1–18-4. https://doi.org/10.1029/2002GL015215
Bird, P., & Kagan, Y. Y. (2004). Plate-tectonic analysis of shallow seismicity: Apparent boundary width, beta-value, corner magnitude, coupled lithosphere thickness, and coupling in 7 tectonic settings. *Bulletin of the Seismological Society of America*, *94*, 2380–2399.
Blaser, L., Kruger, F., Ohrnberger, M., & Scherbaum, F. (2010). Scaling relations of earthquake source parameter estimates with special focus on subduction environment. *Bulletin of the Seismological Society of America*, *100*(6), 2914–2926.
Blaser, L., Ohrnberger, M., Riggelsen, C., Babeyko, A., & Scherbaum, F. (2011). Bayesian network for tsunami early warning. *Geophysical Journal International*, *185*(3), 1431–1443. https://doi.org/10.1111/j.1365-246X.2011.05020.x
Bommer, J. J. (2012). Challenges of building logic trees for probabilistic seismic hazard analysis. *Earthquake Spectra*, *28*, 1723–1735.
Bommer, J. J., & Scherbaum, F. (2008). The use and misuse of logic trees in probabilistic seismic hazard analysis. *Earthquake Spectra*, *24*, 997–1009.
Bonaccorso, A., Calvari, S., Garfí, L., Lodato, L., & Patané, D. (2003). Dynamics of the December 2002 flank failure and tsunami at stromboli volcano inferred by volcanological and geophysical observations. *Geophysical Research Letters*, *30*, 1941. https://doi.org/10.1029/2003GL017702
Bondevik, S., Løvholt, F., Harbitz, C. B., Mangerud, J., Dawson, A., & Svendsen, J. I. (2005). The Storegga slide tsunami—Comparing field observations with numerical simulations. *Marine Petroleum and Geology*, *22*(1–2), 195–209.
Bonneton, P., Barthelemy, E., Chazel, F., Cienfuegos, R., Lannes, D., Marche, F., & Tissier, M. (2011). Recent advances in Serre-Green Naghdi modelling for wave transformation, breaking and runup processes. *European Journal of Mechanics-B/Fluids*, *30*(6), 589–597.
Boring, R., Gertman, D., Joe, G., Marble, J., Galyean, W., Blackwood, L., & Blackman, H. (2005). Simplified expert elicitation guideline for risk assessment of operating events, *Idaho National Laboratory: Department of Energy National Laboratory*. Idaho: Idaho Falls. Retrieved from http://www.inl.gov/technicalpublications/Documents/3310952.pdf
Budnitz, R. J., Apostolakis, G., Boore, D. M., Cluff, L. S., Coppersmith, K. J., Cornell, C. A., & Morris, P. A. (1998). Use of technical expert panels: Applications to probabilistic seismic hazard analysis. *Risk Analysis*, *18*(4), 463–469.
Burbidge, D., Cummins, P. R., Mleczko, R., & Thio, H. K. (2008). A probabilistic tsunami hazard assessment for Western Australia. *Pure and Applied Geophysics*, *165*(11–12), 2059–2088. https://doi.org/10.1007/S00024-008-0421-X
Burnham, K. P., & Anderson, D. R. (2002). *Model selection and multimodel inference: A practical information-theoretic approach* (2nd ed.). New York: Springer-Verlag.
Burroughs, S. M., & Tebbens, S. F. (2005). Power-law scaling and probabilistic forecasting of tsunami runup heights. *Pure and Applied Geophysics*, *162*, 331–342.
Butler, R., Frazer, L. N., & Templeton, W. J. (2016). Bayesian probabilities for M_w 9.0+ earthquakes in the Aleutian Islands from a regionally scaled global rate. *Journal of Geophysical Research: Solid Earth*, *121*, 3586–3608. https://doi.org/10.1002/2016JB012861
Camerlenghi, A., Urgeles, R., & Fantoni, L. (2010). A database on submarine landslides of the Mediterranean Sea. In D. C. Mosher, et al. (Eds.), *Submarine mass movements and their consequences. Advances in Natural and Technological Hazards Research* (Vol. 28, pp. 491–501). Dordrecht: Springer.
Carey, S., Sigurdsson, H., Mandeville, C., & Bronto, S. (2000). Volcanic hazards from pyroclastic flow discharge into the sea: Examples from the 1883 eruption of Krakatau, Indonesia. *Geological Society of America Special Publication*, *345*, 1–14.
Chaytor, J., ten Brink, U. S., Solow, A. R., & Andrews, B. D. (2009). Size distribution of submarine landslides along the U.S. Atlantic Margin. *Marine Geology*, *264*, 16–27.
Choi, B. H., Pelinovsky, E., Kim, K. O., & Lee, J. S. (2003). Simulation of the trans-oceanic tsunami propagation due to the 1883 Krakatau volcanic eruption. *Natural Hazards and Earth System Sciences*, *3*, 321–332.
Choi, B. H., Pelinovsky, E., Ryabov, I., & Hong, S. J. (2002). Distribution functions of tsunami wave heights. *Natural Hazards and Earth System Sciences*, *25*, 1–21.
Chock, G. (2015). The ASCE 7, tsunami loads and effects design standard for the U.S. American Concrete Institute Special Publication 313.
Cisternas, M., Atwater, B. F., Torrejón, F., Sawai, Y., Machuca, G., Lagos, M., & Eipert, A. (2005). Predecessors of the giant 1960 Chile earthquake. *Nature*, *437*(7057), 404–407. https://doi.org/10.1038/nature03943
Cloke, H. L., & Pappenberger, F. (2009). Ensemble flood forecasting: A review. *Journal of Hydrology*, *375*(3–4), 613–626. https://doi.org/10.1016/j.jhydrol.2009.06.005
Comer, R. P. (1980). Tsunami height and earthquake magnitude: Theoretical basis of an empirical relation. *Geophysical Research Letters*, *7*, 445–448.
Cooke, R. (1991). *Experts in uncertainty: Opinion and subjective probability in science*. New York: Oxford University Press.
Cooke, R. M., & Goossens, L. H. J. (1999). Procedures guide for structured expert judgement in accident consequence modelling. *Radiation Protection Dosimetry*, *90*(3), 303–309.
Coppersmith, K. J., Bommer, J. J., Kammerer, A. M., & Ake, J. (2010). *Implementation guidance for SSHAC level 3 and 4 processes. Paper presented at Probabilistic Safety Assessment and Management Conference* (pp. 3068–3078). Seattle, Washington.
Cornell, C. A. (1968). Engineering seismic risk analysis. *Bulletin of the Seismological Society of America*, *58*, 1583–1606.
Corral, A. (2005). Time-decreasing hazard and increasing time until the next earthquake. *Physical Review E*, *71*, 017101. https://doi.org/10.1103/PhysRevE.1171.017101
Crosta, G. B., Imposimato, S., & Roddeman, D. (2016). Landslide spreading, impulse water waves and modelling of the vajont rockslide. *Rock Mechanics and Rock Engineering*, *49*, 2413–2436. https://doi.org/10.1007/s00603-015-0769-z
Cummins, P. (2004). Small threat, but warning sounded for tsunami research, *AusGeo News 75*. Geoscience Australia: Canberra.
Dall'Osso, F., Dominey-Howes, D., Moore, C., Summerhayes, S., & Withycombe, G. (2014). The exposure of Sydney (Australia) to earthquake-generated tsunamis, storms and sea level rise: A probabilistic multi-hazard approach. *Science Reports*, *4*, 7401. https://doi.org/10.1038/srep07401
Davies, G., Griffin, J., Løvholt, F., Glimsdal, S., Harbitz, C., Thio, H. K., … Baptista, A. M. (2017). A global probabilistic tsunami hazard assessment from earthquake sources. In E. M. Scourse, et al. (Eds.), *Tsunamis: Geology, Hazards and Risks*. London: Geological Society of London Spec. Pub., 456. https://doi.org/10.1144/SP1456.1146

Davies, G., Horspool, N., & Miller, V. (2015). Tsunami inundation from heterogeneous earthquake slip distributions: Evaluation of synthetic source models. *Journal of Geophysical Research*, *120*, 6431–6451.
Day, S. J. (2015). Volcanic Tsunamis. In H. Sigurdsson, et al. (Eds.), *Encyplopedia of volcanoes* (2nd ed., pp. 993–1009). London, UK: Academic Press.
Defant, A. (1961). *Physical oceanography*. New York, NY: Pergamon Press.
De Jong, M. P. C., & Battjes, J. A. (2004). Seiche characteristics of Rotterdam Harbour. *Coastal Engineering*, *51*, 373–386. https://doi.org/10.1016/j.coastaleng.2004.04.002
Dengler, L., Uslu, B., Barberopoulou, A., Yim, S. C., & Kelly, A. (2009). The November 15, 2006 Kuril Islands-generated tsunami in Crescent City, California. *Pure and Applied Geophysics*, *166*, 37–53. https://doi.org/10.1007/s00024-008-0429-2
De Risi, R., & Goda, K. (2016). Probabilistic earthquake-tsunami multi-hazard analysis: Application to the Tohoku region, Japan. *Frontiers in Built Environment*, *2*, 2–25. https://doi.org/10.3389/fbuil.2016.00025
Dettmer, J., Hawkins, R., Cummins, P. R., Hossen, J., Sambridge, M., Hino, R., & Inazu, D. (2016). Tsunami source uncertainty estimation: The 2011 Japan tsunami. *Journal of Geophysical Research: Solid Earth*, *121*, 4483–4505. https://doi.org/10.1002/2015JB012764
Dmowska, R., Zheng, G., & Rice, J. R. (1996). Seismicity and deformation at convergent margins due to heterogeneous coupling. *Journal of Geophysical Research*, *101*, 3015–3029.
Downes, G. L., & Stirling, M. W. (2001). Groundwork for development of a probabilistic tsunami hazard model for New Zealand. *ITS2001 Proceeding Session*, *1*, 1–6.
Dragani, W. C., D'Onofrio, E. E., Oreiro, F., Alonso, G., Fiore, M., & Grismeyer, W. (2014). Simultaneous meteorological tsunamis and storm surges at Buenos Aires coast, south-eastern South America. *Natural Hazards*, *74*, 11–24. https://doi.org/10.1007/s11069-013-0836-2
Duputel, Z., Rivera, L., Kanamori, H., & Hayes, G. (2012). W phase source inversion for moderate to large earthquakes (1990–2010). *Geophysical Journal International*, *189*(2), 1125–1147.
Earth Impact Database (EID) (2017). Earth impact database. Retrieved from http://www.passc.net/EarthImpactDatabase/index.html. Accessed 1 February 2017
Emergency Events Database (EM-DAT) (2017). Centre for Research on the Epidemiology of Disasters. Retrieved from http://www.emdat.be
Fernandez, M., Molina, E., Havskov, J., & Atakan, K. (2000). Tsunamis and tsunami hazards in central america. *Natural Hazards*, *22*, 91–116.
Field, E. H., Biasi, G. P., Bird, P., Dawson, T. E., Felzer, K. R., Jackson, D. D., … Zeng, Y. (2015). Long-term, time-dependent probabilities for third Uniform California Earthquake Rupture Forecast (UCERF3). *Bulletin of the Seismological Society of America*, *105*, 511–543. https://doi.org/10.1785/0120140093
Fine, I. V., Rabinovich, A. B., Bornhold, B., Thomson, R. E., & Kulikov, E. A. (2005). The Grand Banks landslide-generated tsunami of November 18, 1929: Preliminary analysis and numerical modelling. *Marine Geology*, *215*, 45–57. https://doi.org/10.1016/j.margeo.2004.11.007
Folch, A., & Marti, J. (2009). Time-dependent chamber and vent conditions during explosive caldera-forming eruptions. *Earth and Planetary Science Letters*, *280*, 246–253. https://doi.org/10.1016/j.epsl.2009.01.035
Frankel, A. (2013). Comment on "Why earthquake hazard maps often fail and what to do about it" by S. Stein, R. Geller, and M. Liu. *Tectonophysics*, *592*, 200–206.
Freundt, A. (2003). Entrance of hot pyroclastic flows into the sea: Experimental observations. *Bulletin of Volcanology*, *65*, 144–164.
Fritz, H., Hager, W. H., & Minor, H.-E. (2003). Landslide generated impulse waves. 2. Hydrodynamic impact craters. *Experiments in Fluids*, *35*, 520–532. https://doi.org/10.1007/s00348-003-0660-7
Fritz, H., Hager, W. H., & Minor, H.-E. (2004). Near field characteristics of landslide generated impulse waves. *Journal of Waterway, Port, Coastal, and Ocean Engineering*, *130*, 287–302. https://doi.org/10.1061/(ASCE)0733-950X(2004)130:6(287)
Fuhrman, D. R., & Madsen, P. A. (2009). Tsunami generation, propagation, and runup with a high-order Boussinesq model. *Coastal Engineering*, *56*(7), 747–758.
Fujii, Y., & Satake, K. (2007). Tsunami source of the 2004 Sumatra-Andaman earthquake inferred from tide gauge and satellite data. *Bulletin of the Seismological Society of America*, *97*(1), 192–207. https://doi.org/10.1785/0120050613
Fujii, Y., & Satake, K. (2013). Slip distribution and seismic moment of the 2010 and 1960 Chilean earthquakes inferred from tsunami waveforms and coastal geodetic data. *Pure and Applied Geophysics*, *170*(9–10), 1493–1509. https://doi.org/10.1007/s00024-012-0524-2
Fujii, Y., Satake, K., Sakai, S. I., Shinohara, M., & Kanazawa, T. (2011). Tsunami source of the 2011 off the Pacific coast of Tohoku Earthquake. *Earth, Planets and Space*, *63*(7), 815–820. https://doi.org/10.5047/eps.2011.06.010
Fukao, Y. (1979). Tsunami earthquakes and subduction processes near deep-sea trenches. *Journal of Geophysical Research*, *84*, 2303–2314.
Gault, D. E., & Sonett, C. P. (1982). Laboratory simulation of pelagic asteroidal impact: Atmospheric injection, benthic topography, and the surface wave radiation field. In L. T. Silver & P. H. Schultz (Eds.), *Geological implications of impacts of large asteroids and comets on the Earth* (Vol. 190, pp. 69–92). Bolder, CO: Geological Society of America Special Paper.
Geist, E. L. (2002). Complex earthquake rupture and local tsunamis. *Journal of Geophysical Research*, *107*(B5), 2086. https://doi.org/10.1029/2000JB000139
Geist, E. L., Chaytor, J. D., Parsons, T., & ten Brink, U. (2013). Estimation of submarine mass failure probability from a sequence of deposits with age dates. *Geosphere*, *9*, 287–298.
Geist, E. L., & Dmowska, R. (1999). Local tsunamis and distributed slip at the source. In *Seismogenic and tsunamigenic processes in shallow subduction zones* (pp. 485–512). Springer.
Geist, E. L., & Lynett, P. J. (2014). Source processes for the probabilistic assessment of tsunami hazards. *Special Issue on Undersea Natural Hazards, Oceanography*, *27*(2), 86–93. https://doi.org/10.5670/oceanog.2014.43
Geist, E. L., & Oglesby, D. D. (2014). Tsunami: Stochastic models of occurrence and generation mechanisms. In A. Meyers (Ed.), *Encyclopedia of Complexity and Systems Science* (pp. 1–29). New York: Springer.
Geist, E. L., & Parsons, T. (2005). Triggering of tsunamigenic aftershocks from large strike-slip earthquakes: Analysis of the November 2000 New Ireland earthquake sequence. *Geochemistry, Geophysics, Geosystems*, *6*, Q10005. https://doi.org/10.1029/2005GC000935
Geist, E. L., & Parsons, T. (2006). Probabilistic analysis of tsunami hazards. *Natural Hazards*, *37*, 277–314. https://doi.org/10.1007/S11069-005-4646-Z
Geist, E. L., & Parsons, T. (2009). Assessment of source probabilities for potential tsunamis affecting the U.S. Atlantic coast. *Marine Geology*, *264*, 98–108.
Geist, E. L., & Parsons, T. (2010). Estimating the empirical probability of submarine landslide occurrence. In D. C. Mosher, et al. (Eds.), *Submarine mass movements and their consequences* (Vol. 28, pp. 377). Advances in Natural and Technological Hazards Research. Dordrecht: Springer
Geist, E. L., & Parsons, T. (2011). Assessing historical rate changes in global tsunami occurrence. *Geophysical Journal International*, *187*, 497–509.

Geist, E. L., & Parsons, T. (2014). Undersampling power-law size distributions: Effect on the assessment of extreme natural hazards. *Natural Hazards*, *72*, 565–595. https://doi.org/10.1007/s11069-013-1024-0

Geist, E. L., & Parsons, T. (2016). Reconstruction of far-field tsunami amplitude distributions from earthquake sources. *Pure and Applied Geophysics*, *172*(12), 3703–3717. https://doi.org/10.1007/s00024-00016-01288-x

Geist, E. L., ten Brink, U., & Gove, M. (2014). A framework for the probabilistic analysis of meteotsunamis. *Natural Hazards*, *74*, 123–142. https://doi.org/10.1007/S11069-014-1294-1

Gelman, A., Carlin, J. B., Stern, H. S., & Rubin, D. B. (2013). *Bayesian data analysis* (Vol. 667). Boca Raton, FA: Chapman & Hall/CRC Press.

Gersonde, R., Kyte, F. T., Bleil, U., Diekmann, B., Flores, J. A., Gohl, K., … Bostwick, J. A. (1997). Geological record and reconstruction of the late Pliocene impact of the Eltanin asteroid in the southern ocean. *Nature*, *390*, 357–363.

Giachetti, T., Paris, R., Kelfoun, K., & Pérez Torrado, F. J. (2011). Numerical modelling of the tsunami triggered by the Güimar debris avalanche, Tenerife Canary Islands: Comparison with field-based data. *Marine Geology*, *284*, 189–202.

Gisler, G., Weaver, R., & Gittings, M. (2011). Calculations of asteroid impacts into deep and shallow water. *Pure and Applied Geophysics*, *168*, 1187–1198. https://doi.org/10.1007/s00024-010-0225-7

Gisler, G. R., Heberling, T., Plesko, C. S., & Weaver, R. P. (2017). Three-dimensional simuations of oblique asteroid impacts into water, *Lunar and Planetary Science, XLVIII*. Los Alamos: Los Alamos National Laboratory.

Glimsdal, S., Pedersen, G. K., Langtangen, H. P., Shuvalov, V., & Dypvik, H. (2007). Tsunami generation and propagation from the Mjølnir asteroid impact. *Meteoritics & Planetary Science*, *42*, 1473–1493. https://doi.org/10.1111/j.1945-5100.2007.tb00586.x

Glimsdal, S., Pedersen, G. K., Harbitz, C. B., & Løvholt, F. (2013). Dispersion of tsunamis: Does it really matter?. *Natural Hazards and Earth System Science*, *13*, 1507–1526. https://doi.org/10.5194/nhess-13-1507-2013

Goda, K., Mai, P. M., Yasuda, T., & Mori, N. (2014). Sensitivity of tsunami wave profiles and inundation simulations to earthquake slip and fault geometry for the 2011 Tohoku earthquake. *Earth Planet Space*, *66*, 105. https://doi.org/10.1186/1880-5981-66-105

González, F. I., Geist, E. L., Jaffe, B., KaNogLu, U., Mofjeld, H., Synolakis, C. E., … Yalciner, A. (2009). Probabilistic tsunami hazard assessment at seaside, oregon, for near- and far-field seismic sources. *Journal of Geophysical Research*, *114*, C11023. https://doi.org/10.1029/2008JC005132

González, F. I., LeVeque, R. J., Adams, L. M., Goldfinger, C., Priest, G. R., & Wang, K. (2014). Probabilistic Tsunami Hazard Assessment (PTHA) for Crescent City, CA. Retrieved from http://hdl.handle.net/1773/25916

Greenspan, H. P. (1956). The generation of edge waves by moving pressure distributions. *Journal of Fluid Mechanics*, *1*, 574–592. https://doi.org/10.1017/S002211205600038X

Grezio, A., Lorito, S., Parsons, T., & Selva, J. (2017). Tsunamis: Bayesian Probabilistic Hazard Analysis. In R.t A. Meyers (Ed.), *Encyclopedia of Complexity and Systems Science* (pp. 1–25). Berlin: Springer. https://doi.org/10.1007/978-3-642-27737-5_645-1

Grezio, A., Marzocchi, W., Sandri, L., & Gasparini, P. (2010). A bayesian procedure for probabilistic tsunami hazard assessment. *Natural Hazards*, *53*, 159–174. https://doi.org/10.1007/s11069-009-9418-8

Grezio, A., Sandri, L., Marzocchi, W., Argnani, A., & Gasparini, P. (2012). Probabilistic tsunami hazard assessment for messina strait area (Sicily, Italy). *Natural Hazards*, *64*, 329–358.

Grezio, A., Tonini, R., Sandri, L., Pierdominici, S., & Selva, J. (2015). A methodology for a comprehensive probabilistic tsunami hazard assessment: Multiple sources and short-term interactions. *Journal of Marine Science and Engineering*, *3*, 23–51. https://doi.org/10.3390/jmse3010023

Griffin, J., Latief, H., Kongko, W., Harig, S., Horspool, N., Hanung, R., … Upi, S. (2015). An evaluation of onshore digital elevation models for modeling tsunami inundation zones. *Frontiers in Earth Science*, *3*, 1–32.

Griffin, J., Pranantyo, I. R., Kongko, W., Haunan, A., Robiana, R., Miller, V., … Latief, H. (2016). Assessing tsunami hazard using heterogeneous slip models in the Mentawai Islands, Indonesia. *Geological Society, London, Special Publications*, *441*(1), 47–70. https://doi.org/10.1144/SP441.3

Grilli, S. T., Shelby, M., Kimmoun, O., Dupont, G., Nicolsky, D., Ma, G., … Shi, F. (2017). Modeling coastal tsunami hazard from submarine mass failures: Effect of slide rheology, experimental validation, and case studies off the US East Coast. *Natural Hazards*, *86*, 74–97. https://doi.org/10.1007/s11069-016-2692-3

Grilli, S. T., Taylor, S. O., Baxter, C. D. P., & Maretzki, S. A. (2009). A probabilistic approach for determining submarine landslides tsunami hazard along the upper east coast of the United States. *Marine Geology*, *264*, 74–97.

Grilli, S. T., & Watts, P. (2005). Tsunami generation by submarine mass failure. I: Modelling, experimental validation, and sensitivity analyses. *Journal of Waterway, Port, Coastal, and Ocean Engineering*, *131*, 283–297. https://doi.org/10.1061/(ASCE)0733-950X(2005)131:6(283)

Gubler, A., Catalán, P. A., & Hayashi, Y. (2013). Probabilistic tsunami hazard assessment for near-field events. *Coastal Dynamics*, *2013*, 759–768.

Gusman, A. R., Tanioka, Y., Matsumoto, H., & Iwasaki, S. I. (2009). Analysis of the Tsunami generated by the great 1977 Sumba earthquake that occurred in Indonesia. *Bulletin of the Seismological Society of America*, *99*(4), 2169–2179.

Gusman, A. R., Tanioka, Y., Sakai, S., & Tsushima, H. (2012). Source model of the great 2011 Tohoku earthquake estimated from tsunami waveforms and crustal deformation data. *Earth and Planetary Science Letters*, *341*, 234–242.

Gutenberg, B., & Richter, C. F. (1941). Seismicity of the Earth. *Geological Society of America Bulletin, Special Papers*, *34*, 1–131.

Gutenberg, B., & Richter, C. F. (1944). Frequency of earthquakes in California. *Bulletin of the Seismological Society of America*, *34*, 185–188.

Gylfadottir, S., Kim, J., Helgason, J. K., Brynjólfsson, S., Höskuldsson, A., Jóhannesson, T., … Løvholt, F. (2017). The 2014 Lake Askja rockslide-induced tsunami: Optimization of numerical tsunami model using observed data. *Journal of Geophysical Research: Oceans*, *122*, 4110–4122. https://doi.org/10.1002/2016JC012496

Hammack, J. L. (1973). A note on tsunamis: Their generation and propagation in an ocean of uniform depth. *Journal of Fluid Mechanics*, *60*, 769–799.

Hanks, T. C., Abrahamson, N. A., Boore, D. M., Coppersmith, K. J., & Knepprath, N. E. (2009). Implementation of the SSHAC guidelines for level 3 and 4 PSHAs—Experience gained from actual applications (US Geological Survey Open-File Report 2009-1093). Reston, VA: US Geological Survey.

Harbitz, C. B. (1992). Model simulations of tsunamis generated by the Storegga slides. *Marine Geology*, *105*, 1–21.

Harbitz, C. B., Glimsdal, S., Løvholt, F., Kveldsvik, V., Pedersen, G. K., & Jensen, A. (2014). Rockslide tsunamis in complex fjords: From an unstable rock slope at Åkerneset to tsunami risk in western Norway. *Coastal Engineering*, *88*, 101–122. https://doi.org/10.1016/j.coastaleng.2014.02.003

Harbitz, C. B., Løvholt, F., & Bungum, H. (2014). Submarine landslide tsunamis: How extreme and how likely? *Natural Hazards*, *72*, 1341–1374. https://doi.org/10.1007/S11069-013-0681-3

Harig, S., Pranowo, W. S., & Behrens, J. (2008). Tsunami simulations on several scales. *Ocean Dynamics*, *58*(5–6), 429–440.

Hatori, T. (1967). The generating area of Sanriku tsunami of 1896 and its comparison with the tsunami of 1933. *Journal of Seismological Society of Japan*, *20*, 164–170. https://doi.org/10.4294/zisin1948.20.3_164
Haugen, K. B., Løvholt, F., & Harbitz, C. B. (2005). Fundamental mechanisms for tsunami generation by submarine mass flows in idealised geometries. *Marine Petroleum and Geology*, *22*(1–2), 209–219.
Heidarzadeh, M., & Satake, K. (2014). The El Salvador and Philippines tsunamis of August 2012: Insights from sea level data analysis and numerical modeling. *Pure and Applied Geophysics*, *171*(12), 3437–3455.
Heidarzaed, M., & Kijko, A. (2011). A probabilistic tsunami hazard assessment for the Makran subduction zone at the northwestern Indian Ocean. *Natural Hazards*, *56*, 577–593.
Heinrich, P., Schindele, F., Guibourg, S., & Ihmlé, P. F. (1998). Modeling of the February 1996 Peruvian tsunami. *Geophysical Research Letters*, *25*, 2687–2690.
Heller, V., & Spinneken, J. (2013). Improved landslide-tsunami prediction: Effects of block model parameters and slide model. *Journal of Geophysical Research: Oceans*, *118*, 1489–1507. https://doi.org/10.1002/jgrc.20099
Hidayat, D., Barker, J. S., & Satake, K. (1995). Modeling the seismic source and tsunami generation of the December 12, 1992 Flores island, Indonesia, earthquake. *Pure and Applied Geophysics*, *144*, 537–554.
Hoechner, A., Babeyko, A. Y., & Zamora, N. (2016). Probabilistic tsunami hazard assessment for the Makran region with focus on maximum magnitude assumption. *Natural Hazards and Earth System Science*, *16*, 1339–1350. https://doi.org/10.5194/nhess-16-1339-2016
Hora, S. C. (2007). Eliciting probabilities from experts. In W. Edwards, R. F. Miles, & D. von Winterfeldt Jr. (Eds.), *Advances in Decision Analysis: From Foundations to Applications*, PART III, (Cap. 8, p. 129–153), https://doi.org/10.1017/CBO9780511611308.009 Cambridge, UK: Cambridge University Press.
Horrillo, J., Grilli, S. T., Nicolsky, D., Roeber, V., & Zhang, J. (2014). Performance benchmarking tsunami models for nthmpõs inundation mapping activities. *Pure and Applied Geophysics*, *172*(3–4), 869–884. https://doi.org/10.1007/s00024-014-0891-y
Horspool, N., Pranantyo, I., Griffin, J., Latief, H., Natawidjaja, D. H., Kongko, W., … Thio, H. K. (2014). A probabilistic tsunami hazard assessment for Indonesia. *Natural Hazards and Earth System Science*, *14*, 3105–3122. https://doi.org/10.5194/Nhess-14-3105-2014
Horvath, K., & Vilibic, I. (2014). Atmospheric mesoscale conditions during the Boothbay meteotsunami: A numerical sensitivity study using a high-resolution mesoscale model. *Natural Hazards*, *74*, 55–74. https://doi.org/10. 1007/978-3-319-12712-5_4
Hunt, J. E., Wynn, R. B., Talling, P. J., & Masson, D. G. (2013). Multistage collapse of eight western Canary Island landslides in the last 1.5 Ma: Sedimentological and geochemical evidence from subunits in submarine flow deposits. *Geochemistry, Geophysics, Geosystems*, *14*, 2159–2181. https://doi.org/10.1002/ggge.20138
Intergovernmental Panel on Climate Change (IPCC) (1998). PRINCIPLES GOVERNING IPCC WORK. Approved at the Fourteenth Session (Vienna, 1–3 October 1998) on 1 October 1998, amended at the Twenty-First Session (Vienna, 3 and 6–7 November 2003), the Twenty-Fifth Session (Mauritius, 26–28 April 2006), the Thirty-Fifth Session (Geneva, 6–9 June 2012) and the Thirty-Seventh Session (Batumi, 14–18 October 2013). Retrieved from http://www.ipcc.ch/pdf/ipcc-principles/ipcc-principles.pdf. Accessed 10 October 2016.
International Tsunami Information Center (2015). Pacific tsunami warning system—A half-century of protecting the Pacific, International Tsunami Information Center.
Ito, Y., Tsuji, T., Osada, Y., Kido, M., Inazu, D., Hayashi, Y., … Fujimoto, H. (2011). Frontal wedge deformation near the source region of the 2011 2011 Tohoku-Oki earthquake. *Geophysical Research Letters*, *38*, L00G05. https://doi.org/10.1029/2011GL048355
Jaimes, M. A., Reinoso, E., Ordaz, M., Huerta, B., Silva, R., Mendoza, E., & Rodríguez, J. C. (2016). A new approach to probabilistic earthquake-induced tsunami risk assessment. *Ocean & Coastal Management*, *119*, 68–75. https://doi.org/10.1016/j.ocecoaman.2015.10.007
Jingming, H., Xiaojuan, L., Ye, Y., & Peitao, W. (2016). Tsunami hazard assessment along the Chinese mainland coast from earthquakes in the Taiwan region. *Natural Hazards*, *81*, 1269–1281. https://doi.org/10.1007/s11069-015-2133-8
Kagan, Y. Y. (1992). Correlations of earthquake focal mechanisms. *Geophysical Journal International*, *110*, 305–320.
Kagan, Y. Y. (1997). Seismic moment-frequency relation for shallow earthquakes: Regional comparison. *Journal of Geophysical Research*, *102*, 2835–2852.
Kagan, Y. Y. (2002). Seismic moment distribution revisited: I. Statistical results. *Geophysical Journal International*, *148*, 520–541.
Kagan, Y. Y. (2002). Seismic moment distribution revisited: II. Moment conservation principle. *Geophysical Journal International*, *149*, 731–754.
Kagan, Y. Y. (2014). *Earthquakes: Models, statistics, testable forecasts* (p. 306). Washington, DC: American Geophysical Union.
Kagan, Y. Y., & Jackson, D. D. (2013). Tohoku earthquake: A surprise?. *Bulleting of the Seismological Society of America*, *103*, 1181–1194.
Kagan, Y. Y., & Schoenberg, F. (2001). Estimation of the upper cutoff parameter for the tapered Pareto distribution. *Journal of Applied Probability*, *38A*, 158–175.
Kaiser, G., Scheele, L., Kortenhaus, A., Løvholt, F., R:omer, H., & Leschka, S. (2011). The influence of land cover roughness on the results of high resolution tsunami inundation modeling. *Natural Hazards and Earth System Sciences*, *11*(9), 2521–2540.
Kaistrenko, V. (2011). Tsunami recurrence versus tsunami height distribution along the coast. *Pure and Applied Geophysics*, *168*, 2065–2069.
Kajiura, K. (1963). The leading wave of a tsunami. *Bulletin of the Earthquake Research Institute*, *41*, 535–571.
Kanamori, H. (1972). Mechanism of tsunami earthquakes. *Physics of the Earth and Planetary Interiors*, *6*, 346–359.
Kanamori, H. (1977). The energy release in great earthquakes. *Journal of Geophysical Research*, *82*(20), 2981–2987. https://doi.org/10.1029/JB082i020p02981
Kanamori, H., & Brodsky, E. E. (2004). The physics of earthquakes. *Reports on Progress in Physics*, *67*, 1429–1496. https://doi.org/10.1088/0034-4885/67/8/R03
Kanamori, H., & Given, J. W. (1981). Use of long-period surface waves for rapid determination of earthquake source parameters. *Physics of the Earth and Planetary Interiors*, *27*, 8–31.
Kanamori, H., & Kikuchi, M. (1993). The 1992 Nicaragua earthquake—A slow tsunami earthquake associated with subducted sediments. *Nature*, *361*, 714–716.
Kanamori, H., & Rivera, L. (2008). Source inversion of W phase: Speeding up seismic tsunami warning. *Geophysical Journal International*, *175*(1), 222–238.
Kawamura, K., Laberg, J. S., & Kanamatsu, T. (2014). Potential tsunamigenic submarine landslides in active margins. *Marine Geology*, *356*, 44–49.
Keating, B. H., & McGuire, W. J. (2000). Island edifice failures and associated tsunami hazards. *Pure and Applied Geophysics*, *157*, 899–955.
Kelfoun, K. (2011). Suitability of simple rheological laws for the numerical simulation of dense pyroclastic flows and long-runout volcanic avalanches. *Journal of Geophysical Research*, *116*, B08209. https://doi.org/10.1029/2010JB007622
Kennedy, A. B., Chen, Q., Kirby, J. T., & Dalrymple, R. A. (2000). Boussinesq modeling of wave transformation, breaking, and runup. I: 1D. *Journal of Waterway, Port, Coastal, and Ocean Engineering*, *126*(1), 39–47.

Kienle, J., Kowalik, Z., & Murty, T. S. (1987). Tsunamis generated by eruptions from Mount St. Augustine Volcano, Alaska. *Science*, *236*, 1442–1447.
Kim, M. K., & Choi, I.-K. (2012). A tsunami PSA methodology and application for NPP site in Korea. *Nuclear Engineering and Design*, *244*, 92–99.
Kim, D. H., Lynett, P. J., & Socolofsky, S. A. (2009). A depth-integrated model for weakly dispersive, turbulent, and rotational fluid flows. *Ocean Modelling*, *27*(3–4), 198–214. https://doi.org/10.1016/j.ocemod.2009.01.005
Kirby, J. T., Shi, F., Tehranirad, B., Harris, J. C., & Grilli, S. T. (2013). Dispersive tsunami waves in the ocean: Model equations and sensitivity to dispersion and Coriolis effects. *Ocean Modeling*, *62*, 39–55.
Knighton, J., & Bastidas, L. A. (2015). A proposed probabilistic seismic tsunami hazard analysis methodology. *Natural Hazards*, *78*, 699–723. https://doi.org/10.1007/S11069-015-1741-7
Knoll, M., Tommasi, A., Logé, R., & Signorelli, J. (2009). A multiscale approach to model the anisotropic deformation of lithospheric plates. *Geochemistry, Geophysics, Geosystems*, *10*, Q08009. https://doi.org/10.1029/2009GC002423
Koketsu, K., Yokota, Y., Nishimura, N., Yagi, Y., Miyazaki, S. I., Satake, K., … Okada, T. (2011). A unified source model for the 2011 Tohoku earthquake. *Earth and Planetary Science Letters*, *310*(3), 480–487.
Korycansky, D. G., & Lynett, P. J. (2007). Runup from impact tsunami. *Geophysical Journal International*, *170*, 1076–1088.
Kowalik, Z., & Murty, T. S. (1993). *Numerical modeling of ocean dynamics* (p. 481). River Edge, NJ: World Scientific.
Kozdon, J. E., & Dunham, E. M. (2014). Constraining shallow slip and tsunami excitation in megathrust ruptures using seismic and ocean acoustic waves recorded on ocean-bottom sensor networks. *Earth and Planetary Science Letters*, *396*, 56–65. https://doi.org/10.1016/j.epsl.2014.04.001
Kulikov, E. A., Rabinovich, A. B., & Thomson, R. (2005). Estimation of tsunami risk for the coasts of Peru and northern Chile. *Natural Hazards*, *35*, 185–209.
Kulkarni, R. B., Youngs, R. R., & Coppersmith, K. J. (1984). Assessment of confidence intervals for results of seismic hazard analysis. In *Proceedings of the Eighth World Conference on Earthquake Engineering*, *1*, San Francisco, California.
Lane, E. M., Gillibrand, P. A., Wang, X., & Power, W. (2013). A probabilistic tsunami hazard study of the Auckland Region, Part II: inundation modelling and hazard assessment. *Pure and Applied Geophysics*, *170*, 1635–1646. https://doi.org/10.1007/s00024-012-0538-9
Lane, E. M., Mountjoy, J. J., Power, W. L., & Mueller, C. (2016). Probabilistic hazard of tsunamis generated by submarine landslides in the Cook Strait Canyon (New Zealand). *Pure and Applied Geophysics*, *173*, 1–18. https://doi.org/10.1007/s00024-016-1410-0
Lane, E. M., Mountjoy, J. J., Power, W. L., & Popinet, S. (2016). Initialising landslide-generated tsunamis for probabilistic tsunami hazard assessment in Cook Strait. *International Journal of Ocean and Climate Systems*, *7*, 4–13. https://doi.org/10.1177/1759313115623162
Lassa, J. (2009). The forgotten disaster? Remembering the Larantuka and Lembata disaster 1979–2009 [in Indonesian]. *Journal of NTT Studies*, *1*, 159–184.
Latief, H., Puspito, N., & Imamura, F. (2000). Tsunami catalog and zones in Indonesia. *Journal of Natural Disaster Science*, *22*, 25–43.
Latter, J. N. (1981). Tsunamis of volcanic origin: Summary of causes with particular references to Krakatoa, 1883. *Bulletin of Volcanology*, *443*, 467–490.
Lauterjung, J., Münch, U., & Rudloff, A. (2010). The challenge of installing a tsunami early warning system in the vicinity of the Sunda Arc Indonesia. *Natural Hazards and Earth System Science*, *10*, 641–646.
Lay, T. (2015). The surge of great earthquakes from 2004 to 2014. *Earth and Planetary Science Letters Invited Front. Pap.*, *409*, 133–146. https://doi.org/10.1016/j.epsl.2014.10.047?
Le Gal, M., Violeau, D., & Benoit, M. (2017). Influence of timescales on the generation of seismic tsunamis. *European Journal of Mechanics B/Fluids*, *65*, 257–273. https://doi.org/10.1016/j.euromechflu.2017.03.008
Le Méhauté, B. L., & Wang, S. (1996). *Water waves generated by underwater explosion*. New Jersey: Advanced Series on Ocean Engineering (World Scientific).
Legros, F., & Druitt, T. H. (2000). On the emplacement of ignimbrite in shallow-marine environments. *Journal of Volcanology and Geothermal Research*, *95*, 9–22.
Leonard, L. J., Rogers, G. C., & Mazzotti, S. (2014). Tsunami hazard assessment of Canada. *Natural Hazards*, *70*, 237–274.
LeVeque, R. J., George, D. L., & Berger, M. J. (2011). Tsunami modelling with adaptively refined finite volume methods. *Acta Numerica*, *20*, 211–289. https://doi.org/10.1017/S0962492911000043
LeVeque, R. J., Waagan, K., González, F. I., Rim, D., & Lin, G. (2016). Generating random earthquake events for probabilistic tsunami hazard assessment. *Pure and Applied Geophysics*, *173*, 3671–3692. https://doi.org/10.1007/s00024-016-1357-1
Li, L., Switzer, A. D., Chan, C.-H., Wang, Y., Weiss, R., & Qiu, Q. (2016). How heterogeneous coseismic slip affects regional probabilistic tsunami hazard assessment: A case study in the South China Sea. *Journal of Geophysical Research*, *121*(8), 6250–6272.
Lin, I.-C., & Tung, C. C. (1982). A preliminary investigation of tsunami hazard. *Bulletin of the Seismological Society of America*, *72*(6A), 2323–2337.
Linstone, H. A., & Turoff, M. (1975). *The Delphi method: Techniques and applications*. Reading: Addison-Wesley Publishing Company Advanced Book Program.
Liu, P. L. F., Cho, Y. S., Yoon, S. B., & Seo, S. N. (1995). Numerical simulations of the 1960 Chilean tsunami propagation and inundation at Hilo, Hawaii, *Tsunami: Progress in prediction, disaster prevention and warning* (pp. 99–115). Netherlands: Springer.
Liu, Y., Santos, A., Wang, S. M., Shi, Y., Liu, H., & Yuen, D. A. (2007). Tsunami hazards along Chinese coast from potential earthquakes in South China Sea. *Physics of the Earth and Planetary Interiors*, *163*, 233–244.
Lomnitz, C. (2004). Major earthquakes of Chile: A historical survey, 1535-1960. *Seismological Research Letters*, *75*(3), 368–378. https://doi.org/10.1785/gssrl.75.3.368
Lorito, S., Romano, F., & Lay, T. (2016). Tsunamigenic earthquakes (2004–2013): Source processes from data inversion. In R. Meyers (Ed.), *Encyclopedia of complexity and systems science*. New York: Springer Science+Business Media New York 2015. https://doi.org/10.1007/978-3-642-27737-5641-1
Lorito, S., Selva, J., Basili, R., Romano, F., Tiberti, M. M., & Piatanesi, A. (2015). Probabilistic hazard for seismically induced tsunamis: Accuracy and feasibility of inundation maps. *Geophysical Journal International*, *200*(1), 574–588. https://doi.org/10.1093/gji/ggu408
Løvholt, F., Bondevik, S., Laberg, J. S., Kim, J., & Boylan, N. (2017). Some giant submarine landslides do not produce large tsunamis. *Geophysical Research Letters*, *44*, 8463–8472. https://doi.org/10.1002/2017GL074062
Løvholt, F., Glimsdal, S., Harbitz, C. B., Horspool, N., Smebye, H., de Bono, A., & Nadim, F. (2014). Global tsunami hazard and exposure due to large co-seismic slip. *International Journal of Disaster Risk Reduction*, *10*, Part B, 406–418. https://doi.org/10.1016/j.ijdrr.2014.04.003
Løvholt, F., Glimsdal, S., Harbitz, C. B., Zamora, N., Nadim, F., Peduzzi, P., … Smebye, H. (2012). Tsunami hazard and exposure on the global scale. *Earth-Science Reviews*, *110*(1), 58–73.

Løvholt, F., Griffin, J., & Salgado-Galvez, M. A. (2015). Tsunami hazard and risk assessment on the global scale. In R. A. Meyers (Ed.), *Encyclopedia of complexity and systems science* (pp. 1–34). Berlin, Heidelberg: Springer. https://doi.org/10.1007/978-3-642-27737-5_642-1

Løvholt, F., Pedersen, G., & Gisler, G. (2008). Oceanic propagation of a potential tsunami from the La Palma Island. *Journal of Geophysical Research*, *113*, C09026. https://doi.org/10.1029/2007JC004603

Løvholt, F., Pedersen, G., Harbitz, C. B., Glimsdal, S., & Kim, J. (2015). On the characteristics of landslide tsunamis. *Philosophical Transactions of the Royal Society A*, *373*, 20140376. https://doi.org/10.1098/rsta.2014.0376

Løvholt, F., Pedersen G., & Harbitz, C. B. (2016). Tsunami-genesis due to retrogressive landslides on an inclined seabed. In G. Lamarche, et al. (Eds.), *Submarine mass movements and their consequences: 7th International Symposium* (Vol. 41, pp. 569–578), Advances in Natural and Technological Hazards Research: Springer, Cham. https://doi.org/10.1007/978-3-319-20979-1_57

Lynett, P. J., Borrero, J., Son, S., Wilson, R., & Miller, K. (2014). Assessment of the tsunami-induced current hazard. *Geophysical Research Letters*, *41*, 2048–2055. https://doi.org/10.1002/2013GL058680

Lynett, P. J., & Liu, P. L.-F. (2002). A numerical study of submarine-landslide-generated waves and runup. *Proceedings of the Royal Society, Series A*, *458*, 20–28. https://doi.org/10.1098/rspa.2002.0973

Lynett, P. J., & Martinez, A. J. (2012). A Probabilistic approach for the waves generate by a submarine landslide. *Coastal Engineering Proceedings*, *N*(33), 1–15. https://doi.org/10.9753/icce.v33.currents.15

Lynett, P. J., Wu, T. R., & Liu, P. L. F. (2002). Modeling wave runup with depth-integrated equations. *Coastal Engineering*, *46*(2), 89–107.

Ma, K.-F., Kanamori, H., & Satake, K. (1999). Mechanism of the 1975 Kalapana, Hawaii, earthquake inferred from tsunami data. *Journal of Geophysical Research*, *104*(13), 153–167.

Ma, G., Shi, F., & Kirby, J. T. (2012). Shock-capturing non-hydrostatic model for fully dispersive surface wave processes. *Ocean Models*, *43–44*, 22–35. https://doi.org/10.1016/j.ocemod.2011.12.002

Maeno, F., & Imamura, F. (2011). Tsunami generation by a rapid entrance of pyroclastic flow into the sea during the 1883 Krakatau eruption, Indonesia. *Journal of Geophysical Research*, *116*, B09205. https://doi.org/10.1029/2011JB008253

Maramai, A., Graziani, L., Alessio, G., Burrato, P., Colini, L., Cucci, L., … Vilardo, G. (2005). Near- and far-field survey report of the 30 December 2002 Stromboli Southern Italy tsunami. *Marine Geology*, *215*, 93–106.

Maretzki, S., Grilli, S., & Baxter, C. D. P. (2007). Probabilistic SMF tsunami hazard assessment for the upper east coast of the United States. In V. Lykousis, D. Sakellariou, & J. Locat (Eds.), *Submarine mass movements and their consequences* (pp. 377–385). Netherlands: Springer.

Marzocchi, W., Sandri, L., & Selva, J. (2010). BET_VH: a probabilistic tool for long-term volcanic hazard assessment. *Bulletin of Volcanology*, *72*(6), 717–733.

Marzocchi, W., Taroni, M., & Selva, J. (2015). Accounting for epistemic uncertainty in PSHA: Logic tree and ensemble modeling. *Bulletin of the Seismological Society of America*, *105*(4), 2151–2159.

Marzocchi, W., & Jordan, T. H. (2014). Testing for ontological errors in probabilistic forecasting models of natural systems. *Proceedings of the National Academy of Sciences of the United States*, *85*, 955–959.

Marzocchi, W., & Zechar, J. D. (2011). Earthquake forecasting and earthquake prediction: Different approaches for obtaining the best model. *Seismological Research Letters*, *82*, 442–448.

Masson, D. G., Harbitz, C. B., Wynn, R. B., Pedersen, G., & Løvholt, F. (2006). Submarine landslides: processes, triggers and hazard prediction. *Philosophical Transactions of the Royal Society A*, *364*, 2009–2039. https://doi.org/10.1098/rsta.2006.1810

Matsui, T., Imamura, F., Tajika, E., Nakano, Y., & Fujiisawa, Y. (2002). Generation and propagation of a tsunami from the Cretaceous-Tertiary impact event. In C. Koerbel & K. G. MacLeod (Eds.), *Catastrophic events and mass extinctions: Impacts and beyond* (Vol. 356, pp. 69–77). Boulder, CO: Geological Society of America Special Paper.

McCaffrey, R. (2008). Global frequency of magnitude 9 earthquakes. *Geology*, *36*, 263–266. https://doi.org/10.1130/G24402A.1

McMurtry, G. M., Watts, P., Fryer, G. J., Smith, J. R., & Imamura, F. (2004). Giant landslides, mega-tsunamis and paleo-sea level in the Hawaiian Islands. *Marine Geology*, *203*, 219–233.

Mofjeld, H. O., Gonzáles, F. I., Titov, V. V., Venturato, A. J., & Newman, J. C. (2007). Effects of tides on maximum tsunami wave heights: Probability distributions. *Journal of Atmospheric and Oceanic Technology*, *24*(1), 117–123.

Mohammed, F., & Fritz, H. (2012). Physical modeling of tsunamis generated by three-dimensional deformable granular landslides. *Journal of Geophysical Research*, *117*, C11015. https://doi.org/10.1029/2011JC007850

Monserrat, S., Vilibić, I., & Rabinovich, A. B. (2006). Meteotsunamis: Atmospherically induced destructive ocean waves in the tsunami frequency band. *Natural Hazards and Earth System Science*, *6*(6), 1035–1051.

Moore, J. G., & Moore, G. W. (1984). Deposit from a giant wave on the island of Lanai, Hawaii. *Science*, *226*, 1312–1315.

Mori, J., Mooney, W. D., Afnimar, Kurniawan, S., Anaya, A. I., & Widiyantoro, S. (2007). The 17 July 2006 tsunami earthquake in West Java, Indonesia. *Seismological Research Letters*, *78*, 201–209.

Mori, N., Takahashi, T., Yasuda, T., & Yanagisawa, H. (2011). Survey of 2011 Tohoku earthquake tsunami inundation and runup. *Geophysical Research Letters*, *38*, L00G14. https://doi.org/10.1029/2011GL049210

Morgan, M. G. (2014). Use (and abuse) of expert elicitation in support of decision making for public policy. *Proceedings of the National academy of Sciences*, *111*(20), 7176–7184. https://doi.org/10.1073/pnas.1319946111

Mueller, C., Power, W., Fraser, S., & Wang, X. (2015). Effects of rupture complexity on local tsunami inundation: Implications for probabilistic tsunami hazard assessment by example. *Journal of Geophysical Research: Solid Earth*, *120*, 488–502. https://doi.org/10.1002/2014JB011301

Muhammad, A., Goda, K., & Alexander, N. (2016). Tsunami hazard analysis of future megathrust sumatra earthquakes in Padang, Indonesia using stochastic tsunami simulation. *Frontiers in Built Environment*, *2*, 33. https://doi.org/10.3389/fbuil.2016.00033

Murotani, S., Miyake, H., & Koketsu, K. (2008). Scaling of characterized slip models for plate-boundary earthquakes. *Earth, Planets and Space*, *60*, 987–991. https://doi.org/10.1186/BF03352855

Murotani, S., Satake, K., & Fujii, Y. (2013). Scaling relations of seismic moment, rupture area, average slip, and asperity size for *M*9 subduction-zone earthquakes. *Geophysical Research Letters*, *40*, 5070–5074. https://doi.org/10.1002/grl.50976

Murphy, S., Scala, A., Herrero, A., Lorito, S., Festa, G., Trasatti, E., … Nielsen, S. (2016). Shallow slip amplification and enhanced tsunami hazard unravelled by dynamic simulations of mega-thrust earthquakes. *Scientific Reports*, *6*, 35007.

Musson, R. M. W. (2005). Against fractiles. *Earthquake Spectra*, *21*(3), 887–891.

Natawidjaja, D. H., Sieh, K., Ward, S. N., Cheng, H., Edwards, R. L., Galetzka, J., & Suwargadi, B. W. (2004). Paleogeodetic records of seismic and aseismic subduction from central Sumatran microatolls, Indonesia. *Journal of Geophysical Research*, *109*, B04306. https://doi.org/10.1029/2003JB002398

Newcomb, K. R., & McCann, W. R. (1987). Seismic history and seismotectonics of the Sunda Arc. *Journal of Geophysical Research*, *92*, 421–439.

Newman, A. V., Hayes, G., Wei, Y., & Convers, J. (2011). The 25 October 2010 Mentawai tsunami earthquake, from real-time discriminants, finite-fault rupture, and tsunami excitation. *Geophysical Research Letters*, *38*, L05302. https://doi.org/10.1029/2010GL046498

Newman, A. V., & Okal, E. A. (1998). Teleseismic estimates of radiated seismic energy: The E/M_0 discriminant for tsunami earthquakes. *Journal of Geophysical Research*, *103*, 26,885–26,898.

Nomanbhoy, N., & Satake, K. (1995). Generation mechanism of tsunamis from the 1883 Krakatau eruption. *Geophysical Research Letters*, *224*, 509–512.

Nomura, S., Ogata, Y., Komaki, F., & Toda, S. (2011). Bayesian forecasting of recurrent earthquakes and predictive performance for a small sample size. *Journal of Geophysical Research*, *116*, B04315. https://doi.org/10.1029/2010JB007917

Nosov, M. A., Bolshakova, A. V., & Kolesov, S. V. (2014). Displaced water volume, potential energy of initial elevation, and tsunami intensity: Analysis of recent tsunami events. *Pure and Applied Geophysics*, *171*, 3515–3525.

Nosov, M. A., & Kolesov, S. V. (2011). Optimal initial conditions for simulation of seismotectonic tsunamis. *Pure and Applied Geophysics*, *168*, 1223–1237. https://doi.org/10.1007/s00024-010-0226-6

Nwogu, O. (1993). Alternative form of Boussinesq equations for nearshore wave propagation. *Journal of Waterway, Port, Coastal, and Ocean Engineering*, *119*(6), 618–638.

Okada, Y. (1985). Surface deformation due to shear and tensile faults in a half-space. *Bulletin of the seismological society of America*, *75*(4), 1135–1154.

Okal, E. A. (1988). Seismic parameters controlling far-field tsunami amplitudes: A review. *Natural Hazards*, *1*, 67–96.

Okal, E. A. (2015). The quest for wisdom: Lessons from 17 tsunamis, 2004–2014. *Philosophical Transactions of the Royal Society A*, *20140370*, 373. https://doi.org/10.1098/rsta.2014.0370

Okal, E. A., & Synolakis, C. E. (2003). A theoretical comparison of tsunamis from dislocations and landslides. *Pure and Applied Geophysics*, *160*, 2177–2188. https://doi.org/10.1007/s00024-003-2425-x

Omira, R., Baptista, M. A., & Matias, L. (2015). Probabilistic tsunami hazard in the northeast atlantic from near- and far-field tectonic sources. *Pure and Applied Geophysics*, *172*, 901–920. https://doi.org/10.1007/S00024-014-0949-X

Orfanogiannaki, K., & Papadopoulos, G. (2007). Conditional probability approach of the assessment of tsunami potential: Application in three tsunamigenic regions of the Pacific Ocean. *Pure and Applied Geophysics*, *164*, 593–603.

Paris, R. (2015). Source mechanisms of volcanic tsunamis. *Philosophical Transactions of the Royal Society, A*, *373*, 20140380.

Paris, R., Coello Bravo, J. J., Martín González, M. E., Kelfoun, K., & Nauret, F. (2017). Explosive eruption, flank collapse and mega-tsunami at Tenerife ca. 170 ky ago. *Nature Communications*, *8*, 15246. https://doi.org/10.1038/ncomms15246

Paris, R., Giachetti, T., Chevalier, J., Guillou, H., & Frank, N. (2011). Tsunami deposits in Santiago Island Cape Verde archipelago as possible evidence of a massive flank failure of Fogo volcano. *Sedimentary Geology*, *239*, 129–145.

Paris, R., Switzer, A. D., Belousova, M., Belousov, A., Ontowirjo, B., Whelley, P. L., & Ulvrova, M. (2014). Volcanic tsunami: A review of source mechanisms, past events and hazards in Southeast Asia Indonesia, Philippines, Papua New Guinea. *Natural Hazards*, *70*, 447–470.

Park, J. O., Tsuru, T., Kodaira, S., Cummins, P. R., & Kaneda, Y. (2002). Splay Fault branching along the Nankai subduction zone. *Science*, *297*, 1157–1160.

Parsons, T. (2008a). Earthquake recurrence on the south Hayward fault is most consistent with a time dependent, renewal process. *Geophysical Research Letters*, *36*, L21301. https://doi.org/10.1029/2008GL035887

Parsons, T. (2008b). Monte Carlo method for determining earthquake recurrence parameters from short paleoseismic catalogs: Example calculations for California. *Journal of Geophysical Research*, *113*, B03302. https://doi.org/10.1029/2007JB004998

Parsons, T. (2012). Paleoseismic interevent times interpreted for an unsegmented earthquake rupture forecast. *Geophysical Research Letters*, *39*, L13302. https://doi.org/10.1029/2012GL052275

Parsons, T., & Geist, E. L. (2009). Tsunami probability in the Caribbean region. *Pure and Applied Geophysics*, *165*, 2089–2116. https://doi.org/10.1007/s00024-008-0416-7

Patchett, J., Gisler, M., & Ross, G. (2017). Deep water impact ensemble data set, Representative data set for Intel in their continued system development for Trinity. *Report Web, Los Alamos National Laboratory 2017-02-24*.

Paté-Cornell, E. (2012). On "Black Swans" and "Perfect Storms": Risk analysis and management when statistics are not enough. *Risk Analysis*, *32*, 1823–1833. https://doi.org/10.1111/j.1539-6924.2011.01787.x

Paté-Cornell, M. E. (1996). Uncertainties in risk analysis: Six levels of treatment. *Reliability Engineering & System Safety*, *54*, 95–111.

Pattiaratchi, C. B., & Wijeratne, E. M. S. (2014). Observations of meteorological tsunamis along the south-west Australian coast. *Natural Hazards*, *74*, 281–303. https://doi.org/10.1007/978-3-319-12712-5_16

Pattiaratchi, C. B., & Wijeratne, E. M. S. (2015). Are meteotsunamis an underrated hazard?. *Philosophical Transactions of the Royal Society A*, *373*, 20140377. https://doi.org/10.1098/rsta.2014.0377

Pedersen, G. (2008). Modeling runup with depth integrated equation models. In P. L.-F. Liu, H. Yeh, & C. E. Synolakis (Eds.), *Advanced numerical models for simulating tsunami waves and runup* (Vol. 10, pp. 3–41). Singapore: World Scientific.

Pelayo, A. M., & Wiens, D. A. (1992). Tsunami earthquakes—Slow thrust-faulting events in the accretionary wedge. *Journal of Geophysical Research*, *97*, 15,321–15,337.

Pelinovsky, E., Zahibo, N., Dunkley, P., Edmonds, M., Herd, R., Talipova, T., … Nikolkina, I. (2004). Tsunamis generated by the volcano eruption on July 12–13, 2003 at Montserrat, Lesser Antilles. *Science of Tsunami Hazards*, *22*, 44–57.

Pellikka, H., Rauhala, J., Kahma, K. K., Stipa, T., Boman, H., & Kangas, A. (2014). Recent observations of meteotsunamis on the Finnish coast. *Natural Hazards*, *74*, 197–215. https://doi.org/10.1007/978-3-319-12712-5_11

Pérez Torrado, F. J., Paris, R., Cabrera, M. C., Schneider, J. L., Wassmer, P., Carracedo, J. C., … Santana, F. (2006). The Agaete tsunami deposits Gran Canaria: Evidence of tsunamis related to flank collapses in the Canary Islands. *Marine Geology*, *227*, 137–149.

Pisarenko, V. F., Sornette, A., Sornette, D., & Rodkin, M. V. (2014). Characterization of the tail of the distribution of earthquake magnitudes by combining the GEV and GPD descriptions of extreme value theory. *Pure and Applied Geophysics*, *171*, 1599–1624.

Polet, J., & Kanamori, H. (2000). Shallow subduction zone earthquakes and their tsunamigenic potential. *Geophysical Journal International*, *142*, 684–702. https://doi.org/10.1046/j.1365-246X.2000.00205.x

Polet, J., & Kanamori, H. (2016). Tsunami earthquakes. In R. A. Meyers (Ed.), *Encyclopedia of complexity and systems science* (pp. 9577–9592). Berlin Heidelberg: Springer Publishing. https://doi.org/10.1007/978-3-642-27737-5_567-2

Polet, J., & Thio, H. K. (2003). The 1994 Java Tsunami earthquake and its 'Normal' Aftershocks. *Geophysical Research Letters*, *30*, 1474. https://doi.org/10.1029/2002GL016806

Popinet, S. (2011). Quadtree-adaptive tsunami modelling. *Ocean Dynamics*, *61*(9), 1261–1285. https://doi.org/10.1007/s10236-011-0438-z

Power, W., Clark, K., King, D. N., Borrero, J., Howarth, J., Lane, E. M., & Reid, C. (2017). Tsunami runup and tide-gauge observations from the 14 November 2016 M7. 8 Kaikōura earthquake, New Zealand. *Pure and Applied Geophysics*, *174*, 2457–2473. https://doi.org/10.1007/s00024-017-1566-2

Power, W., Wang, X., Lane, E. M., & Gillibrand, P. A. (2013). A probabilistic tsunami hazard study of the Auckland region, Part I: Propagation modelling and tsunami hazard assessment at the shoreline. *Pure and Applied Geophysics*, *170*, 16–21. https://doi.org/10.1007/s00024-012-0543-z

Proudman, J. (1929). The effects on the sea of changes in atmospheric pressure. *Geophysical Supplements of Monthly Notices of the Royal Astronomical Society*, *2*(4), 197–209.

Rabinovich, A. B., & Monserrat, S. (1998). Generation of meteorological tsunamis (large amplitude seiches) near the Balearic and Kuril islands. *Natural Hazards*, *18*, 27–55.

Ramalho, R. S., Winclker, G., Madeira, J., Helffrich, G. R., Hipo'lito, A. R., Quartau, R., … Schaefer, J. M. (2015). Hazard potential of volcanic flank collapses raised by new megatsunami evidence. *Science Advances*, *1*, e1500456.

Reid, H. F. (1910). The mechanics of the earthquake, The California earthquake of April 18, 1906, *Report of the State Investigation Commission* (Vol. 2). Washington, DC: Carnegie Institution of Washington.

Renault, L., Vizoso, G., Jansá, A., Wilkin, J., & Tintoré, J. (2011). Toward the predictability of meteotsunamis in the Balearic Sea using regional nested atmosphere and ocean models. *Geophysical Research Letters*, *38*, L10601. https://doi.org/10.1029/2011GL047361

Rikitake, B. T., & Aida, I. (1988). Tsunami hazard probability in Japan. *Bulletin of the Seismological Society of America*, *78*, 1268–1278.

Romano, F., Piatanesi, A., Lorito, S., D'Agostino, N., Hirata, K., Atzori, S., … Cocco, M. (2012). Clues from joint inversion of tsunami and geodetic data of the 2011 Tohoku-Oki earthquake. *Science Reports*, *2*, 385. https://doi.org/10.1038/srep00385

Romano, F., Trasatti, E., Lorito, S., Piromallo, C., Piatanesi, A., Ito, Y., … Cocco, M. (2014). Structural control on the Tohoku earthquake rupture process investigated by 3D FEM, tsunami and geodetic data. *Science Reports*, *4*, 5631. https://doi.org/10.1038/srep05631

Ruff, L., & Kanamori, H. (1980). Seismicity and the subduction process. *Physics of the Earth and Planetary Interiors*, *23*, 240–252.

Rumpf, C. M., Lewis, H. G., & Atkinson, P. M. (2017). Asteroid impact effects and their immediate hazards for human populations. *Geophysical Research Letters*, *44*, 3433–3440. https://doi.org/10.1002/2017GL073191

Ryan, K. J., Geist, E. L., Barall, M., & Oglesby, D. D. (2015). Dynamic models of an earthquake and tsunami offshore Ventura, California. *Geophysical Research Letters*, *42*, 6599–6606. https://doi.org/10.1002/2015GL064507

Sakai, T., Takeda, T., Soraoka, H., Yanagisawa, K., & Annaka, T. (2006). Development of a probabilistic tsunami hazard analysis in Japan. In *Proceedings of ICONE14 International Conference on Nuclear Engineering*, Miami, Florida USA. ICONE14-89183.

Satake, K. (2007). Tsunamis. In G. Schubert, & H. Kanamori (Eds.), *Treatise on geophysics earthquake seismology* (Vol. 4, pp. 483–511). Amsterdam: Elsevier.

Satake, K., & Atwater, B. F. (2007). Long-term perspectives on giant earthquakes and tsunamis at subduction zones. *Annual Review of Earth and Planetary Sciences*, *35*, 349–74. https://doi.org/10.1146/annurev.earth.35.031306.140302

Satake, K., Fujii, Y., Harada, T., & Namegaya, Y. (2013). Time and space distribution of coseismic slip of the 2011 Tohoku earthquake as inferred from tsunami waveform data. *Bulletin of the Seismological Society of America*, *103*, 1473–1492.

Satake, K., & Kanamori, H. (1991). Abnormal tsunamis caused by the June 13, 1984, Torishima, Japan, earthquake. *Journal of Geophysical Research*, *96*, 19933–19939.

Satake, K., & Kato, Y. (2001). The 1741 Oshima-Oshima eruption: Extent and volume of submarine debris avalanche. *Geophysical Research Letters*, *28*, 427–430.

Satake, K., & Tanioka, Y. (1999). Sources of tsunami and tsunamigenic earthquakes in subduction. *Pure and Applied Geophysics*, *154*, 467–483.

Savage, J. C. (1994). Empirical earthquake probabilities from observed recurrence intervals. *Bulletin of the Seismological Society of America*, *84*, 219–221.

Scherbaum, F., & Kuehn, N. M. (2011). Logic tree branch weights and probabilities: Summing up to one is not enough. *Earthquake Spectra*, *27*(4), 1237–1251.

Scholz, C. (1990). *The mechanics of earthquakes and faulting*. Cambridge, UK: Cambridge University Press.

Scholz, C. H., & Small, C. (1997). The effect of seamount subduction on seismic coupling. *Geology*, *25*, 487–490.

Schorlemmer, D., Gerstenberger, M. C., Wiemer, S., Jackson, D. D., & Rhoades, D. A. (2007). Earthquake likelihood model testing. *Seismological Research Letters*, *78*, 17–29.

Schwartz, D. P., & Coppersmith, K. J. (1984). Fault behavior and characteristic earthquakes: Examples from the Wasatch and San Andreas Fault Zones. *Journal of Geophysical Research*, *89*(B7), 5681–5698. https://doi.org/10.1029/JB089iB07p05681

Selva, J., Costa, A., Marzocchi, W., & Sandri, L. (2010). BET_VH: exploring the influence of natural uncertainties on long-term hazard from tephra fallout at Campi Flegrei (Italy). *Bulletin of Volcanology*, *72*(6), 705–716.

Selva, J., Iqbal, S., Taroni, M., Marzocchi, W., Cotton, F., Courage, W., … Smerzini, C. (2015). Deliverable D3.1: Report on the effects of epistemic uncertainties on the definition of LP-HC events. STREST project: Harmonized approach to stress tests for critical infrastructures against natural hazards.

Selva, J., & Sandri, L. (2013). Probabilistic Seismic Hazard Assessment: Combining Cornell-like approaches and data at sites through Bayesian inference. *Bulletin of the Seismological Society of America*, *103*(3), 1709–1722. https://doi.org/10.1785/0120120091

Selva, J., Tonini, R., Molinari, I., Tiberti, M. M., Romano, F., Grezio, A., … Lorito, S. (2016). Quantification of source uncertaintiesin seismic probabilistic tsunami hazard analysis (SPTHA). *Geophysical Journal International*, *205*, 1780–1803. https://doi.org/10.1093/gji/ggw107

Senior Seismic Hazard Analysis Commission (SSHAC) (1997). Recommendations for probabilistic seismic hazard analysis: Guidance on uncertainty and use of experts (U.S. Nuclear Regulatory Commission Report NUREG/CR-6372). Washington, DC.

Seno, T. (2002). Tsunami earthquakes as transient phenomena. *Geophysical Research Letters*, *29*(10), 58-1–58-4. https://doi.org/10.1029/2002GL014868

Seno, T., & Hirata, K. (2007). Did the 2004 Sumatra-Andaman earthquake involve a component of tsunami earthquakes?. *Bulletin of the Seismological Society of America*, *97*, 296–306. https://doi.org/10.1785/0120050615

Šepić, J., Medugorac, I., Janeković, I., Dunić, N., & Vilibić, I. (2016). Multi-meteotsunami event in the Adriatic Sea generated by atmospheric disturbances of 25-26 June 2014. *Pure and Applied Geophysics*, *173*, 4117–4138. https://doi.org/10.1007/s00024-016-1249-4

Šepić, J., Vilibić, I., & Monserrat, S (2016). Quantifying the probability of meteotsunami occurrence from synoptic atmospheric patterns. *Geophysical Research Letters*, *43*, 10,377–10,384. https://doi.org/10.1002/2016GL070754

Setiyono, U., Gusman, A. R., Satake, K., & Fujii, Y. (2017). Pre-computed tsunami inundation database and forecast simulation in Pelabuhan Ratu, Indonesia. *Pure and Applied Geophysics*, *174*(8), 3219–3235. https://doi.org/10.1007/s00024-017-1633-8

Shi, F., Kirby, J. T., Harris, J. C., Geiman, J. D., & Grilli, S. T. (2012). A high-order adaptive time-stepping TVD solver for Boussinesq modeling of breaking waves and coastal inundation. *Ocean Models*, *43–44*, 36–51. https://doi.org/10.1016/j.ocemod.2011.12.004

Shimazaki, K., & Nakata, T. (1980). Time-predictable recurrence model for large earthquakes. *Geophysical Research Letters*, *7*, 279–282.

Shin, J. Y., Chen, S., & Kim, T.-W. (2015). Application of Bayesian Markov Chain Monte Carlo method with mixed gumbel distribution to estimate extreme magnitude of tsunamigenic earthquake. *Journal of Civil Engineering*, *19*(2), 366–375. https://doi.org/10.1007/s12205-015-0430-0

Shuvalov, V. V. (2003). *Numerical modeling of the Eltanin impact*, Paper presented at Lunar and Planetary Science Conference, pp. 34,1101. Houston.

Shuvalov, V. V., & Trubetskaya, I. A. (2007). Numerical modeling of the formation of the Eltanin submarine impact structure. *Solar System Research*, *41*, 56–64. https://doi.org/10.1134/S0038094607010066

Simons, M., Minson, S. E., Sladen, A., Ortega, F., Jiang, J., Owen, S. E., … Helmberger, D. V. (2011). The 2011 magnitude 9.0 Tohoku-Oki earthquake: Mosaicking the megathrust from seconds to centuries. *Science*, *332*(6036), 1421–1425.

Smit, A., Kijko, A. J., & Stein, A. (2017). Probabilistic tsunami hazard assessment from incomplete and uncertain historical catalogues with application to tsunamigenic regions in the Pacific Ocean. *Pure and Applied Geophysics Springer International Publishing*, *174*, 3065–3081. https://doi.org/10.1007/s00024-017-1564-4

Solheim, A., Berg, K., Forsberg, C. F., & Bryn, P. (2005). The Storegga slide complex: Repetitive large scale sliding with similar cause and development. *Marine and Petroleum Geology*, *22*, 97–107. https://doi.org/10.1016/j.marpetgeo.2004.10.013

Song, Y. T., Mohtat, A., & Yim, S. C. (2017). New insights on tsunami genesis and energy source. *Journal of Geophysical Research: Oceans*, *122*, 4238–4256. https://doi.org/10.1002/2016JC012556

Sørensen, M. B., Spada, M., Babeyko, A., Wiemer, S., & Grünthal, G. (2012). Probabilistic tsunami hazard in the Mediterranean Sea. *Journal of Geophysical Research*, *117*, B01305. https://doi.org/10.1029/2010JB008169

Stein, S., Geller, R. J., & Liu, M. (2012). Why earthquake hazard maps often fail and what to do about it? *Tectonophysics*, *562*, 1–25.

Stein, S., & Mazzotti, S. (2007). Continental intraplate earthquakes: Science, hazard, and policy issues. *Geological Society of America Special Paper*, *425*, 1–47.

Stein, S., & Okal, E. A. (2007). Ultralong period seismic study of the December 2004 Indian Ocean earthquake and implications for regional tectonics and the subduction process. *Bulletin of the Seismological Society of America*, *97*(1), 297–295. https://doi.org/10.1785/0120050617

Stern, R. J. (2002). Subduction zones. *Reviews of Geophysics*, *40*(4), 1012. https://doi.org/10.1029/2001RG000108

Stix, J., & Kobayashi, T. (2008). Magma dynamics and collapse mechanisms during four historic caldera-forming events. *Journal of Geophysical Research*, *113*, B09205. https://doi.org/10.1029/2007JB005073

Strasser, F. O., Arango, M. C., & Bommer, J. J. (2010). Scaling of the source dimensions of interface and intraslab subduction-zone earthquakes with moment magnitude. *Seismological Research Letters*, *81*(6), 941–950.

Suppasri, A., Hasegawa, N., Makinoshima, F., Imamura, F., Latcharote, P., & Day, S. (2016). An analysis of fatality ratios and the factors that affected human fatalities in the 2011 Great East Japan tsunami. *Frontiers in Built Environment*, *2*, 32. https://doi.org/10.3389/fbuil.2016.00032

Suppasri, A., Imamura, F., & Koshimura, S. (2012). Probabilistic tsunami hazard analysis and risk to coastal populations in Thailand. *Japan Earthquake & Tsunami*, *06*, 1250011, 27 Pages. https://doi.org/10.1142/S179343111250011x

Synolakis, C. E. (1987). The runup of solitary waves. *Journal of Fluid*, *185*, 523–545.

Synolakis, C. E. (1991). Tsunami runup on steep slopes: How good linear theory really is, *Tsunami hazard* (pp. 221–234). Netherlands: Springer.

Synolakis, C. E., Bardet, J. P., Borrero, J. C., Davies, H. L., Okal, E. A., Silver, E. A., … Tappin, D. R. (2002). The slump origin of the 1998 Papua New Guinea tsunami. *Proceedings of the Royal Society A: Mathematical, Physical and Engineering Sciences*, *458*(2020), 763–789. https://doi.org/10.1098/rspa.2001.0915, URL https://doi.org/10.1098/rspa.2001.0915

Synolakis, C. E., & Bernard, E. N. (2006). Tsunami science before and beyond Boxing Day 2004.*Philosophical Transactions of the Royal Society A*, *364*, 2231–2265. https://doi.org/10.1098/rsta.2006.1824

Synolakis, C. E., Bernard, E. N., Titov, V. V., Kânoglu, U., & González, F. I. (2008). Validation and verification of tsunami numerical models. *Pure and Applied Geophysics*, *165*, 2197–2228.

Synolakis, C. E., & Kânoglu, U. (2015). The Fukushima accident was preventable. *Philosophical Transactions of the Royal Society A*, *373*, 20140379. https://doi.org/10.1098/rsta.2014.0379

Tanaka, K., Gohara, S., Koga, T., Yamaguchi, R., & Yamada, F. (2014). Abiki oscillations in Sakitsu Bay, west Kyushu, Japan. *Natural Hazards*, *74*, 233–250. https://doi.org/10.1007/978-3-319-12712-5_13

Tanioka, Y., Ruff, L., & Satake, K. (1997). What controls the lateral variation of large earthquake occurrence along the Japan Trench? *The Island Arc*, *6*, 261–266. https://doi.org/10.1111/j.1440-1738.1997.tb00176.x

Tanioka, Y., & Satake, K. (1996). Tsunami generation by horizontal displacement of ocean bottom. *Geophysical Research Letters*, *23*, 861–864.

Tappin, D., Watts, P., & Grilli, S. T. (2008). The Papua New Guinea tsunami of 17 July 1998: Anatomy of a catastrophic event. *Natural Hazards and Earth System Science*, *8*, 243–266. https://doi.org/10.5194/nhess-8-243-2008

Tatsumi, D., Calder, C. A., & Tomita, T. (2014). Bayesian near-field tsunami forecasting with uncertainty estimates. *Journal of Geophysical Research: Oceans*, *119*, 2201–2211. https://doi.org/10.1002/2013JC009334

Taubenböck, H., Goseberg, N., Setiadi, N., Lämmel, G., Moder, F., Oczipka, M., … Birkmann, J. (2009). "Last-Mile" preparation for a potential disaster—Interdisciplinary approach towards tsunami early warning and an evacuation information system for the coastal city of Padang, Indonesia. *Natural Hazards and Earth System Sciences*, *9*(4), 1509–1528.

Taubenböck, H., Post, J., Roth, A., Zosseder, K., Strunz, G., & Dech, S. (2008). A conceptual vulnerability and risk framework as outline to identify capabilities of remote sensing. *Natural Hazards and Earth System Science*, *8*, 409–420.

ten Brink, U. S., Andrews, B. D., & Miller, N. C. (2016). Seismicity and sedimentation rate effects on submarine slope stability. *Geology*, *44*, 563–566.

ten Brink, U. S., Chaytor, J. D., Geist, E. L., Brothers, D. S., & Andrews, B. D. (2014). Assessment Of tsunami hazard to the U.S. Atlantic margin. *Marine Geology*, *353*, 31–54.

ten Brink, U. S., Geist, E. L., & Andrews, B. D. (2006). Size distribution of submarine landslides and its implication to tsunami hazard in Puerto Rico. *Geophysical Research Letters*, *33*, L11307. https://doi.org/10.1029/2006GL026125

ten Brink, U. S., Lee, H. J., Geist, E. L., & Twichell, D. (2009). Assessment Of tsunami hazard to the U.S. East Coast using relationships between submarine landslides and earthquakes. *Marine Geology*, *264*, 65–73.

Thio, H. K., Somerville, P. G., & Ichinose, G. (2007). Probabilistic analysis of strong ground motion and tsunami hazards in Southeast Asia. *Journal of Earthquake And Tsunami*, *01*, 119. https://doi.org/10.1142/S1793431107000080

Thio, H. K., Somerville, P. G., & Polet, J. (2010). Probabilistic tsunami hazard in California. *Pacific Earthquake Engineering Research Center Report*, *108*, 331.

Thio, H. K., Wei, Y., Chock, G., & Li, W. (2017). Development of offshore probabilistic tsunami exceedance amplitudes for ASCE 7-16. In *Proceedings of the Sixteenth World Conference on Earthquake Engineering*, Santiago.

Thomson, R. E., Rabinovich, A. B., Fine, I. V., Sinnott, D. C., McCarthy, A., Sutherland, N. A. S., & Neil, L. K. (2009). Meteorological tsunamis on the coasts of British Columbia and Washington. *Physics and Chemistry of the Earth*, *34*, 971–988. https://doi.org/10.1016/j.pce.2009.10.003

Toth, Z., & Kalnay, E. (1993). Ensemble forecasting at NMC: The generation of perturbations. *Bulletin of the American Meteorological Society*, *74*, 2317–2330. https://doi.org/10.1175/1520-0477(1993)074-2.0.CO;2

Tinti, S., Bortolucci, E., & Chiavetteri, C. (2001). Tsunami exitation by submarine landslides in shallow-water approximation. *Pure and Applied Geophysics*, *158*, 759–797. https://doi.org/10.1007/PL00001203

Tinti, S., Pagnoni, G., & Zaniboni, F. (2006). The landslides and tsunamis of the 30th of December 2002 in Stromboli analysed through numerical simulations. *Bulletin of Volcanology*, *68*, 462–479.

Titov, V. V., & Synolakis, C. E. (1995). Modeling of breaking and non-breaking long-wave evolution and runup using VTCS-2. *Journal of Waterway, Port, Coastal, and Ocean Engineering*, *121*(6), 308–316.

Torsvik, T., Paris, R., Didenkulova, I., Pelinovsky, E., Belousov, A., & Belousova, M. (2010). Numerical simulation of explosive tsunami wave generation and propagation in Karymskoye Lake, Russia. *Natural Hazards and Earth System Sciences*, *10*, 2359–2369.

Ulvrova, M., Paris, R., Kelfoun, K., & Nomikou, P. (2014). Numerical simulations of tsunami generated by underwater volcanic explosions at Karymskoye Lake Kamchatka, Russia and Kolumbo volcano Aegean Sea, Greece. *Natural Hazards and Earth System Sciences*, *14*, 401–412.

Ulvrova, M., Paris, R., Nomikou, P., Kelfoun, K., Leibrandt, S., Tappin, D. R., & McCoy, F. W. (2016). Source of the tsunami generated by the 1650 AD eruption of Kolumbo submarine volcano (Aegean Sea, Greece). *Journal of Volcanology and Geothermal Research*, *321*, 125–139.

Ulvrova, M., Selva, J., Paris, R., Brizuela, B., Costa, A., & Grezio, A. (2016). Probabilistic tsunami hazard assessment related to underwater explosions in the Campi Flegrei caldera: Gulfs of Napoli and Pozzuoli (Tyrrhenian Sea, Italy). In *EGU General Assembly 2016*, Vienna, Austria. Geophysical Research Abstracts, Vol. 18, EGU2016-16366.

Urgeles, R., & Camerlenghi, A. (2013). Submarine landslides of the Mediterranean Sea: Trigger mechanisms, dynamics, and frequency-magnitude distribution. *Journal of Geophysical Research: Earth Surface*, *118*, 2600–2618. https://doi.org/10.1002/2013JF002720

U.S. Environmental Protection Agency (2011). Exposure Factors Handbook: 2011 Edition. EPA/600/R-090/052F, Retrieved from http://www.epa.gov, (accessed September 2011).

U.S. Nuclear Regulatory Commission (USNRC) (2012). Practical implementation guidelines for SSHAC Level 3 and 4 hazard studies. Prepared by AM Kammerer and JP Ake, NRC Project Manager: R Rivera- Lugo, NUREG-2117.

Utsu, T. (1999). Representation and analysis of the earthquake size distribution: A historical review and some new approaches. *Pure and Applied Geophysics*, *155*, 509–535.

Vick, M. (2002). *Degrees of belief: Subjective probability and engineering judgment* (p. 455). Reston, VA: ASCE Press.

Vilibić, I., Šepić, J., Rabinovich, A. B., & Monserrat, S. (2016). Modern approaches in meteotsunami research and early warning. *Frontiers in Marine Science*, *3*, 57. https://doi.org/10.3389/fmars.2016.00057

Wald, D. J., & Graves, R. W. (2001). Resolution analysis of finite fault source inversion using one-and three-dimensional Green's functions: 2. Combining seismic and geodetic data. *Journal of Geophysical Research*, *106*(B5), 8767–8788.

Wang, D., Becker, N. C., Walsh, D., Fryer, G. J., Weinstein, S. A., McCreery, C. S., … Shiro, B. (2012). Real-time forecasting of the April 11, 2012 Sumatra tsunami. *Geophysical Research Letters*, *39*, L19601. https://doi.org/10.1029/2012GL053081

Wang, R., Martín, F. L., & Roth, F. (2003). Computation of deformation induced by earthquakes in a multi-layered elastic crust-FORTRAN programs EDGRN/EDCMP. *Computers and Geosciences*, *29*(2), 195–207.

Wang, X., Li, K., Yu, Z., & Wu, J. (1987). Statistical characteristics of seiches in Longkou Harbour. *Journal of Physical Oceanography*, *17*, 1963–1966.

Wang, X., Power, W. L., Lukovic, B., & Mueller, C. (2017). Effect of explicitly representing buildings on tsunami inundation: A pilot study of Wellington CBD. In *Proceedings, New Zealand Society for Earthquake Engineering Conference 2017*. Wellington, New Zealand. http://db.nzsee.org.nz/2017/O3C.3_Wang.pdf

Ward, S. N. (2001). Landslide tsunami. *Journal of Geophysical Research*, *106*(B6), 11201–11215. https://doi.org/10.1029/2000JB900450

Ward, S. N. (2002). Tsunamis. In R. A. Meyers (Ed.), *The encyclopedia of physical science and technology* (Vol. 17, pp. 175–191). London, UK: Academic Press.

Ward, S. N., & Asphaug, E. (2000). Asteroid impact tsunami: A probabilistic hazard. *Icarus*, *145*(1), 64–78. https://doi.org/10.1006/icar.1999.6336

Ward, S. N., & Day, S. J. (2003). Ritter Island volcano--Lateral collapse and the tsunami of 1888. *Geophysical Journal International*, *154*, 891–902.

Watanabe, H. (1972). Statistical studies on the wave-form and maximum height of large tsunamis. *Journal of the Oceanographical Society of Japan*, *28*, 229–241. https://doi.org/10.1007/BF02109293

Watts, P. (2000). Tsunami features of solid block underwater landslides. *Journal of Waterway, Port, Coastal, and Ocean Engineering*, *126*, 144–152.

Watts, P. (2004). Probabilistic predictions of landslide tsunamis of Southern California. *Marine Geology*, *203*, 281–301.

Watts, P., & Waythomas, C. F. (2003). Theoritical analysis of tsunami generation by pyroclastic flows. *Journal of Geophysical Research*, *108*(B12), 2563. https://doi.org/10.1029/2002JB002265

Wei, Y., Thio, H. K., Titov, V., Chock, G., Zhou, H., Tang, L., & Moore, C. (2017). Inundation modeling to Create 2,500-year return period tsunami design zone maps for the ASCE 7-16 standard. In *Proceedings of the Sixteenth World Conference on Earthquake Engineering*, Santiago.

Wells, D., & Coppersmith, K. (1994). New empirical relationships among magnitude, rupture length, rupture width, rupture area, and surface displacement. *Bulletin of the Seismological Society of America*, *84*(4), 974–1002.

Wesnousky, S. G. (1986). Earthquakes, quaternary faults, and seismic hazard in California. *Journal of Geophysical Research*, *91*(B12), 12587–12631. https://doi.org/10.1029/JB091iB12p12587

Whitmore, P., & Knight, B. (2014). Meteotsunami forecasting: Sensitivities demonstrated by the 2008 Boothbay Maine event. *Natural Hazards*, *74*, 11–23. https://doi.org/10.1007/978-3-319-12712-5_2

Woessner, J., Danciu, L., Giardini, D., Crowley, H., Cotton, F., Grünthal, G., … the SHARE consortium (2015). The 2013 European seismic hazard model—Key components and results. *Bulletin of Earthquake Engineering*, *13*, 3553–3596. https://doi.org/10.1007/s10518-015-9795-1

Wood, N., Jones, J., Spielman, S., & Schmidtlein, M. (2015). Community clusters of tsunami vulnerability in the US Pacific Northwest. *Proceedings of the National Academy of Sciences*, *112*(17), 5353–5359. http://www.pnas.org/content/early/2015/04/09/1420309112

Wünnemann, K., Collins, G. S., & Weiss, R. (2010). Impact of a cosmic body into Earth's ocean and the generation of large tsunami waves: Insight from numerical modeling. *Reviews of Geophysics*, *48*, RG4006. https://doi.org/10.1029/2009RG000308

Wünnemann, K., & Weiss, R. (2015). The meteorite impact-induced hazard. *Philosophical Transactions of the Royal Society A*, *373*, 20140381.
Yadav, R. B. S., Tripathi, J. N., & Kumari, T. S. (2013). Probabilistic assessment of tsunami recurrence in the Indian Ocean. *Pure and Applied Geophysics*, *170*, 373–389. https://doi.org/10.1007/s00024-012-0487-3
Yadav, R. B. S., Tsapanos, T. M., Tripathi, J. N., & Chopra, S. (2013). An evaluation of tsunami hazard using Bayesian approach in the Indian Ocean. *Tectonophysics*, *593*, 172–182.
Yavari-Ramshe, S., & Ataie-Ashtiani, B. (2016). Numerical modeling of subaerial and submarine landslide-generated tsunami waves—Recent advances and future challenges. *Landslides*, *13*, 1325–1368. https://doi.org/10.1007/s10346-016-0734-2
Yeh, H. (2010). Gender and age factors in tsunami casualties. *ASCE Natural Hazards Review*, *11*, 29–34.
Yokoyama, I. (1987). A scenario of the 1883 Krakatau tsunami. *Journal of Volcanology and Geothermal Research*, *34*, 123–13.
Yoshida, Y., Ueno, H., Muto, D., & Aoki, S. (2011). Source process of the 2011 off the Pacific coast of Tohoku Earthquake with the combination of teleseismic and strong motion data. *Earth, Planets and Space*, *63*(7), 565–569.
Zachariasen, J., Sieh, K., Taylor, F. W., Edwards, R. L., & Hantoro, W. S. (1999). Submergenceand uplift associated with the giant 1833 Sumatran subduction earthquake: Evidence from coral microatolls. *Journal of Geophysical Research*, *104*, 895–919.
Zöller, G. (2013). Convergence of the frequency-magnitude distribution of global earthquakes: Maybe in 200 years. *Geophysical Research Letters*, *40*, 3873–3877. https://doi.org/10.1002/grl.50779